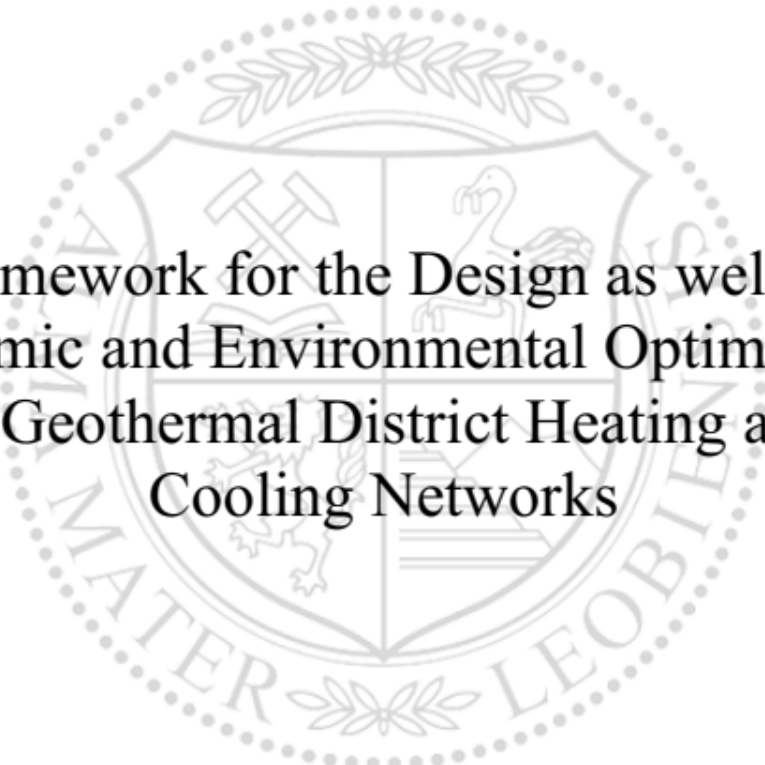Chair of Thermal Processing Technology

Master's Thesis

Framework for the Design as well as Economic and Environmental Optimization of Geothermal District Heating and Cooling Networks

Paul Stipper, BSc

May 2024

EIDESSTATTLICHE ERKLÄRUNG

Ich erkläre an Eides statt, dass ich diese Arbeit selbstständig verfasst, andere als die angegebenen Quellen und Hilfsmittel nicht benutzt, den Einsatz von generativen Methoden und Modellen der künstlichen Intelligenz vollständig und wahrheitsgetreu ausgewiesen habe, und mich auch sonst keiner unerlaubten Hilfsmittel bedient habe.

Ich erkläre, dass ich den Satzungsteil „Gute wissenschaftliche Praxis" der Montanuniversität Leoben gelesen, verstanden und befolgt habe.

Weiters erkläre ich, dass die elektronische und gedruckte Version der eingereichten wissenschaftlichen Abschlussarbeit formal und inhaltlich identisch sind.

Datum 09.05.2024

_____

Unterschrift Verfasser/in
Paul Stipper

Signiert von:	Paul Gregor Stipper
Datum:	10.05.2024 10:02:53

TRUST

Dieses Dokument ist digital signiert!
Dieses mit einer qualifizierten elektronischen Signatur versehene Dokument hat gemäß Art. 25 Abs. 2 der Verordnung (EU) Nr 910/2014 vom 23. Juli 2014 ("eIDAS-VO") die gleiche Rechtswirkung wie ein handschriftlich unterschriebenes Dokument.

Prüfinformation: Informationen zur Prüfung der elektronischen Signatur finden Sie unter: www.a-trust.at/pdf

Master's Thesis

Framework for the Design as well as Economic and Environmental Optimization of Geothermal District Heating and Cooling Networks

compiled by

Chair of Thermal Processing Technology

Submitted by:

Paul Stipper, BSc

01602585

Supervisor:

Dipl.-Ing. Christoph Gatschelhofer

Univ. Prof. Dipl.-Ing. Dr.techn. Harald Raupenstrauch

Leoben, 13.05.24

Abstract:

Climate Change and the provision of affordable, reliable energy have become an increasingly prevalent subject of discussion. Over the past decade, the European Union has made significant efforts to decarbonize its electricity sector, while the heating and cooling sector, responsible for half of Europe's final energy consumption, has received less attention. District heating and cooling systems exemplify best practice approaches for delivering locally available, cost-effective, and low-carbon thermal energy. Furthermore, they provide interesting possibilities for the substitution of climate-damaging generation technologies through greener options in the heating and cooling sector on a large-scale. In particular, the exploitation of the shallow geothermal potential presents interesting opportunities, prompting intensive research into how technologies such as heat pumps and auxiliary devices like thermal energy storages can be effectively integrated into these networks. One objective of this work is to provide an understanding of the district heating and cooling sector and identify measures that can be implemented for its sustainable development, with a focus on the exploitation of geothermal energy. Therefore, the thesis first examines the functionality and historical development of district heating and cooling systems, aiming to provide an understanding of the status quo and anticipate future trends. Building up-on this knowledge, relevant technologies for their retrofitting, and how these technologies can be effectively integrated into such networks, are explained. The second objective, which is the main focus of this work, is to offer a framework for designing and optimizing geothermal generation facilities in district heating and cooling networks. In the design process, a hypothetical district heating and cooling network demand from Madrid, Spain was used as a representative example. Two Python-based programs were written to enable a high degree of automation in the design and optimisation process, as well as to facilitate handling large amounts of data. In order to get insights into the thermodynamic behaviour of such a system, a generation facility, which exploits the shallow geothermal potential, was modelled in the simulation environment TRNSYS. With the generated data, a sensitivity analysis concerning the power plant's topology was conducted to examine the impact of varying topology parameters on the levelized cost of energy, specific CO_2 emissions, as well as the heating and cooling coverage achievable. The results indicate the optimal sizes for heat and cold storage systems, as well as the optimal number of reversible heat pumps.

Kurzfassung:

Der Klimawandel und die zuverlässige Bereitstellung kostengünstiger Energie rücken immer mehr in den Fokus der öffentlichen Diskussion. Im letzten Jahrzehnt hat die Europäische Union erhebliche Anstrengungen unternommen, um ihren Stromsektor zu dekarbonisieren, während dem Heiz- und Kühlsektor, der für die Hälfte des gesamten europäischen Endenergieverbrauchs verantwortlich ist, weniger Aufmerksamkeit zugekommen ist. Fernwärme- und Fernkältesysteme entsprechen bewährten Methoden zur Bereitstellung lokal verfügbarer, günstiger und kohlenstoffarmer thermischer Energie. Sie bieten zudem vielseitige Möglichkeiten, klimaschädliche Erzeugungstechnologien im Heiz- und Kühlsektor, im großen Maßstab, durch umweltfreundlichere Varianten zu ersetzen. In diesem Kontext scheint insbesondere die Nutzung des oberflächennahen geothermischen Potentials interessante Lösungsansätze zu bieten. Deshalb beschäftigt sich kontemporäre Forschung intensiv damit wie Technologien wie Wärmepumpen und thermische Energiespeicher effektiv in solche Netze integriert werden können. Ein Ziel dieser Arbeit ist es, ein Verständnis für den Fernwärme und -kälte Sektor zu schaffen und Maßnahmen zu identifizieren, die zu seiner nachhaltigen Entwicklung beitragen können, wobei der Schwerpunkt hierbei auf der Nutzung von Geothermie liegt. Dazu werden zunächst die Funktionsweise und historische Entwicklung von Fernwärme- und Fernkältesystemen beschrieben, um den Status quo besser zu verstehen und zukünftige Trends abzuschätzen. Aufbauend auf diesem Wissen werden relevante Technologien zur Nachrüstung sowie Wege zu deren effektiven Integration erläutert. Das zweite Ziel, welches den Hauptfokus dieser Arbeit darstellt, ist die Bereitstellung eines Rahmens für das Design und die Optimierung von geothermischen Erzeugungsanlagen in Fernwärme- und Fernkältenetzwerken. Im Designprozess wurde ein hypothetisches Lastprofil eines Fernwärme- und Fernkältenetzes aus Madrid, Spanien, als repräsentatives Beispiel verwendet. Zwei Programme wurden in Python geschrieben, um einen hohen Grad an Automatisierung im Design- und Optimierungsprozess zu ermöglichen sowie die Verarbeitung großer Datenmengen zu erleichtern. Um Einblicke in das thermodynamische Verhalten eines solchen Systems zu gewinnen, wurde eine Erzeugungsanlage, welche das oberflächennahe geothermische Potenzial nutzt, in der Simulationsumgebung TRNSYS modelliert. Mit den generierten Daten wurde eine Sensitivitätsanalyse bezüglich der Kraftwerkstopologie durchgeführt, um die Auswirkungen variierender Topologieparameter auf die Erzeugungskosten, spezifischen CO_2-Emissionen sowie die Deckung des Heiz- und Kühlbedarfs zu untersuchen. Die Ergebnisse zeigen die optimalen Größen für den Wärme- und Kältespeicher sowie die optimale Anzahl an reversiblen Wärmepumpen.

Table of contents

List of abbreviations, formulae, and symbols

General abbreviations

AHP	*absorption heat pump*
APF	*annual performance factor*
ASHP	*air source heat pump*
ATES	*aquifer thermal energy storage*
BHX	*borehole heat exchanger*
BTES	*borehole thermal energy storage*
CAPEX	*capital expenditures*
CC	*compression chiller*
CHP	*combined heat and power*
COP	*coefficient of performance*
COP_C	*coefficient of performance for cooling*
COP_H	*coefficient of performance for heating*
CTES	*cavern thermal energy storage*
DC	*district cooling*
DH	*district heating*
DHC	*district heating and cooling*
DHW	*domestic hot water*
DSM	*demand side management*
EU	*European Union*
GSHP	*ground source heat pump*
HP	*heat pump*
HR	*heat ratio*
HX	*heat exchanger*
KPI	*key performance indicator*

IEA .... *International Energy Agency*

LCOE .... *levelized cost of energy*

LNG .... *liquefied natural gas*

NPV .... *net present value*

OPEX .... *operational expenditures*

PCM .... *phase change material*

PH .... *process heating*

PTES .... *pit thermal energy storage*

PtH .... *Power-to-Heat*

RES .... *renewable energy sources*

RHP .... *reversible heat pump*

SCOP .... *seasonal coefficient of performance*

$SCOP_C$ .... *seasonal coefficient of performance for cooling*

$SCOP_H$ .... *seasonal coefficient of performance for heating*

SH .... *space heating*

TES .... *thermal energy storage*

TTES .... *tank thermal energy storage*

UPM .... *Universidad Politécnica de Madrid*

Formula symbols

c_p .... *specific heat capacity at constant pressure*

CS .... *cooling share*

d .... *depth*

D .... *demand*

f .... *factor*

h_v .... *enthalpy of evaporation*

l .... *lifetime*

m .... *mass*

Nr .... *Number*

P_C .... *cooling capacity*

P_H .... *heating capacity*

PV .... *present value*

Q .... *heat*

r .... *discount rate*

T .... *temperature*

V .... *Volume*

W .... *electrical work*

η .... *efficiency factor*

Chemical formulas and symbols

CO_2 .... *carbon dioxide*

H_2O ....*water*

LiBr ....*lithium bromide*

NH_3 .... *ammonia*

List of figures

List of tables

1 Challenge and objective outline

This opening chapter explains to what field of interest this thesis can be generally ascribed, why the conducted work is relevant, and what the methodological approach applied in the course of this work looks like. Therefore, initially, an overview of the future market prospects of the district heating and cooling (DHC) sector is given. Subsequently, the research relevance is discussed, and the statement of task is formulated. Finally, the methodology that was applied in the course of this work, to meet the scientific criterion of reproducibility, is described.

1.1 Market outlook for district energy networks

In the pursuit of a climate-neutral society, as outlined in the Paris Agreement, our current reliance on fossil fuels for electrical and thermal power generation presents a significant challenge. These conventional energy sources contribute to the ever-rising greenhouse gas emissions, primarily carbon dioxide (CO_2), highlighting the urgent need for transformative strategies to decarbonize our cities and their critical facilities. In the last decade, the European Union (EU) has made significant efforts to decarbonize its electricity sector, whereas the heating and cooling sector, a critical yet often overlooked component of Europe's energy systems, has received less attention. This sector accounts for half of Europe's energy consumption and about 70 % of the energy is generated by the use of fossil fuels. This indicates that the potential for decarbonization and greater energy independence through Europe's heating and cooling sector is substantial but remains largely untapped. [1, 2]

DHC systems play a vital role in the transitions towards a greener future and are considered one of the key enablers to phase out fossil fuels. District heating (DH) as well as district cooling

(DC) networks, e.g., present a highly efficient alternative to stand-alone boilers and air condition units. This is because district energy systems exemplify best practice approaches for delivering locally available, affordable, and low-carbon thermal energy, by offering possibilities for the substitution of climate-damaging generation technologies through greener options in the heating and cooling sector on a large-scale. However, the adoption of renewable energy sources (RES) into these systems remains limited, though 2022 saw a record increase in heat pump (HP) installations due to high gas prices. Furthermore, without their adoption, 22 million old individual heating appliances and several thousand large old fossil-based heating units are at risk of being replaced by fossil boilers, undermining the EU's long-term security of supply and the goal of more affordable, clean energy for end consumers. At the same time, the global cooling demand has risen at more than double the rate of the overall energy demand in buildings in the past decade and will continue to grow rapidly as incomes, population sizes and temperatures rise. Europe has experienced repeated summers with extraordinary seasonal temperatures, which lead to an escalation in cooling demands, primarily met by individual cooling units. Moreover, studies show that the diffusion of air-conditioning units in the residential sector has developed dramatically across the surveyed countries within the last 20 years. [1, 2]

Nevertheless, the war in Ukraine has exposed Europe's dependency on fossil fuels and created new momentum for decarbonizing the thermal energy sector. The situation has led policymakers to seek ways to expedite transformation in the heat market, enacting policies aimed at decarbonizing the sector and enhancing security of supply by valorising local resources. In 2021, Europe announced 13 new geothermal heating and cooling plants connected to district energy systems, including the development of Europe's largest geothermal DH facility in Aarhus, Denmark, set to be partly operational by 2025. In this context, HPs and compression chillers (CCs) are considered key solutions for the fossil fuel phase out, with their use within DHC networks expected to increase significantly across Europe. Investment plans from some of the largest DHC operators, e.g., indicate that the large HP capacity is going to increase by at least 80 % by 2030, representing changes in the generation portfolio and growth of networks. Furthermore, a publication of the International Energy Agency (IEA) from 2022 highlights that individual units fit perfectly in rural and low-heat density areas, while DH networks are the infrastructure of choice to support the deployment of large HPs in urban areas. The report emphasises that in particular large-scale HPs can help to reduce fossil fuel dependency, e.g., by allowing heat recovery from wastewater or by increasing the temperature at local substations where needed. [1, 2]

The REPowerEU Plan and the EU Commission's Heat Pump Action Plan aim to accelerate the deployment of RES and energy efficiency measures, including the doubling of current HP deployment rates in buildings as well as promoting large HPs and CCs for DHC networks. The Energy Efficiency Directive, which sets new, tighter targets for efficient heating and cooling solutions, further underscores the EU's commitment to decarbonizing DHC and advancing clean energy use within the sector. Furthermore, the new geopolitical and energy market realities demand a drastically accelerated transition in the energy sector. In March 2023, as part of the European Green Deal and the REPowerEU Plan, the EU provisionally agreed on stronger laws to speed up the rollout of RES, setting ambitious targets to double their share by 2030. Moreover, the Fit-for-55 package, which provides the regulatory instruments to reduce greenhouse gas emissions in the EU, recognises the importance of DHC networks in the energy transition. The package reflects positive trends in legislation and represents opportunities for growth of the DHC market. [1]

However, DHC systems are not on track to meet the climate targets set for 2050 by the IEA, so that in 2021 nearly 90 % of district heat globally was still generated via fossil fuels. Nevertheless, existing networks are expected to expand alongside new urban developments and new projects are materialising in Europe. This underscores the urgency for rapid improvement and greater integration of RES into contemporary DHC networks, to allow them to fully realize their potential in the energy transition. Especially, DC networks require more attention, as currently no comprehensive framework exists at the EU level to recognize its benefits and to address the cooling challenge. [1]

1.2 Research relevance and statement of task

As explained above, despite the crucial role RES play in the transition of DHC networks, most thermal energy needs today are still, directly or indirectly, met by fossil fuel-based technology. This underscores the vast potential for improvement through the integration of the less deployed greener alternatives. In this context, DHC networks equipped with Power-to-Heat (PtH) or "electrification" technologies such as HPs and CCs stand out for their potential to significantly reduce carbon emissions and air pollution in cities linked to thermal energy provision, while at the same time increasing security of supply. Moreover, PtH technologies integrated into those systems, offer the opportunity to provide flexibilities for electric grids. Particularly, the exploitation of the shallow geothermal potential via PtH technologies and the combination with auxiliary thermal energy storages (TES) presents interesting opportunities. Nonetheless, despite their potential to enhance the overall performance of integrated energy

systems and environmental benefits, the incorporation of these technologies into DH and DC networks remains underutilised. [1, 2]

With DH and DC systems gaining traction in an increasing number of cities worldwide, the need for modernization to meet the demands of the future carbon-free integrated energy system is evident, which is why the following research question was formulated for this thesis:

What are the requirements of a systematic approach for the design and optimisation of DHC power plants, specifically exploiting geothermal potential, and what could it look like in particular, given that large data volumes are involved?

To answer this question, at first, the characteristics, functioning and historical development of district energy networks are discussed in Chapter 2. Subsequently, an overview of the global position of district energy systems, with focus on Europe, is given in Chapter 3. This is followed by three case studies of such networks in Chapter 4. As the focus of this thesis lies on the exploitation of the shallow geothermal potential via HPs, CCs and TESs, in Chapter 5 and 6 the functioning of these technologies as well as their role in DH and DC systems are described in detail. It should be mentioned that the technology behind compression HPs and CCs is basically the same with regard to their functionality, but in the scope of this thesis a distinction is made between these machines due to their different applications. Therefore, within the context of this work, HPs are always referred to when heating is provided, while the term CCs is used for the provision of cooling. In Chapter 7, which focuses on the practical aspect, a geothermal power plant supplying a hypothetical DHC network situated in Madrid, Spain, was designed and modelled using the simulation environment TRNSYS. Subsequently, a sensitivity analysis regarding the power plant's topology was conducted to optimise the system in terms of cost, emissions as well as heating and cooling coverage. The results of this analysis are discussed in Chapter 8. In Chapter 9, conclusions are drawn, and a future outlook is given, including recommendations for potential next steps, enhancements of the sensitivity analysis and promising areas for future research.

1.3 Methodology

In the following, the methodical procedure that was applied in the course of this work to accomplish what is outlined in Chapter 1.2 is described.

Initially, an extensive literature review was undertaken to gain insights into DH and DC systems as well as the various technologies and their operational mechanisms, potentially relevant to the task. Following this, an in-depth literature research was carried out focusing on

the specific technologies chosen for incorporation into the TRNSYS model which was used to simulate the thermodynamic behaviour of the system. In the resulting literature section, those technologies and their application in DH and DC systems are described in detail. TRNSYS is an extremely flexible graphically based software environment used to simulate the behaviour of transient systems. While the vast majority of simulations are focused on assessing the performance of thermal and electrical energy systems, TRNSYS can equally well be used to model other dynamic systems such as traffic flow or biological processes.

Once the power plant's topology consisting of reversible heat pumps (RHPs), borehole heat exchangers (BHX) and TESs was determined, a TRNSYS model and a calculation scheme consisting of key performance indicators (KPIs) were defined to quantify the optimisation target values and thus ensure comparability for the results of the sensitivity analysis. Target values were identified as the specific CO_2 emissions, the levelized cost of energy (LCOE) as well as the RHP coverage.

To limit the scope of the sensitivity analysis to a manageable number of combinations, the load profile of the hypothetical heating and cooling network was analysed to narrow down the range for the number of RHPs deployed in the power plant. For this purpose, a program was written in Python, which has been attached to this work in Appendix 2: load_data_analysis.py. This program accepts arbitrary load data in the form of .txt or .csv files as input, analyses them fully automatically, and outputs the results graphically.

The next step was the determination of the input data for the calculation scheme. On the one hand, through further literature research, input values such as specific capital expenditures (CAPEX) of the various technologies, electricity prices, gas prices, CO_2 certificate prices, emission factors, etc., were determined. On the other hand, the TRNSYS model was utilised to compute the thermodynamic quantities necessary for all cases analysed in the course of the sensitivity analysis.

Following this, a second Python program, which has been attached as Appendix 3: result_analysis.py, was written to execute the sensitivity analysis. This program automatically imports all the data generated in TRNSYS, calculates the calculation scheme's KPIs, and graphically displays the outcomes. Finally, the generated results were compared, interpreted and checked for plausibility.

Furthermore, it must be mentioned that AI-based tools such as ChatGPT and DeepL were used to support the writing of this thesis. Table 1 provides insight into their application in the course of this work and the extent of the AI-generated output's share in the overall result. Additionally, a document with representative examples of the applied prompts was created,

which is available on request at the Chair of Thermal Processing Technology at the Montanuniversität Leoben. It should be explicitly mentioned that the content of this thesis was not generated with these tools, as they were merely used to reproduce the content in another language and to enhance the code. During the literature research, these tools were used to assist in finding relevant literature, while the extraction of the relevant information was carried out independently.

Table 1: Declaration of AI-based tools

Application	*AI contribution*	*Tool*	*Document*
Translation	40 %	*DeepL* *ChatGPT-4*	*Available on request at the Chair of Thermal Processing Technology at Montanuniversität Leoben at the following email address:* *tpt@uniloben.ac.at*
Improvement of linguistic correctness	40 %	*ChatGPT-4*	
Rephrasing	30 %	*DeepL* *ChatGPT-4*	
Code generation	20 %	*ChatGPT-4*	
Literature research	5 %	*ChatGPT-4*	

2 Fundamentals of district energy networks

The following chapter provides an overview of the characteristics and basic mode of operation of DH and DC systems. This is done first using DH systems as an example, and then DC systems are introduced on the basis of this knowledge. In addition to that, possible load management measures for DH and DC networks as well as their importance are described. Furthermore, the historical development of these systems is outlined.

2.1 Characteristics and basic topology of district energy networks

DH and DC systems are centralised systems that provide heating and cooling energy for multiple buildings, also called thermal loads. These systems are designed to deliver thermal energy in a more cost-effective, efficient, and environmentally friendly manner than if each of these thermal loads were heated or cooled individually. In addition to the advantages of the economy of scale, the independence of a single heat/cold source in modern DH and DC systems increases the security of supply. Further benefits are less climate-damaging refrigerant utilization and leakage in HPs and CCs due to fewer decentralised units, more flexibility and efficiency in the overall energy system through possibilities in sector coupling and reduced fuel consumption as well as emissions due to the improved efficiency. [1, 3–5]

The basic components of these systems are a central plant where the heat or cold is generated, a network of pipes through which the thermal energy is distributed, heat exchangers (HXs), also called substations, to transfer heat from the primary network circuit into the secondary one, pumps, control and measurement systems as well as the thermal loads. These loads could be single or multifamily dwellings, large commercial and institutional

buildings, industrial facilities, settlements, offices or hospitals. Figure 1 illustrates a traditional DH system with a substation showing the essential components. [3–5]
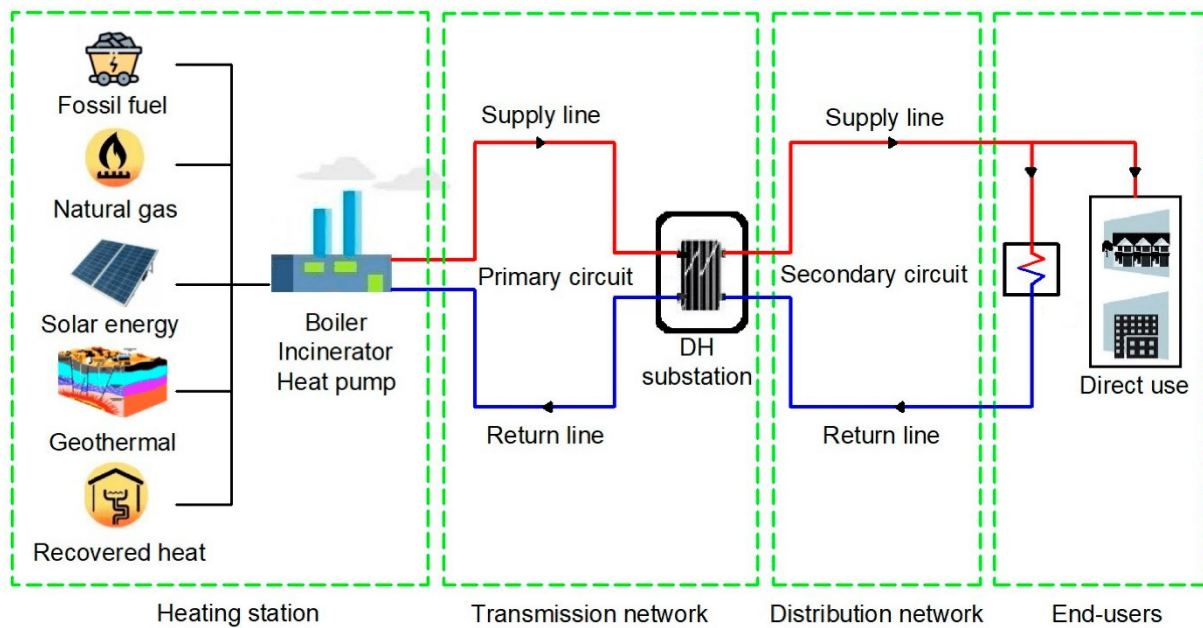
Figure 1: Essential components of a traditional DH system with substation [6]

2.1.1 Heat sources in district heating networks

Modern DH systems can provide energy for entire cities as well as smaller communities. As already mentioned, one of the most important characteristics of these systems is the use of an energy source that offers a significant cost difference compared to heat generated by other means, such as boilers or direct electric heating. This cost difference finances the high upfront costs of the necessary infrastructure. Especially in systems built in the past, the heat used was usually a by-product of electricity generation. Therefore, a typical heat source for city-wide systems is steam extraction from major combined heat and power (CHP) stations. For this purpose, steam can be extracted at multiple points within power plants, which then allows the DH water to be heated up by HXs connected in series. Furthermore, this approach enables a reduction in flow temperature at times of part load, thus achieving better efficiency. Other typical sources for large systems are excess heat from waste incineration plants and industrial processes. For smaller communities, small-scale CHP plants, biomass-fired boilers or waste heat from local industry can be used as heat sources. In each case, TESs are typically installed to increase the flexibility of the system. This flexibility offered by TESs enables the efficient integration of other technologies that are drawing increasingly more attention. One of them, solar thermal energy, has already been deployed on a large-scale as an extension of some networks. This combination is of particular interest as it allows the cheap, renewable surplus

heat generated in summer to be stored until winter. Furthermore, with the increasing decarbonization of the energy system, the use of large-scale HPs to exploit shallow geothermal potentials is on the rise and will continue to grow in the future. Due to the ever-increasing number of HPs, heat can be generated at little cost when electricity prices are low and stored in TESs, which in the future will not only depend on demand but also on the amount of renewable generation from solar and wind. Therefore, in times of low electricity demand and high renewable generation, it will be beneficial for the overall system to have HPs convert surplus electricity efficiently into heat. Furthermore, through sector coupling like this, particularly when used in conjunction with TESs, flexibility can be provided for electrical grids as they allow to decouple the DH network's electricity demand from its heat demand. In certain places of the earth, it is also possible to use deep geothermal potentials as a heat source for the network. Moreover, in integrated future energy systems, fuel cells operating as CHP plants could supply smaller networks and recovering heat losses from electrolysis processes for hydrogen production can increase overall system efficiency. [1, 4, 6]

2.1.2 Thermal energy transport in district heating networks

Generally, liquid water or steam is used for the thermal energy transport in DH networks. In addition to the advantages such as easy availability, low cost, non-toxicity and simple disposal, water has a high thermal conductivity and heat capacity. The energy, in form of high temperature heat, is then transported through large underground pipelines by pumps. The carrier pipes can be made of steel, polybutylene or polyethylene. Typically, pre-insulated pipe systems are used, in which the carrier pipe is enclosed in polyurethane foam insulation, with an outer casing for mechanical protection against damage and groundwater penetration. Control valves and heat meters ensure regulation of the mass flow rate, safe operation, and the measurement of the supplied heat. Next to the location of the load, the heat is typically transferred to a lower network level by means of HXs, also referred to as substations, although this is not necessarily the case. In this context, a basic distinction can be made between transmission networks and distribution networks. HXs installed at the customer's site separate the general network from the local customer circuit. Topologies like this offer the advantage of decoupling the pressure and temperature of the different network levels. After passing the substation, the fluid in the transmission network has cooled down and is pumped back to the heat source, where the water is heated up again to restart the cycle. The heat transferred into the distribution network is then conveyed further to the load. The final purpose at the end-user can be for instance space heating (SH), preparation of domestic hot water (DHW) or process heating (PH) services. In today's DH networks typical yearly average supply temperature levels

lie between 75 and $90\,°C$ and annual average return temperatures between 40 and $50\,°C$. After the heat has been extracted from the distribution network by the consumer, the water is pumped back to the substation. The transferred heat $\dot{Q}$ in W can be calculated according to formula (2-1) where $\dot{m}$ is the mass flow in kg/s, c_p is the specific heat capacity at constant pressure in $J/(kg\,K)$, and T_{inlet} as well as T_{outlet} are the inlet and outlet water temperatures in K. [4, 6, 7]

$$\dot{Q} = \dot{m} * c_p * (T_{inlet} - T_{outlet}) \tag{2-1}$$

When DH demand increases, DH providers typically increase the supply temperature. However, this change in the network propagates relatively slowly. If the change in supply temperature is not sufficient to cover the demand, the mass flow through the pipes is increased, allowing the power to be delivered to the consumer much faster. Yet, this can lead to higher pumping costs, higher return temperatures and consequently higher network losses as well as lower DH production plant efficiencies. Another problem is that due to the increased mass flow and the associated higher flow velocities, higher pressure drops occur. This can lead to insufficient differential pressure in the DH area attached to the transmission pipe, which in turn leads to insufficient delivery of the heat demanded by the customer. The latter problem can also occur when the network is expanded. This undesirable situation can be prevented if the DH providers increase the supply temperature in advance. However, this requires reliable short-term load forecasts, which is why it is important to understand the individual consumer behaviour well. [5]

2.1.3 District cooling networks

DC networks are typically smaller than DH networks and supply service and industrial sectors. As well as for DH systems the main advantage of these networks is the economic gain they can achieve in comparison to individual cooling solutions. The thermal energy distribution in DC systems follows the same principles as for DH systems, except that instead of high temperature heat, low temperature heat is provided. Similar to DH, a DC network consist of three main components: A chilled water generation facility (central plant), a piping system (network) and customer-building interconnections (HXs also called substations). Supply temperatures usually range from 4 to $8\,°C$, while return temperatures lie between 13 and $16\,°C$. Depending on economic factors, the piping systems can be either insulated or left uninsulated. If uninsulated, corrosion protections for piping materials are required. The principal equipment, including different chiller technologies, pumps, chemical treatment systems, controls, and heat dissipation equipment, is located in the central plant. [4, 6, 8, 9]

Water chillers are classified as either mechanical vapor CCs or thermochemical chillers also called absorption heat pumps (AHPs). Other ways to provide low temperature heat to the network are natural cooling, where cold water from lakes, rivers or the sea is used to supply cooling energy or the integration of excess cold streams into the network. Furthermore, DC systems can be used in combination with CHP as AHPs offer the possibility to use the waste heat of the combustion process as prime driver for the chillers during the cooling season, thus increasing CHP efficiency as excess heat does not have to be discarded. Moreover, in combination with DH, it is possible to generate a useful heating and a useful cooling affect simultaneously with the same HP/CC. The absorbed heat at the loads location (or "transferred cold") $\dot{Q}$ in W can be calculated according to formula (2-2) where $\dot{m}$ is the mass flow in kg/s, c_p is the specific heat capacity at constant pressure in $J/(kg\ K)$, and T_{inlet} as well as T_{outlet} are the inlet and outlet water temperatures in K. [4, 6, 8, 9]

$$\dot{Q} = \dot{m} * c_p * (T_{outlet} - T_{inlet}) \tag{2-2}$$

2.1.4 Measures for dealing with load variations

An aggregated load profile in a DH system consists of many different loads such as loads related to SH, DHW preparation, DH-driven absorption cooling or heat for industrial processes and exhibits different types of variations, namely seasonal (consequences of variations in outdoor temperature), daily (mostly due to customer behaviour), and weather-related ones. As a result, the demand has a highly varying character. The same principles also apply to DC networks. [5, 10, 11]

Depending on the climatic conditions of the region, different load profiles for heating and cooling result throughout the year. Figure 2 shows a possible annual heating and cooling load profile for a hypothetical DHC network. In this scenario, the highest load peaks occur in the winter months for heating purposes. With the arrival of summer, the heating demand decreases strongly and gets finally completely replaced by cooling demand. In the transitional period, an overlap between heating and cooling demand can be observed. Furthermore, two characteristic patterns of DHC load profiles can be identified. On one hand, the high volatility of DHC demand is evident, while on the other it is noticeable that for most hours of the year relatively little power is required compared to the peak demand periods. [5, 10–12]
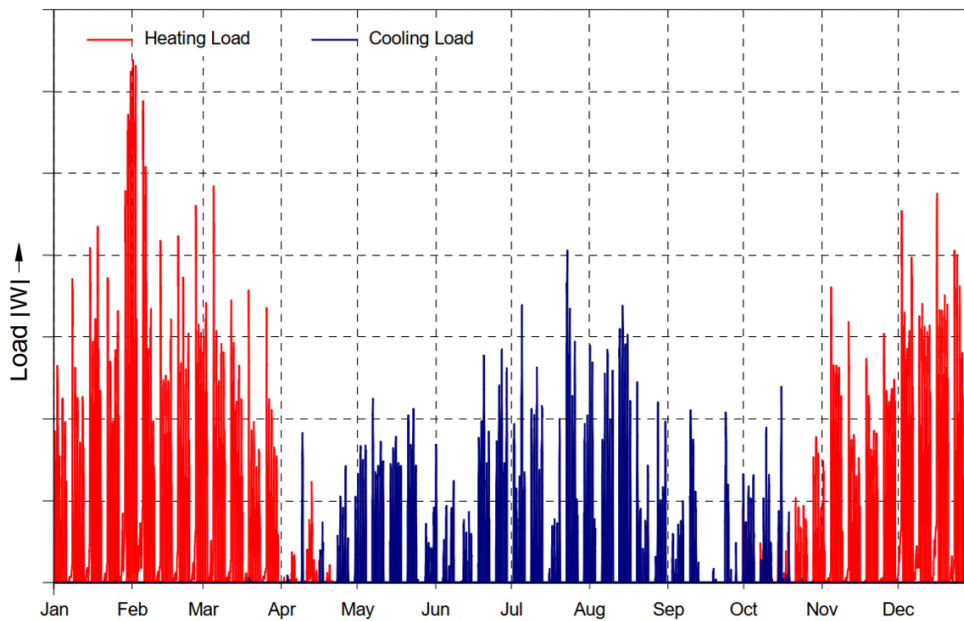
Figure 2: Heating and cooling load profile for a hypothetical DHC network [10]

Another way of displaying this data is the so-called annual load duration curve. This curve shows the amount of thermal energy required from the heating and load in a cumulative manner for each hour of the year. The x-axis represents the hours of the year, while the y-axis shows the power, arranged starting from the highest peak of demand down to the lowest. Figure 3 shows the annual load duration curve for the heat and cold load profile shown in Figure 2. This form of representation clearly shows that peak loads are present only for a very few hours throughout the year. [10]
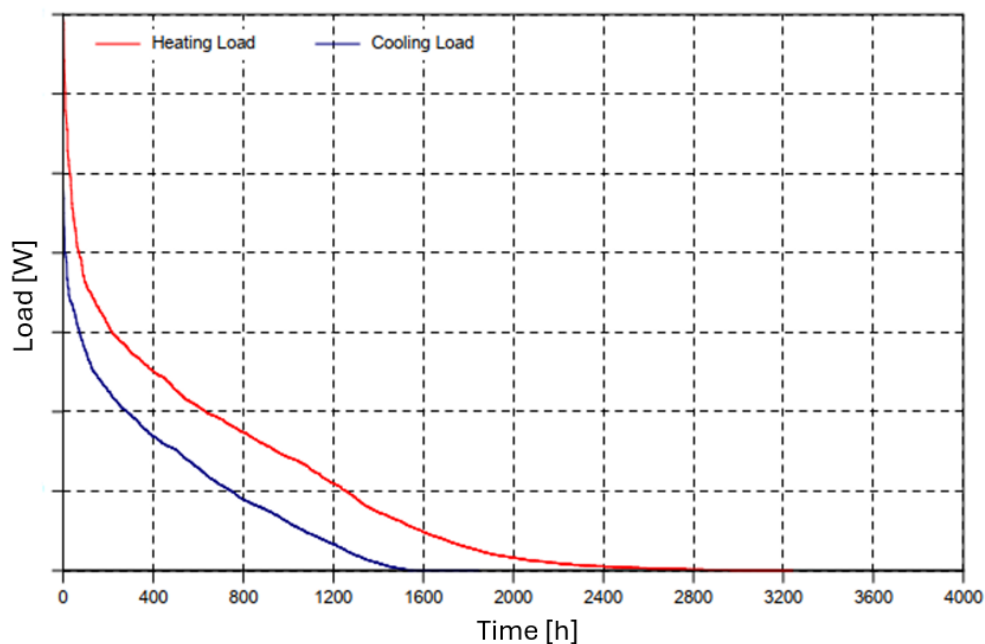
Figure 3: Annual load duration curve [10]

If typical base load plants which are characterized by high investment but low operational cost, would be dimensioned to cover these peak demands, this would result in energy generation that exceeds the network demand on a regular basis or low-capacity utilization and full load hours, i.e., in a low degree to which the installed capacity is actually exploited. As central low-cost generating units such as CHP plants or large-scale HPs and CCs should be operated with as many full load hours per year as possible, it is not economical to deploy them for peak load coverage. Thus, they are generally not designed to cover the peak loads of the network and will typically supply 60 to 80 % of the annual demand. This may correspond to an installed capacity of only about 30 to 60 % of the highest load peak. To cover the remaining peak loads, so-called backup units are integrated into the networks. In DH these backup units are usually fossil fuel fired and characterized by low investment cost and flexible adjustment, but high operational cost. Thus, peak demands in DH systems today are not only associated with higher cost, but also with increased greenhouse gas emissions. These backup units are often deployed decentralised in the network to provide additional security of supply rather than at the location of the primary heat source. Figure 4 illustrates this division into peak and baseload generation units. [4–6, 8, 10, 11]
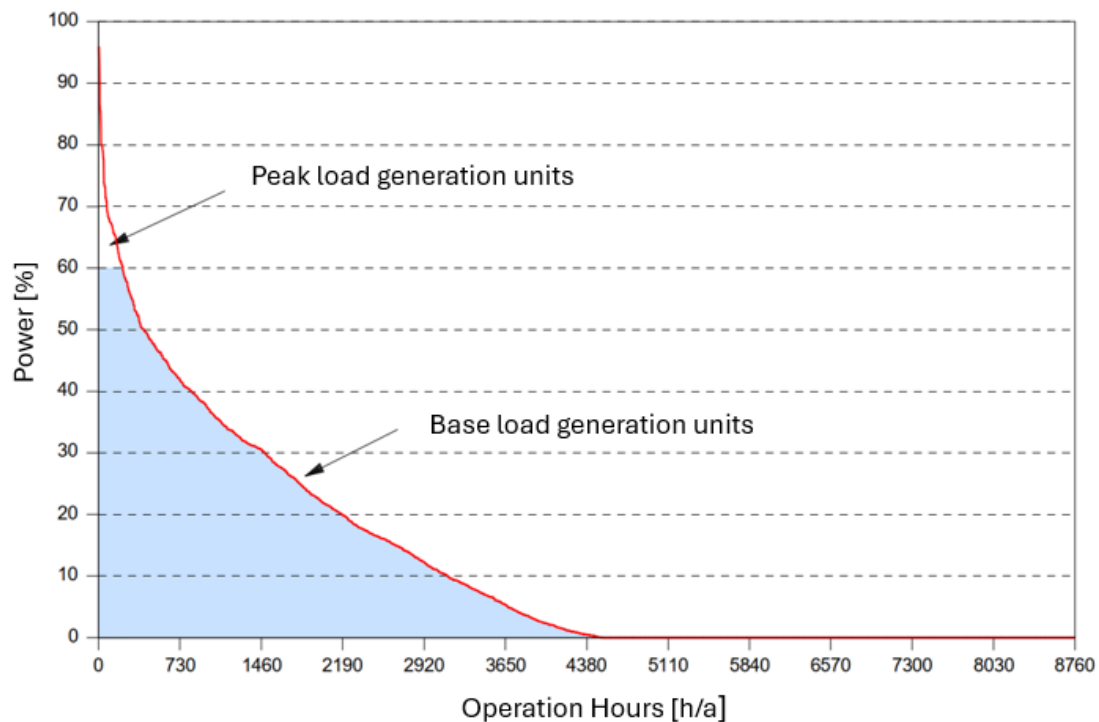
Figure 4: Division into peak and baseload generation units [10]

The duration curve shows that sizing a generation unit to 60 % of the highest peak demand results in a reduction of less than 10 % in the total annual energy supplied. In conventional DH systems, the base load is typically provided by CHP plants, while the peak load is covered by

fossil fuel fired heat only boilers and TESs. In DC systems central base load CCs can be supplemented with TESs as well. However, there are other possibilities to deal with peak loads, so that modern DH and DC load management can be divided into three main categories: [4–6, 8, 10, 11, 13]

1. **TESs:** TESs can be used for peak load coverage and load shifting in DH and DC networks, hence enabling a flexible load profile of the system. In DH systems daily load peaks typically occur in the morning and evening hours due to hot tap water use. To even out these daily variations, small, decentralised short-term TES units located close to individual dwellings (e.g. small buffer tanks) or in the individual dwellings (e.g. floor thermal storage systems) are usually sufficient. However, it is also possible to install centralised short-term TES units to supply aggregated loads. Therefore, short-term TESs can decrease generation cost and greenhouse gas emissions across the entire system, as they can be charged up with cheap heat from baseload units during periods of low demand to use it later for peak load coverage. In order to compensate seasonal fluctuations, long-term TESs are necessary. Just as centralised short-term TES, long-term TES can increase capacity utilization and full load hours of base load plants as heat for peak load coverage can be provided at times of low demand, which in turn results in reduced cost and emissions. Additionally, they allow exploiting solar collectors in combination with DH systems at their best, making it possible to harness cheap heat in summer for peak load coverage in winter. Thus, TESs allow for covering peak loads while at the same time increasing the economical as well as the ecological performance of the system. Furthermore, they serve as the gateway for enabling sector coupling between electrical grids and DHC systems supplied by PtH technologies like HPs and CCs. In this context, thermal energy for peak load coverage can be provided when electricity prices are low. [5, 10, 11, 13]

2. **Complementing DH production:** In today's DH networks centralised peak load boilers are used to complement DH base load generation systems. Furthermore, decentralised boilers and HPs, which can be connected to both the primary and the secondary network circuit, are options for dealing with peak loads. Whether coal, gas or oil is used as a fuel for the boilers differs from country to country and is primarily dependent on the fuel market conditions. Besides fossil fuel boilers, there are also electric and biomass fired variants. These units are usually characterized by low investment cost and flexible power output, but by high operational cost. From an economic point of view, depending on the price of electricity, HPs could compete with boilers, especially when combined with TESs. The economic and energy benefits of using distributed HPs to adjust temperature in secondary networks are even higher when the base load generation plants include

CHP with a flue gas heat recover system. This is due to the fact that by using distributed HPs, the return water temperatures would be lower, which in turn would not only reduce network losses but also increase the amount of recoverable heat from turbine exhaust steam and flue gases. Thus, the use of HPs could offer not only energetic and economic benefits, but also ecological ones. Another possible technology to complement DH production is fuel cell CHP. Just like HPs or electric boilers, in combinations with TESs, these could be used for sector coupling in DH networks. In the case of too much heat in the network, it can be dissipated using cooling towers, whereas in this case it is more sensible to install TESs or power AHPs to generate cold. In DC systems decentralised peak load CCs can be used to cover peak demands. [5, 10, 11, 14–17]

Other technologies that have drawn more and more attention in recent years are hydrogen boilers and hydrogen-natural gas blend boilers. In principle, they work like natural gas boilers, but adapted to the reactive nature and flame speed of hydrogen and up to a certain degree such boilers could use existing infrastructure. However, one problem with hydrogen is the significant supply chain energy loss especially in hydrogen production, which is why the logical use of hydrogen in a future decarbonised energy system will be in hard to electrify sectors, such as industrial processes that require high temperatures. [16, 18, 19]

3. **Demand side management measures:** Other measures that have recently gained interest are summarized under the term demand side management (DSM). DSM measures try to cause desirable changes in the DH/DC load profile in order to optimise the overall system. Measures such as strategic demand increase include, e.g., valley filling, which implies finding ways for increasing the DH demand during periods with low demand. The goal here is to increase capacity utilization and full load hours of base load generation units. An interesting approach for valley filling is to provide heating for cooling. A well-known strategy to achieve this is the integration of DH-driven AHPs since the cooling demand reaches its maximum in summer while the heating demand is at its lowest. Another DMS measure is demand response which is applied to the existing demand. Demand response strategies, such as load shifting, rely on demand-side flexibilities and require advanced monitoring, control and communication systems between DH/DC providers and customers. For more information regarding DMS, please refer to the literature. [5, 11]

2.2 Historical development of district energy networks

Since the introduction of district energy systems, they have been continuously improved and have spread all over the world. This development can be classified into five different generations. The evolution shows a trend from networks fed by centralised fossil fuel fired heat sources with poor systemic efficiency and high temperatures towards a smart and efficient thermal grid with low operating temperature composed of many different decentralised RESs where thermal energy can be exchanged throughout the whole district or network. Distinctions can be made mainly in terms of efficiency, fluid temperatures, the heat transport media used, thermal application, network size, installed components and energy sources. Figure 5 shows the development of DH networks from the first to the fifth generation over the last 150 years. [2, 20–22]
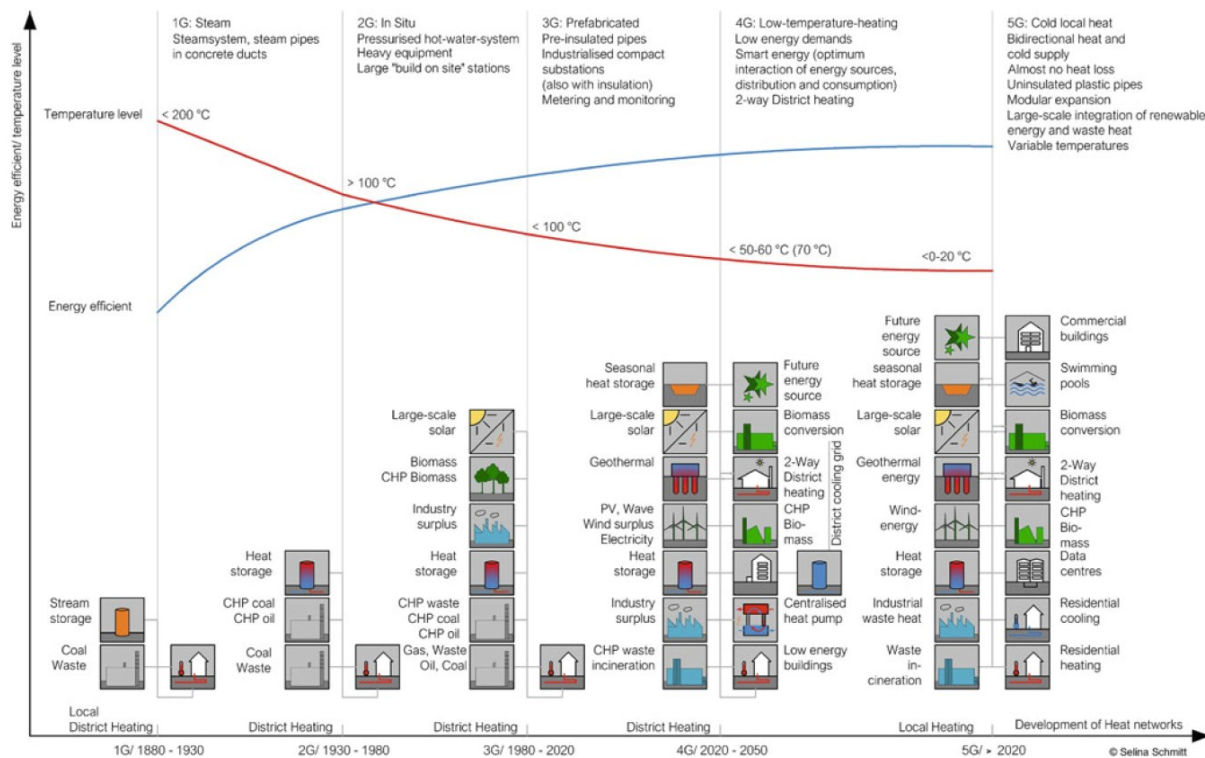
Figure 5: Development of DH networks over the last 150 years [21]

Most of the DH and DC systems existing in cities today can be categorized as belonging to the first three generations and need to be modernised in order to meet the standards of the fourth and fifth generation. Driver for these future generations is the cross-sector integration of DH, DC, electrical networks, and gas grids in order to exploit synergies and make the overall energy system more efficient and flexible. This integration will allow for the intelligent incorporation of variable RES into the networks, therefore facilitating the transition to the

carbon-neutral energy system of the future. The five generations of DH and DC networks as well as their historical development over the past one and a half centuries are described below, with focus on the fourth and fifth generation, as these point the way into the future. [2, 20, 21, 23, 24]

First generation DH systems were introduced in the 1880s in the USA and used pressurised steam at temperatures of 120 to 200 °C as the heat carrier which was typically generated by the combustion of coal. Typical components were non-insulated steel pipes in concrete ducts, steam traps and compensators. However, these systems have issues with high energy losses and safety concerns due to steam explosions and are considered today as an outdated technology. DC systems were introduced in the late 19th century and consisted of centralised condensers combined with decentralised or centralised evaporators. As distribution fluid refrigerants or brine were used. [2, 6, 20, 21, 23, 25]

Second generation DH systems emerged in the 1930s, utilizing pressurized superheated water with supply temperatures of over 100 °C as the heat carrier. These networks aimed for better efficiency and more flexibility by utilizing coal and oil-fired CHP generation, in situ insulated steel pipes and TES systems. Water pipes in concrete ducts, large shell-and-tube HXs as well as material-intensive, large and heavy valves are typical features, which are still common in existing systems. The second generation of DC was introduced in the 1960s and used large CCs for centralised cold generation and replaced refrigerants and brine with water as the cold distribution fluid. [2, 6, 20, 21, 23, 25]

Third generation DH systems were introduced around the 1980s, using hot water with lower supply temperatures of around 70 to 100 °C. This generation focused on energy efficiency mainly related to improved CHP generation as well as the use of better construction material and techniques such as prefabricated, pre-insulated pipes directly buried into the ground, insulated compact substations with plate stainless steel HXs and material lean components. In addition, metering and monitoring systems as well as other heat sources such as large-scale solar plants, biomass CHP, heat from waste incineration or surplus heat from industrial processes were integrated into the systems. Due to the lower temperature levels, better materials, and construction techniques, the efficiency could be increased significantly. Main drivers for the development were security of supply in relation to the two oil crises and replacing oil with various local and/or cheaper fuels such as coal, biomass or industrial waste heat. Third generation DC systems appeared in the 1990s and are characterized by a more diversified cold supply using excess cold streams and natural cooling from lakes in addition to CCs. Other features include heat recovery from cooling operations and cold storages. Chilled water is used as the distribution medium. [2, 6, 20, 21, 23, 25]

Fourth generation DH systems are comprehensive technological and institutional frameworks. Efforts have been made to reduce the operating temperatures as much as possible, resulting in supply temperatures as close as possible to the level of the end user's demand of about 30 to $70\,°C$. In addition to the significantly improved efficiency, the lower temperatures also allow for the integration of heat sources at lower temperature levels. They aim to support sustainable development by integrating thermal grids into the overall energy systems (i.e. integrated electricity, gas, and thermal grids), thereby enabling the incorporation of a high share of variable RES such as wind, solar, and shallow geothermal energy. Within those systems, heat is efficiently supplied to low-energy buildings with minimal grid losses. This concept also encompasses the establishment of an institutional and organizational structure that promotes appropriate cost structures and motivations, thus facilitating the transition to the carbon-neutral energy system of the future. Similar to fourth generation DH networks, fourth generation DC networks work in collaboration with other energy sectors and provide a high degree of flexibility. The primary motivation of these systems is the cross-sectoral integration of energy systems and the exploitation of synergies between cooling, heating, and electricity grids, thus facilitating the deployment of RES. These systems utilise both centralised and/or decentralised cold sources, such as electric CCs, AHPs, ambient sources, surplus cold flows as well as cold storage facilities, to meet the cooling needs of residential, commercial, and industrial sectors. Since DH and DC networks are interconnected from the fourth generation onwards, from this point on they can also be referred to as DHC networks. [2, 6, 20, 21, 23, 25]

Fifth generation stands for a DHC system that is non-linear, bi-directional, decentralised, and operates with fluid temperatures around the surrounding soil temperature of about 0 to $25\,°C$, also referred to as the ambient or free-floating temperature range. These networks could be considered as an extension of ground source heat pump (GSHP) systems at district scale. Due to the low operating temperature, small to medium sized distributed HPs and CCs are required at consumer sites. In the absence of a return flow, what is consumed as heat is essentially supplied back as cold, and vice versa. The aim is to close energy loops to the maximum extent possible by using warm flows returning from the cooling system and cold flows returning from the heating systems, while exploiting RES to fill the supply-demand gap. The system's architecture allows for a significant degree of flexibility, due to the integrated framework of heating, cooling, and electrical infrastructures. Geothermal energy storages, also called balancing units, act as an effective heat source or sink when heating and cooling loads are not compensated between buildings and/or do not take place simultaneously. Modularity allows for the addition of diverse consumer types and sources of heat and cold. Figure 6 illustrates a fifth generation DHC network. [6, 21, 22, 24]
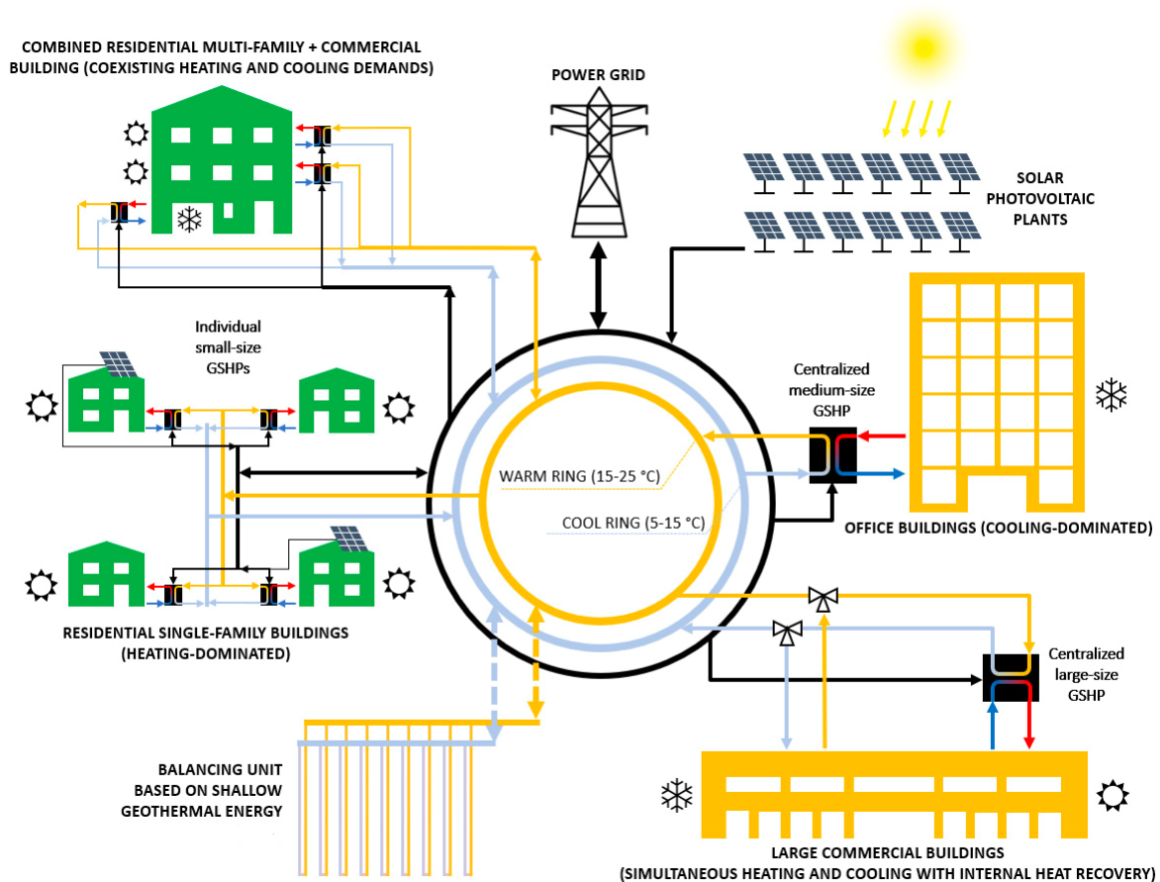
Figure 6: Illustration of a fifth generation DHC network [22]

It should be noted that there are many different definitions for fifth generation DHC systems in the current literature, as it is a relatively new development, which is why in the following the most important characteristics of such networks are described:

- **Low free-floating temperature:** For the operation of fifth generation networks, supply temperature setpoints are not useful anymore. Both the warm and cold pipelines have free-floating temperatures that can oscillate according to the admissible range of HP performance and the balancing unit. These temperatures are near ambient ground temperature, thereby minimizing network losses, insulation needs and related costs to almost zero. Since these temperatures are unsuitable for direct heating purposes, at the consumer's site the temperature is raised to the desired level with the aid of HPs and CCs. [21–24]

- **Non-linear, bi-directional, decentralised, and modular design:** Traditional DH and DC systems are designed in a linear fashion, where heat or cold is produced at a source and then conducted to consumers via pipes. These systems include a return water flow that has no energy value. In contrast, fifth generation DHC systems are set up in a

non-linear, bi-directional, and decentralised manner. Essentially, every energy consumer also acts as an energy supplier, also called "prosumer". Instead of featuring return flows, these systems utilise separate warm and cold water pipelines. Buildings are equipped with HPs and CCs connected to these two water lines. When heating is needed, the building draws from the warm water line, increases the temperature via a HP, and then discharges the chilled water into the cold line. Conversely, when cooling is required, the process is reversed and water is drawn from the cold line, passed through a CC, and then discharged into the warm line. Ideally, there should be an almost equal demand for both heating and cooling, in which case the system can be almost circular. Furthermore, the fifth generation DHC system is modular, allowing for the addition of various heat and cold sources as it expands. [22–24]

- **Closed loop nature and different loads:** A fifth generation DHC system is a closed loop system and supplies a diverse range of consumers, including households, industrial plants, and offices, each with unique load profiles. Rather than simply conveying heat or cold from a central source to the different loads, the warm and cold grid facilitate the exchange of residual heat or cold between connected buildings. Some of them are balanced over the year while others are heat or cold dominated. [24]

- **TESs:** Since there is no central heat source anymore TES facilities and balancing units serve as buffers to bridge temporal gaps between demand and supply, thus acting as subsidiary heat provider or consumer for the network. Incorporating both short-term and seasonal TESs is a crucial feature. Short-term storage allows for dealing with the problem of intermittency of RES, therefore closing the temporal gap between supply and demand of heat and cold loads. Seasonal storage enables surplus heat generated in the summer to meet part of the heating demand in winter. In particular, the exploitation of geothermal heat sources offers the possibility to tackle the seasonal storage problem, thus contributing to flexibility in the network. Furthermore, the use of sufficient storage capacity can considerably reduce the necessary power output of HPs and CCs, thus reducing investment cost. [23, 24]

- **Integration of RES**: In fifth generation DHC systems, electricity is inextricably linked to thermal energy generation, because using ambient-temperature water as heat source can only be an energy vector if combined with electrically driven HPs. Furthermore, just like the HPs, CCs also require electrical power for the provision of cooling, which is why renewable electricity generation is indispensable in designing and planning efficient fifth generation networks. During periods when renewable electricity is abundant, it powers transport pumps, HPs and CCs whereas in times of lower availability, the systems rely on buffers and building thermal mass. Therefore, the fifth generation of DHC offers a

way to integrate classical RES like solar and wind, alongside low temperature renewable heat sources such as geothermal energy, sewage and surface water as well as solar thermal and waste heat, which otherwise could not be utilised. [21, 22, 24]

Figure 7 shows an overview of an individual connection point in a fifth generation DHC network. Different temperature levels can be distinguished in the figure and each temperature level has its own dedicated device. If regular HPs are not able to reach sufficiently high temperatures, optional booster HPs for DHW preparation can be used. CCs are used for cooling provision. The temperature is adjusted as close as possible to the connection point. [24]
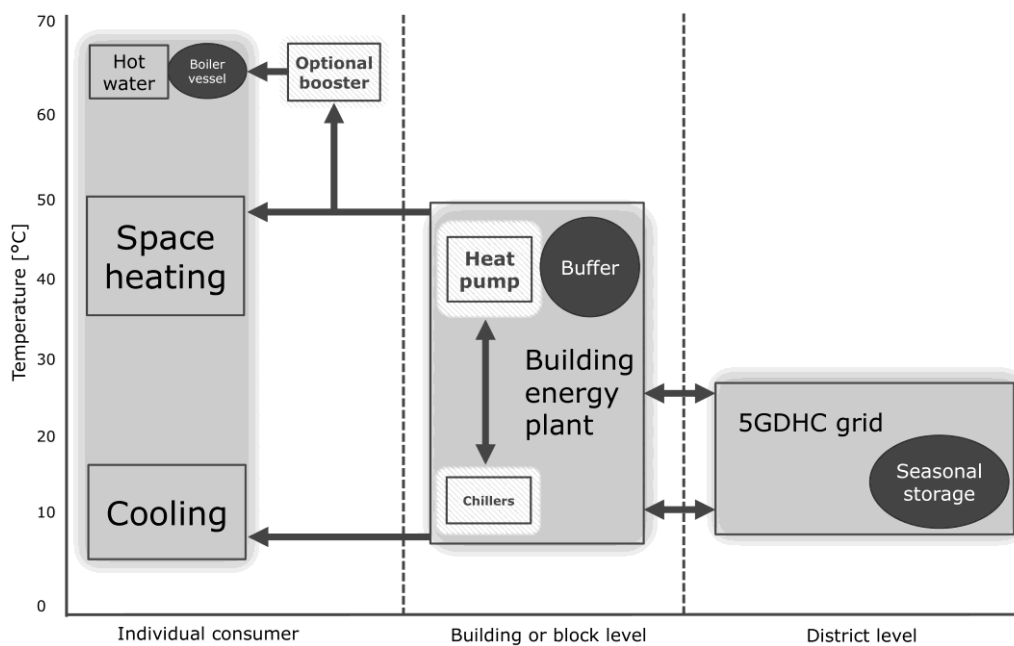
Figure 7: Individual connection point in a fifth generation DHC network [24]

3 Global position of district energy networks

In the following chapter a comprehensive overview of the global situation and deployment of DH and DC networks is given. Furthermore, the chapter details three concrete examples of such systems that have been successfully installed. It is important to note that established expertise in DH has paved the way for the introduction and deployment of DC networks. DC systems are therefore neither as common nor as extensive and, in comparison to DH, still in their early days. Therefore, relatively little has been published on the subject which is why the focus of this chapter lies on DH systems.

3.1 Global position of district energy networks

The subsequent section provides an overview of the global position of DH and DC systems in 2017, examining their status across five key areas: market trends, technical development, supply considerations, environmental impacts, and future outlooks. Furthermore, some deeper insights into European conditions are given.

3.1.1 Market context

Nowadays, major DH systems appear in cities as Moscow, St. Petersburg, Beijing, New York, Kiev, Seoul, Warsaw, Berlin, Hamburg, Helsinki, Stockholm, Copenhagen, Paris, Prague, Sofia, Bucharest, Vienna, and Milan. The total number of systems is estimated at 80,000, of which around 12,000 are located in Europe. Within the European sector, the total installed capacity is estimated to be around $300\,GW$. The main user categories of DH are

industry, the service sector and residential buildings. Nevertheless, when compared to other methods of heat provision, the average global and European utilization of DH is still relatively low. However, there are also high implementation rates of around and above 50 % in certain countries such as Iceland, Denmark, Sweden, Finland, Estonia, Latvia, Lithuania, Poland, Russia and northern China. Large DC systems can be found in cities such as Singapore, Tokyo, Stockholm, Paris, Dubai, Chicago, Toronto, Berlin, Helsinki, Barcelona, Vienna or Courbevoie outside Paris. There is no exact data on the total number of DC systems in the world, but around 150 European systems are in operation. In comparison to DH, the global volume of DC deliveries in 2017 was low and at an international level, the dominant user category is service sector buildings. Nevertheless, the absolute proportion of service sector buildings where cold is supplied via DC is still very small. [1, 26]

3.1.2 Technical context

The technical context is divided into three further sub-areas, namely supply, distribution and delivery methods:

1. **Supply methods:** Both globally and in Europe, the most common heat sources for DH networks are direct use of fossil fuels, direct use of RES (geothermal, biomass and waste), recovered heat from renewable CHP (waste and biomass), recovered heat from fossil CHP and industrial waste heat. Internationally, the deployment of CHP plants is the strongest argument for the introduction of DH networks, as they allow the unavoidable heat losses from thermal power plants to be used for heating purposes. The EU has a higher share of recycled heat (72 %) and heat from RES (27 %) compared to the rest of the world with a share of 56 % and 9 %, respectively. Therefore, at an international level the supply of heat through DH networks still relies to a large extent on the direct use of fossil fuels via large boilers. The low share of CHP plants (around 50 %) in both Russia and China makes a major contribution to this low global level of heat recovery. Short-term TESs are used in some networks to compensate for daily heat load fluctuations but virtually no seasonal TESs were installed until around 2017. However, since that time, relatively large, long-term TESs have been installed in connection with new solar DH networks in small Danish towns and villages. The supply of cold is managed by utilizing natural and excess cold resources through HXs, exploiting excess heat via AHPs as well as CCs with or without heat recovery and the deployment of cold storage systems. [26]

2. **Distribution methods:** Most first generation DH networks have been either retrofitted to water systems or decommissioned, as steam is today considered an inefficient heat

transfer medium due to losses and maintenance costs. Current DH networks use second or third generation technologies with a wide variation of temperature levels applied. However, the Manhattan system in New York and the central system in Paris continue to use steam as a heat transfer medium. These two networks are still viable as the population density is very high, resulting in relatively short piping systems and therefore a low proportion of distribution costs. The total length of DH pipelines is estimated at around $600,000\ km$ worldwide and around $200,000\ km$ in the EU. The different applied temperature levels, insulation qualities and network lengths lead to unavoidable distribution losses of between 5 and $35\ \%$. Most customers in Europe are connected to primary distribution networks via substations, which means all customers are supplied with heat at the same temperature level. Sometimes, however, secondary networks with lower distribution temperatures are connected to these primary networks. Overall control systems are based on four different and independent control systems. Flow controls and heat demand controls are located in customer's heating systems and in substations, while heat providers are responsible for the centralised differential pressure and supply temperature control. In DC instead of hot water, chilled water is pumped through the networks with a relatively small temperature difference between the cold supply and the warmer return temperature. Therefore, compared to DH grids, the distribution losses are relatively low. The control systems for DH and DC essentially function in the same way. In terms of infrastructure, no data was available for global trench lengths. However, the cooling networks in Europe represent $1,358\ km$ of pipes in 2021, with $70\ \%$ of the total based in Sweden, France and Finland. [1, 26]

3. **Delivery methods:** Substations supply heat to buildings for SH and DHW preparation with or without HXs. Generally, industrial facilities are connected to the networks in the same way although a special pipe connection can be used to achieve a different temperature level if the industrial customer is located close to the supply plant. Furthermore, in Russia, there are also some networks that use DH water directly to provide hot water to customers by blending it with cold water. The resulting water difference is then compensated for by a corresponding supply of additional water into the distribution network. In Europe, the use of heat meters to measure the amount of heat supplied to each customer is the best available technology. Nowadays, these provide automatic measurements that are transmitted by cable or wireless methods to the supplier for billing purposes. However, in Russia and China it is common to charge a fixed annual fee depending on the floor area used. A disadvantage of this method is that customers have no incentive to change their heat consumption behaviour. Cold deliveries are managed in the same way as heat deliveries but as the temperature

difference between the supply and return lines is smaller, HXs with longer thermal lengths are used. [26]

3.1.3 Supply context

Globally, the proportion of heat delivered through DH from fossil fuels remains significantly high at 90 %, and this figure is also substantial within the EU at 70 %. This is because fossil fuels are still the primary energy source for both CHP and boiler systems. In Russia, where natural gas is the main fuel, and in China, where coal is the main fuel, this is particularly pronounced. To reduce CO_2 emissions, new non-fossil heat sources like recovered heat from waste incineration and industrial processes, nuclear reactors with heat recovery, geothermal heat, large-solar collector fields or biofuels must replace the current fossil generation. Another interesting option is to recover excess heat from large electricity consumers such as big data centres that offer cloud services, where continuous power consumption can reach up to 100 MW. This type of heat recovery is already in operation in Stockholm and Helsinki, where several large HPs utilise heat from the cooling of data centres as source to supply DH systems. In addition, surplus electricity generated from volatile RES such as wind and solar can be used in DH systems through large electric boilers and HPs. These possibilities have already been explored in Denmark, Sweden, China, USA, and Russia. However, achieving this requires CHP plants to allow for a more flexible operation to compensate for the variable power generation and large TESs must be integrated into the networks. In DC systems, various cold resources such as CCs, AHPs TESs, natural cold and excess cold can be used for cooling supply. Traditionally, large mechanical CCs, with or without heat recovery, are deployed for centralised cooling in DC systems since larger units have better efficiencies than smaller individual ones. If the heat is recovered, it can be used in DH systems as a heat source for large HPs. In this scenario the CC supplies heat and cold to the two different networks at the same time. Furthermore, AHPs allow excess heat to be used for cooling purposes. This cold supply option can be found in Korea, Germany, Spain (Barcelona), Austria (Vienna), and Sweden (Göteborg and Linköping). Thus, both AHPs and CCs create valuable synergies between DH and DC. TESs are important for covering cooling peaks on hot summer days, as these days are characterised by large differences between daytime and nighttime cold loads. In countries with cold winters, natural cold reservoirs are available in the deep sea as well as in lakes and can be used during summer for DC. Examples of such systems can be found in Toronto, Geneva, Stockholm, Amsterdam, and at Cornell University. A major advantage of these systems is that there are no operational expenditures (OPEX) apart from pumping costs. If

industrial processes generate excess cold as a by-product, this can also be used for DC. Here, one example is the cold recovery from the liquefied natural gas (LNG) terminal in Barcelona. This system will be the first DC network at the global level to make use of surplus cold form an LNG terminal. This example shows the adaptability of DC local conditions and its ability to valorise energy streams that would otherwise be wasted. [1, 26]

3.1.4 Environmental context

Compared to conventional heating technologies, DH achieves significantly lower CO_2 emissions by replacing the traditional fossil primary energy supply with recovered heat that would otherwise have been wasted. Nevertheless, the global specific CO_2 emissions associated with DH have remained almost constant on a level of $198\ kg/MWh$ since 1990. This value is strongly influenced by the low share of CHP plants of around 50 % in both Russia and China. In particular, the expansion of coal-based DH in China has counteracted the decline in emissions in other countries in recent years. Furthermore, no plan exists in the Russian energy strategy to increase the share of CHP plants in the heat supply. In the EU, specific emissions have been reduced by 35 % since 1990 to a level of about $111{,}6\ kg/MWh$, which is 43,6 % lower than the specific emissions worldwide. This change is due to the higher proportion of CHP plants and RES in the European heat supply. The main conclusion that can be drawn here is that neither DH systems worldwide nor in the ones in the EU have yet taken full advantage of the opportunities to reduce CO_2 emissions. For the CO_2 emissions associated with DC no data was available. [26]

3.1.5 Future context

The future prospects for DH systems are likely to be promising, as they can offer greater security of supply, lower cost as well as lower CO_2 emissions compared to other alternatives. Nevertheless, international and European DH systems have not been significantly expanded in the last two decades, even though energy policy makers are looking for technologies with these favourable characteristics. The international DH sector has rather stable heat deliveries and therefore not the same expansion rate as the whole global energy system, which is why new methods need to be used to raise awareness of the potential of DH systems. A major challenge is that DH is strongly tied to local conditions such as urban demand and local heating and cooling resources. This is in stark contrast to the fossil fuel society, where generic solutions are applied throughout the entire world. Local conditions need to be aggregated and quantified at regional, national and international level as they are not known in current energy statistics,

which poses a great challenge. Furthermore, deployed DH technology must be enhanced as the current third generation networks are designed for fossil fuels and feature buildings with high heating demands. Therefore, fourth and fifth generation networks must integrate a high proportion of RES and buildings with low heating requirements. In the coming decades, new systems using advanced technology must be built and existing systems retrofitted. For DC systems around the world, the future prospects are also likely to be promising, as only a small proportion of current cooling needs is covered by DC. [26]

4 Case studies

In the subsequent chapter, the research outcomes for three instances of real DHC networks are given. The research included the examination of both the DH and DC networks in Vienna, as well as an investigation of a fifth generation district energy network that features a large-scale geothermal collector.

4.1 District heating network of Vienna

Until about the end of World War II, Vienna was heated primarily with wood and coal. After the war these energy carriers started to be replaced by cleaner, grid-based energy sources, i.e. gas, electricity and DH. In 2016, the situation was such that around $44\,\%$ of the heat demand was covered by DH, $46\,\%$ by natural gas, $4\,\%$ by electricity and the rest by solar energy, HPs, biomass or fuel oil. This transition was accompanied by a significant reduction in CO_2 emissions, primary energy consumption and air pollutant emissions like particulate matter, nitrogen oxides and sulphur oxides. [27]

The almost $1{,}300\ km$ long DH network in Vienna is one of the largest in Europe and is divided into a primary and secondary network. In the primary network (main pipelines) water with a temperature of up to $160\ °C$ and a maximal pressure of $22{,}5\ bar$ is transported through Vienna. Subsequently the heat gets transferred into the secondary network (local pipes) from where it reaches individual buildings for SH and DHW preparation purposes. Here the water has a temperature of $63\ °C$ to $95\ °C$ and a maximal pressure of $10\ bar$. In the return line the water has a temperature of about $60\ °C$. The network supplies around $430{,}000$ homes (more than a third of all households in Vienna) and around $7{,}700$ large customers. Figure 8 shows Vienna's

DH network in 2022. The red lines in the figure correspond to the primary network and the blue ones to the secondary network. [27–30]
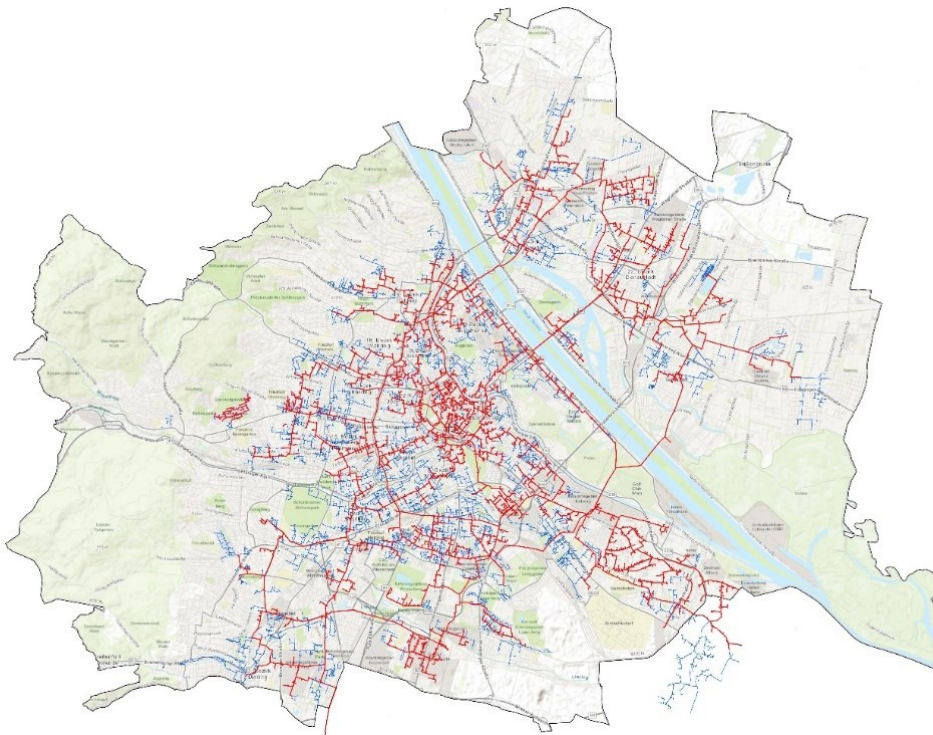
Figure 8: Primary (red) and secondary (blue) DH network of Vienna in 2022 [31]

In 2021 about one third of the thermal energy was provided by waste incineration plants and a biomass plant. The remaining two thirds came from CHP plants and industrial waste heat. To cover peak loads, gas boilers, electric boilers, a large TESs and HPs were used. Although HPs currently still play a subordinate role, a trend towards more deployment is observable. This is mainly due to the fact that the technology is developing rapidly, has low OPEX and can be used for cooling as well. [27]

In the climate-neutral scenario 2040, it is envisaged that heat generation through gas and heating oil in the building sector is to be completely replaced by DH and individual HPs. Thus, by 2040, more than half of the total low-temperature (less than $100\,°C$) heat demand in Vienna should be covered by DH while at the same time, the generation structure of the DH system is to be diversified and decarbonized. In 2019, Vienna had a DH demand of around $6{,}550\,TWh$, of which more than $50\,\%$ was covered by natural gas. The remaining portion was almost entirely provided by thermal waste treatment. Biomass, HPs and electrical heating played a negligible role. In 2040 the forecasted DH demand amounts to more than $7{,}550\,TWh$. Figure 9 shows the development of the DH demand and generation mix in Vienna in GWh per year. [27, 32, 33]
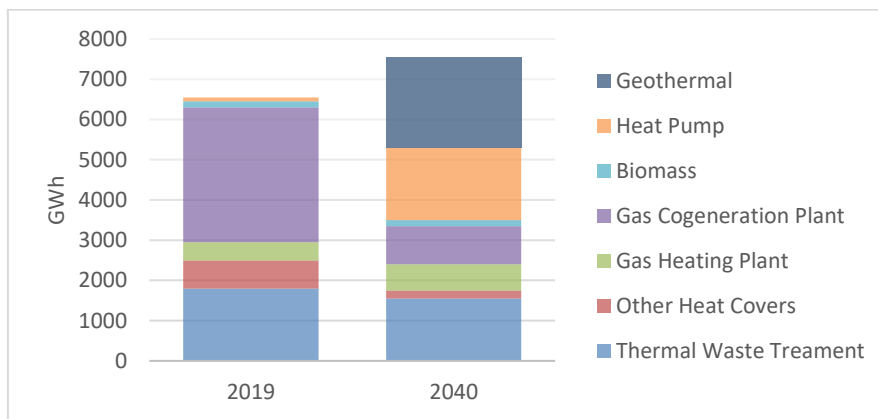
Figure 9: DH demand and generation mix Vienna (Climate Neutral 2040) [32]

More than 50 % of the demand is to be covered by deep geothermal energy, biomass and large HPs. Around 20 % should be generated via renewable gas and the rest mainly by thermal waste treatment plants equipped with carbon capture and storage facilities. In this scenario, the main baseload technologies will be thermal waste treatment plants and geothermal plants, as they can produce heat virtually all year round except for maintenance intervals in summer. HPs will also have a high-capacity utilization of around 6000 to 7000 full load hours. Investments in short-term as well as seasonal TES facilities are also under consideration when deriving the future asset portfolio, as they enable the withdrawal of heat from the network when generation exceeds consumption. Thus, the key technologies for the complete decarbonization of Vienna's DH systems are deep geothermal energy, HPs, TESs, CO_2 sequestration and the exclusive use of green gas. The latter in particular for peak load coverage in winter via CHP plants or heat only boilers. Figure 10 shows the annual load duration curve in GWh per day and the DH production mix of Vienna in 2040 for the climate neutral scenario. [27, 32]

Figure 10: Annual duration curve DH Vienna (Climate Neutral 2040) [32]

Furthermore, due to the strong deployment of large HPs and deep geothermal energy, the electricity demand for DH production will increase significantly from $50\,GWh$ in 2019 to $850\,GWh$ in 2040. However, due to the many full load hours of HPs and geothermal plants, electrical peak loads related to DH production, despite high annual quantities, remain moderate in comparison, reaching a maximum of about $140\,MW$ in 2040. [32]

4.2 District cooling network of Vienna

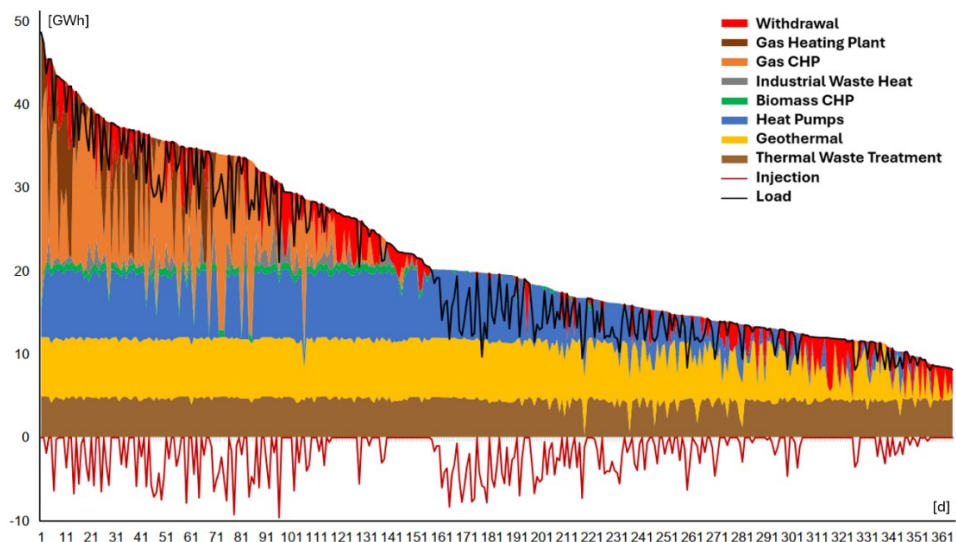Since 2007, in addition to the DH network, there is also a DC network in Vienna. The whole system consists of 7 DC centres connected to a common grid and another 14 decentralised cooling units. The cold is supplied into the system via CCs and AHPs. In the $24\,km$ network, water is pumped through insulated pipes to the cold load at 5 to $7\,°C$ and a maximum operating pressure of $16\,bar$. At the loads site, the water is then heated to about $16\,°C$ and recirculated to the cooling plant. Compared to conventional systems, this efficient form of cooling saves up to $70\,\%$ in energy consumption and around $50\,\%$ of the associated CO_2 emissions. A further advantage is that the use of climate-damaging refrigerants can be significantly reduced. In buildings connected to the DC grid, the water is used to operate loads such as chilled ceilings and fan coils to cool rooms, appliances and other devices. The cold is provided mainly for the service sector and less to residential buildings. Currently, around 180 buildings such as hospitals, train stations, museums, universities, office buildings or hotels are supplied with cooling energy through the network. For planned expansion projects, priority is given to areas with a high share of commercial activity, such as Vienna's city centre, as the density of cooling demand is highest there. [28, 30, 32, 34]

In contrast to DH, in DC in the climate-neutral scenario for 2040, not only does the amount of required electrical energy increase significantly, but also the electrical peak loads. In 2019, the annual demand for electricity used for cooling and air conditioning in Vienna was around $300\,GWh$, with power peaks of about $200\,MW$. In addition to the use of individual cooling units, part of the demand was already covered by the more efficient DC network. In the climate neutral scenario 2040, the electrical energy demand is forecasted to increase to $1050\,GWh$, with power peaks of around $900\,MW$. These high peak loads result from the weather dependency of air conditioning and the resulting strong concentration of demand on the summer months. [32]

4.3 Fifth generation district energy network

Fifth generation DHC systems are a rather new development in the field of DH and DC systems, which is why only a few of these systems have been built in Europe so far. In the existing ones, groundwater and shallow geothermal energy are used most often as heat sources. In the following, one of these networks, which was built in Bad Nauheim in Germany, is described in detail. [35]

The existing installation uses a double layer large-scale geothermal collector system with $11{,}000\ m^2$ of area per layer to extract heat from the ground. One of the layers is located at a depth of $1{,}5\ m$ and the other at a depth of $3\ m$. This geothermal collector is connected to a $12\ km$ long fifth generation DHC network through a $600\ m$ long feeding pipe which works as an extension of the collector and provides about $2{,}3\ GWh$ of source heat per year to more than 400 residential units. Three feeding pumps are installed to ensure a permanent fluid flow. At times of peak load two of these three pumps are operated at full capacity. The other pump is installed for redundancy to ensure security of supply and to keep wear as balanced as possible pumps are operated alternately. By means of approximately 180 decentralised HPs, the heat provided by the collector is harnessed and raised to the desired temperatures. Furthermore, due to the temperature levels in the soil around the collector system, cooling provision during the summer period is possible. Investigations have shown that, in the late winter months, the temperature in the soil between the two collector layers falls below the freezing point of water, which leads to significant icing around and between the collector pipes. The ice, which stores thermal energy at a low temperature level, remains in the ground until summer and can be used for cooling purposes. This type of operation is made possible by individual control of the two layers. From spring until the early summer months, mostly the upper layer is used to provide source heat since at this time of the year solar irradiation and precipitation will lead to rapid regeneration. During summer, mainly the lower layer is utilised to meet the buildings cooling demand, while the excess heat from the buildings is used to regenerate this layer. This process, in turn, allows for the storage of heat in the soil surrounding the lower layer, which can then be tapped again in winter. During this time, both layers are in operation. [21]

For one of the HPs installed, an analysis of the coefficient of performance (COP) and seasonal coefficient of performance (SCOP) over the course of one year was carried out. The exact definition and explanation of these quantities can be found in Chapter 5.2.1 but essentially, it is a measurement for the efficiency of the machine. During the monitoring period, the COP values varied between $2{,}8$ and $5{,}6$, and for the SCOP a value of $3{,}9$ was determined. Furthermore, the source temperature, which was measured directly at the HP, fluctuated

between $0{,}5$ and $15{,}3\,°C$. Another interesting observation was that the source temperature around the collector was lower than the source temperature measured directly at the HPs throughout the whole heating season. This shows the enormous potential of the network itself to act as a heat source. While the collector system was operating at temperatures of around $0\,°C$, the network was able to provide heat that was around $2\,K$ higher. This indicates that the further away the heat source is from the settlement and the lower the fluid temperature, the more energy can be generated by the network itself. As the higher temperatures allow the HPs to be operated more efficiently, this improves the efficiency of the whole system. [21]

5 Shallow geothermal energy for heating and cooling provision

In the following chapter, the fundamentals of the exploitation of the shallow geothermal potential in DHC systems are described as this is the basic energy source for heating and cooling provision in the TRNSYS model used in the course of this work. Subsequently, the functionality of compression HPs, CCs and RHPs is explained in detail as they are used to harness this potential. For the sake of completeness, the functionality of AHPs is explained as well, although they play a subordinate role in the context of this work since only compression machines are included in the TRNSYS model. Furthermore, it is discussed how HPs, CCs, RHPs and AHPs can be efficiently integrated into DHC systems.

5.1 Exploitation of the shallow geothermal potential

Geothermal energy is considered one of the most promising RES, along with solar, wind and tidal. Yet, one problem is that high enthalpy geothermal energy is only available in very few places on earth. However, low enthalpy geothermal energy at $100\,°C$ or less is much more widespread and if the temperature of these reservoirs can be kept constant, machines such as HPs can be operated efficiently. Unlike most other RES, geothermal energy is available around the clock, therefore making it baseload capable. Furthermore, as tapping the geothermal potential enables sustainable electrification of DHC systems, it makes geothermal energy an important pillar of the energy transition. [21]

Generally, the geothermal potential can be divided into three different types. Up to a depth of $10\,m$ and temperatures of around $10\,°C$ the term very shallow geothermal source is used. In a depth of 10 to $400\,m$, with temperatures around 10 to $20\,°C$, one speaks about shallow geothermal energy and everything below this depth is called a deep geothermal source. From this depth on temperature levels above $20\,°C$ are available. Figure 11 illustrates the subdivisions of the geothermal potential. [21]
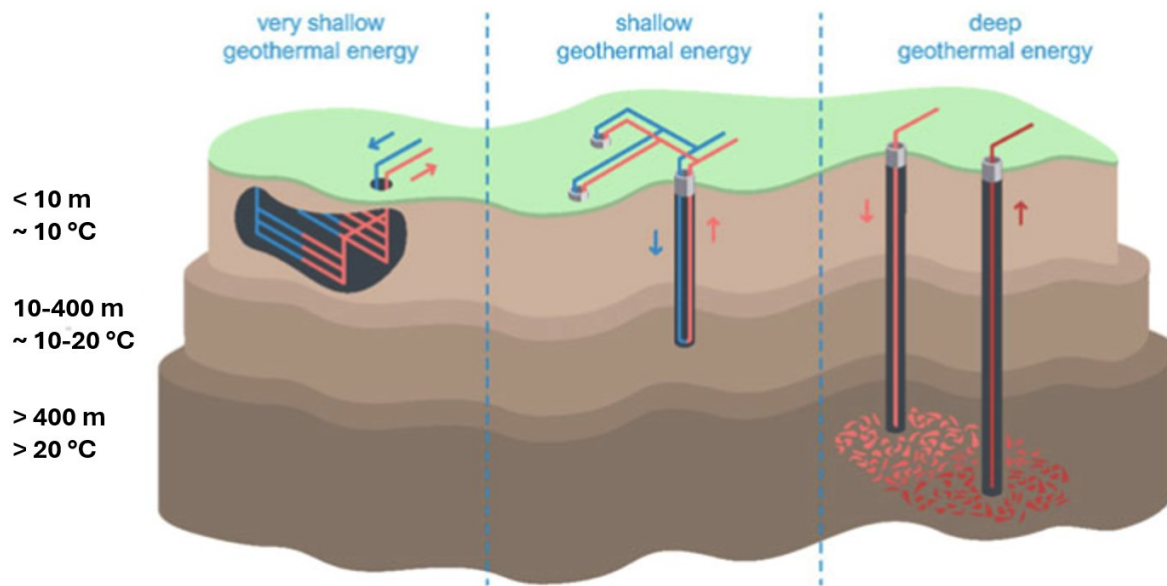
Figure 11: Subdivisions of the geothermal potential [21]

Within the context of fourth and fifth generation DHC systems very shallow and shallow geothermal sources seem to be a perfect fit, as they provide the low temperature levels required for GSHP operation. When aiming to tap into these potentials, the consideration of soil parameters plays a crucial role in allowing for efficient exploitation. The most important thermal properties of the soil are thermal conductivity, thermal diffusivity, and heat capacity, which are mainly influenced by parameters such as bulk density, water content and soil texture. In the case of very shallow geothermal energy, solar irradiation and precipitation as well have a crucial impact on the geothermal potential. [21]

GSHP systems primarily utilise two types of heat exchange methods: open loop and closed loop. Open loop systems involve extracting groundwater, whereas closed loop systems circulate fluid through either a vertical or horizontal circuit. Vertical systems are typically chosen when space is restricted. To implement them, drilling equipment is used to create narrow boreholes with depths of between 25 to $100\,m$. The pipes for fluid circulation are placed inside these BHXs. In combination with fifth generation DHC networks and GSHPs, such systems

offer the possibility to provide heat as well as cold, as they also act as a TES. Figure 12 illustrates a closed loop vertical BHX in winter and summer operation. [10, 21, 36]
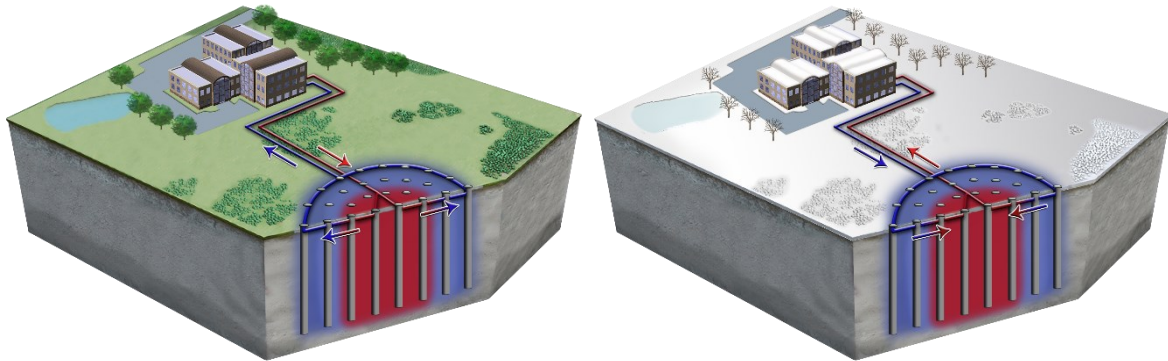
Figure 12: Closed loop vertical BHX in winter and summer operation [36]

In contrast, in horizontal systems the HXs are installed horizontally and at a shallow depth, therefore requiring larger areas, which limits the potential future use of the land on which the HXs are deployed. Another disadvantage of horizontal HX systems is their higher sensitivity to precipitation and changes in ambient temperature compared to vertical systems, which results from their proximity to the earth's surface. This sensitivity to changes may result in lower GSHP efficiencies. Nevertheless, the exploitation of the very shallow potential today is mainly achieved by horizontally installed ground HXs, as the installation costs and drilling technology requirements are considerably lower. Figure 13 illustrates a large-scale horizontal single layer geothermal collector system. [10, 21]
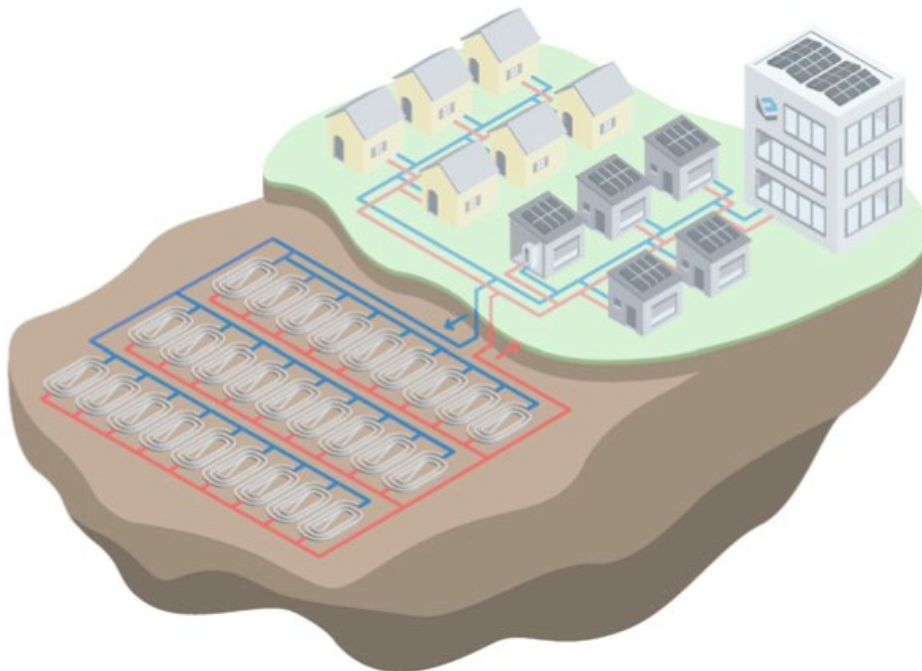
Figure 13: Large-scale single layer geothermal collector system [21]

By using dual or multi-layer collector installations, the specific heat extraction per square meter can be increased up to a point where local icing of the surrounding soil occurs. One the one hand, this so-called frozen soil storage acts as a heat source as it extracts environmental heat from the surrounding soil, solar irradiation, precipitation and groundwater flows. On the other hand, it can also act as a latent heat storage, allowing to store large amounts of low temperature heat with high energy density by freezing the ground. Figure 14 illustrates a large-scale multi-layer geothermal collector system with frozen soil storage. [21]
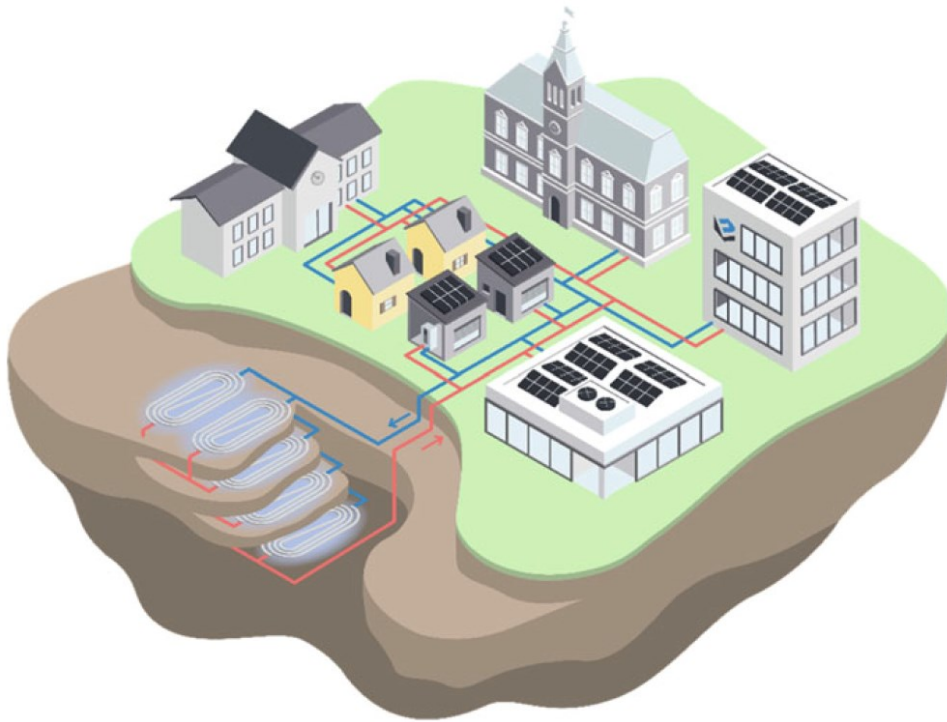
Figure 14: Multi-layer geothermal collector system with frozen soil storage [21]

During winter, heat is extracted from the reservoir by the collector system, which causes the surrounding soil to freeze. Through the fifth generation network the heat then reaches connected buildings where the temperature is raised to the desired level by means of decentralised GSHPs. In spring and summer, solar irradiation, precipitation and higher outside temperatures lead to a natural recovery of the upper layers. In contrast, the lower layers must be regenerated actively as the upper layer shields them from natural regeneration. To achieve this, the cold required in the buildings during summer is provided mainly by the lower layers of the storage without any significant energy input, which results in defrosting the ground. This defrosting, in turn, enables the seasonal storage of the excess heat transferred into the collector systems by providing cooling energy for the buildings. During fall, as the heating season begins, heat is extracted from the frozen soil storage and the cycle starts again. Figure 15 illustrates the different operation modes of a frozen soil storage. [21]
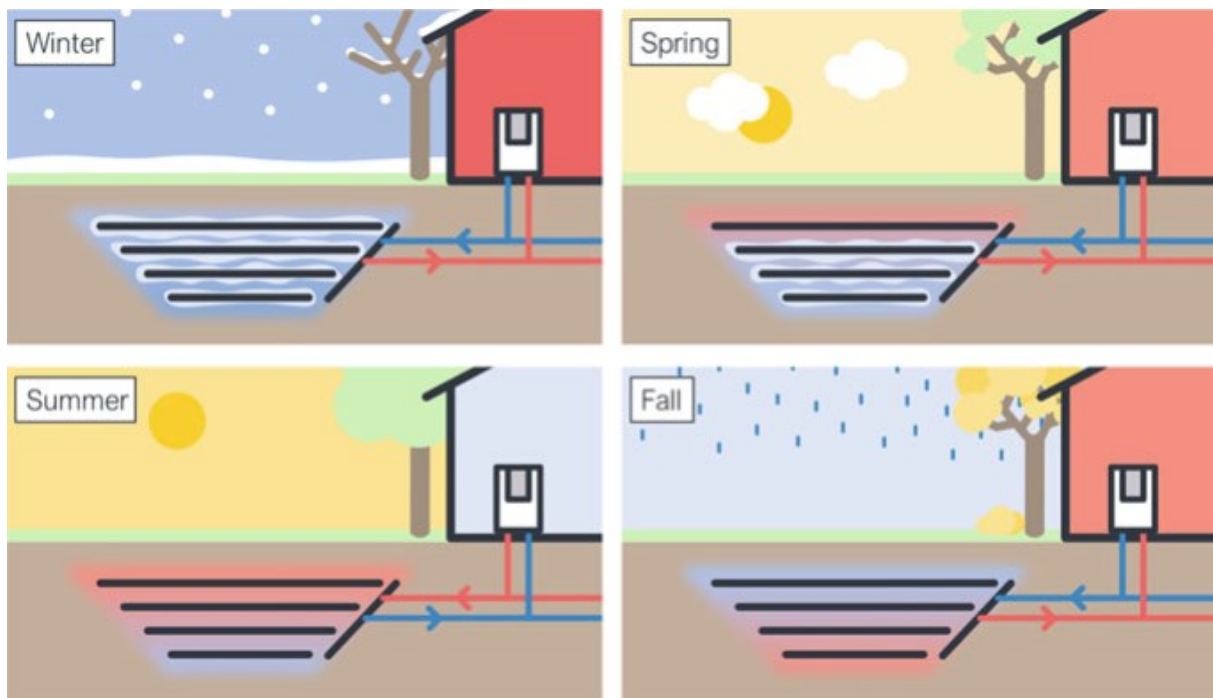
Figure 15: Operation modes of a multi-layer frozen soil storage [21]

Another noteworthy aspect of fifth generation DHC networks is that the network itself can act as an energy source, since the pipes essentially function as large horizontal HX. This implies that a portion of the low-temperature source heat can be provided by the network itself. However, the prerequisite for this is that the fluid temperature is lower than the ambient temperature. In case of a network temperature higher than the ambient temperature, losses occur. Yet, in the case of cooling systems, this can also be an advantage. Therefore, it can be said as a rule of thumb that the longer the pipe network and the higher the temperature gradient to the environment, the more heat can be drawn from the earth or released to it. [21]

5.2 Working principles of compression and absorption machines

In the following section, the basic thermodynamic relationships and the operating principle of HPs, CCs, RHPs and AHPs are explained. However, the focus here is clearly on compression machines, as these are key components of the TRNSYS model used in this work. Nevertheless, for the sake of completeness, AHPs are also included. As already mentioned, the technology behind compression HPs and CCs is basically the same, but in the scope of this thesis a distinction is made due to their different applications. Therefore, within the context of this work, HPs are always referred to when heating is provided, while the term CCs is used for the provision of cooling.

5.2.1 Compression machines

In the following the working principle of compression HPs and CCs is explained. This is done by first using the example of a CC and then, building up on this knowledge, the functioning of HPs is described. An ideal cooling machine makes use of a thermodynamic cycle in which heat is extracted from one location, also called the heat source, and then released at another location, called the heat sink. In the simplest case, the system consists of the four components which are shown in Figure 16 and explained in the following. [37]
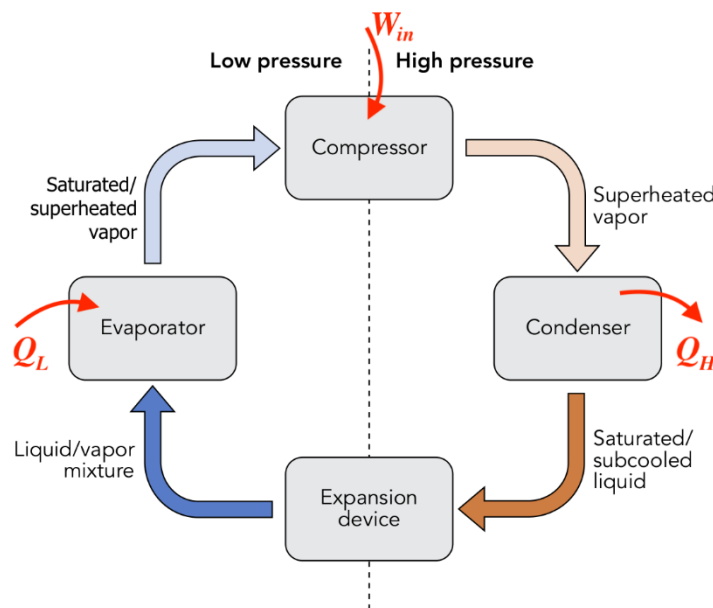
Figure 16: Basic components of HPs and CCs [37]

Evaporator: In the evaporator heat (Q_L) is extracted from the heat source by means of a refrigerant in a liquid-vapor state at low pressure and temperature. Due to the transferred heat, the refrigerant undergoes a phase transition from the liquid to the gaseous state. This phase transition extracts, depending on the enthalpy of vaporization, a significant amount of energy from the source, capturing it within the working fluid mainly as latent heat. After this process the refrigerant is in the state of saturated or superheated vapor. [37–39]

Compressor: In the compressor, work (W_{in}) in the form of electrical energy is fed into the system, causing an increase in the system's pressure and temperature. The refrigerant is still in the state of superheated vapor. [37–39]

Condenser: In the condenser, heat (Q_H) is released at high pressure into the heat sink, causing the working fluid to undergo another phase transition. The refrigerant is now either in a saturated or subcooled liquid state. [37–39]

Expansion device: To return the pressure and temperature of the refrigerant to their original levels, it is passed through an expansion valve. After passing through the expansion valve, the refrigerant is again in a liquid-vapor state, and the cycle repeats. [37–39]

The purpose of a CC is to achieve a cooling effect by removing heat from the source and releasing it at the sink. Therefore, the amount of heat that can be removed from the source per unit of electrical energy is used as a measure of the performance for such a machine. In this work, this dimensionless ratio is referred to as the coefficient of performance for cooling (COP_C). The ideal COP_C can be calculated according to formula (4-1) and depends on the average temperature levels at which heat is supplied (T_L) and removed (T_H). [37–39]

$$\text{COP}_{C_{ideal}} = \frac{desired\ output}{required\ input} = \frac{Q_L}{W_{in}} = \frac{Q_L}{Q_H - Q_L} = \frac{1}{\frac{Q_H}{Q_L} - 1} = \frac{T_L}{T_H - T_L} \tag{4-1}$$

Since the formula (4-1) is an idealised view of the system, the so-called efficiency factor η_C is used to determine the real COP_C. Values for this efficiency factor lie between $0{,}4$ and $0{,}6$. [39]

$$\text{COP}_C = COP_{C_{ideal}} * \eta_C \tag{4-2}$$

Typical values for the COP_C found in the literature range from 3 to 6, which means that between 3 and $6\ kWh$ of thermal energy can be provided per kWh of electricity. Generally, it can be said that the higher the COP_C, the better the chiller. [21, 40–42]

As already mentioned, the COP_C depends primarily on the temperature levels at which heat supply and heat removal take place and is better the closer these temperatures are to each other. Other influencing factors are the thermodynamic properties of the refrigerant, friction losses in the compressor and pipes, full and partial load operation, the type of heat source and sink as well as the HX designs (evaporator and condenser) and therefore the heat transfer coefficients, maintenance and quality of insulation. [10, 38, 43–47]

In a HP, the exact same thermodynamic cycle which is shown in Figure 16 is used to generate useful heat. The HP absorbs heat from a source and releases it at the sink, along with the energy supplied by the compressor. In contrast to the CC, the objective of the HP is to provide heat at the sink. Therefore, the amount of heat released at the sink per unit of electrical energy supplied is used to measure the performance of such machines. In this work, this dimensionless ratio is referred to as the coefficient of performance for heating (COP_H). The ideal COP_H can be calculated according to formula (4-3) and is a function of the temperature difference between the heat source (T_L) and the heat sink (T_H). [37–39]

$$\text{COP}_{H_{ideal}} = \frac{desired\ output}{required\ input} = \frac{Q_H}{W_{in}} = \frac{Q_H}{Q_H - Q_L} = \frac{\frac{Q_H}{Q_L}}{\frac{Q_H}{Q_L} - 1} = \frac{T_H}{T_H - T_L} \tag{4-3}$$

Since the formula (4-3) is an idealised view of the system, the so-called efficiency factor η_H is introduced to determine the real COP_H. Values for this efficiency factor lie between $0,45$ and $0,55$. [7]

$$COP_H = COP_{H_{ideal}} * \eta_H \qquad\qquad\qquad\qquad (4\text{-}4)$$

Typical values for the COP_H found in the literature range from 2 to 8 and generally it can be said that the higher the COP_H, the better the HP. [2, 7, 8, 21, 42, 47, 48]

As previously noted, the COP_H is influenced by the temperature difference between source and sink and becomes higher the smaller this difference is. Other influencing factors are the thermodynamic properties of the refrigerant, friction losses in the compressor and pipes, full and partial load operation, the type of heat source and sink as well as the HX designs (evaporator and condenser) and therefore the heat transfer coefficients, maintenance and quality of insulation. [10, 38, 43, 44, 47, 49]

Figure 17 illustrates the relationship between the COP and the temperature difference between heat source and sink. [7, 39]
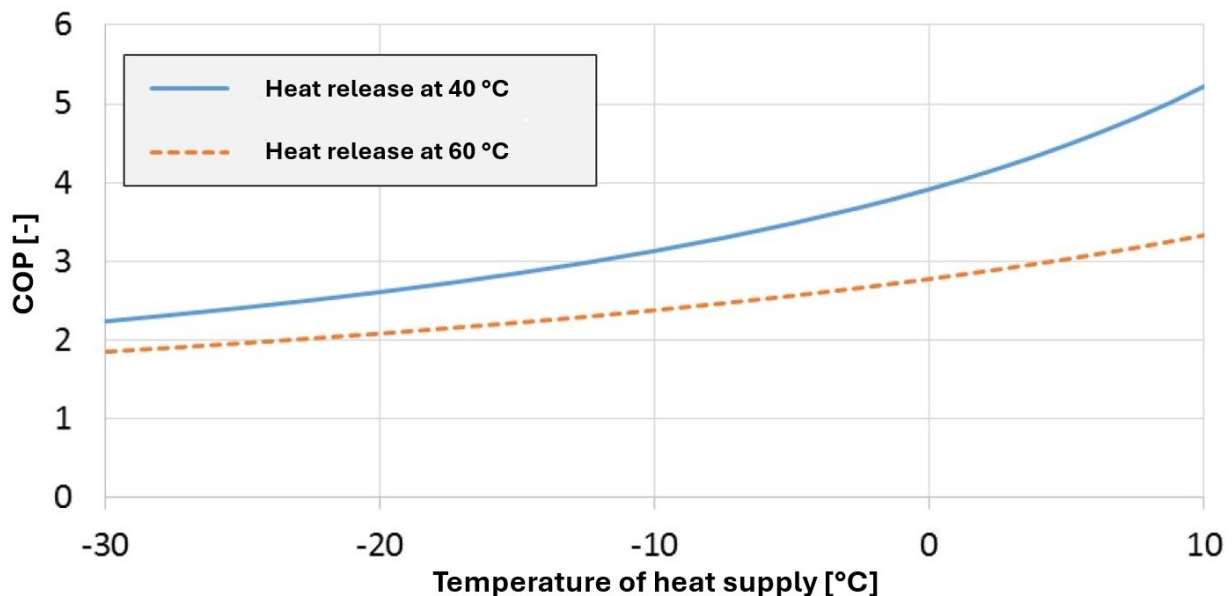
Figure 17: Relationship between the COP and the temperature difference [7]

Furthermore, it must be mentioned that the COP is an instantaneous measurement. Thus, to determine the COP, both the electrical energy consumed and the thermal energy delivered are measured at a specific given point in time. However, due to factors such as fluctuating source temperatures throughout the year or full and part load operations, the COP is not constant and varies over time. To take this variation into account the SCOP is introduced. The SCOP is a metric used to evaluate the efficiency of HPs and CCs over a range of different

operating conditions for a certain period of time, e.g. a whole year or a complete heating and cooling season. By considering not only a single outdoor temperature or operating point, the SCOP offers a more realistic evaluation of the system's performance. The SCOP for heating purposes ($SCOP_H$) can be calculated according to formula (4-5), typically using hours as time steps. [21, 42, 49, 50]

$$SCOP_H = \frac{Total\ Seasonal\ or\ Annual\ Heating\ Output\ [kWh]}{Total\ Seasonal\ or\ Annual\ Electrical\ Energy\ Input\ [kWh]} = \frac{\sum_{j=1}^{j=n} Q_H}{\sum_{j=1}^{j=n} W_{in}} \tag{4-5}$$

Figure 18 shows the analysis of the hourly efficiency of a monitored HP installed in a fifth generation DHC network in comparison to the average monthly source temperature which was measured directly at the HP. The daily COP of the HP is shown in the boxplot diagram for monthly analysis. The centreline in the boxes shows the average COP during that month. [21]
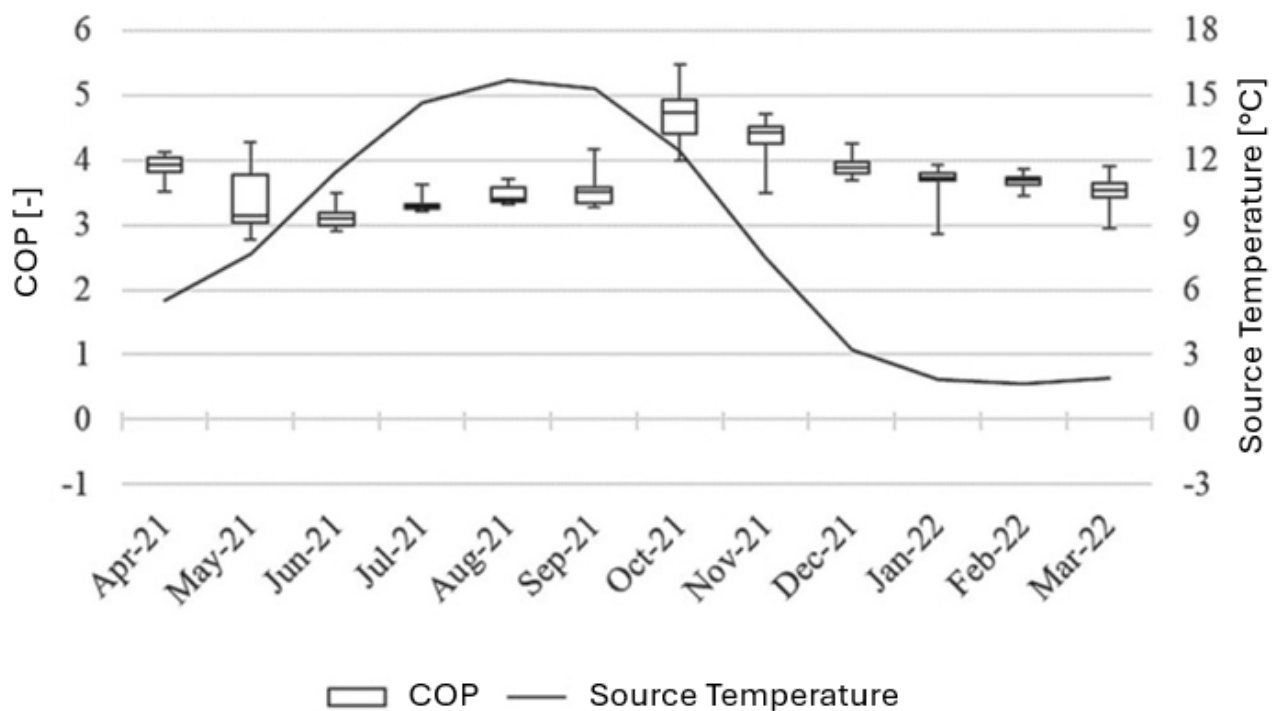
Figure 18: Analysis of a HPs monitoring data and its source temperatures [21]

During the summer months, the HP is only used for DHW preparation, which results in low efficiencies even though the source temperature is relatively high. In October, the demand for SH starts and the HP reaches its peak performance as the source temperature is still high, but the required sink temperature is lower. During the winter months, the COP decreases again due to the lower source temperature. Typical values for the $SCOP_H$ found in the literature from studies in Germany, Estonia, Denmark, Spain, China, and Japan range from 2,9 to 4,7. [21, 42, 50–52]

The definition of the SCOP for cooling purposes ($SCOP_C$) is basically analogous, except that instead of the heating output, the cooling output is of interest. The $SCOP_C$ can be calculated according to formula (4-6), typically using hours as time steps. Values for the $SCOP_C$ found in the literature from studies carried out in Germany, Estonia, China, and Japan range from $2,2$ to $4,7$. [21, 50, 51]

$$SCOP_C = \frac{Total\ Seasonal\ or\ Annual\ Cooling\ Output\ [kWh]}{Total\ Seasonal\ or\ Annual\ Electrical\ Energy\ Input\ [kWh]} = \frac{\sum_{j=1}^{j=n} Q_L}{\sum_{j=1}^{j=n} W_{in}} \tag{4-6}$$

5.2.2 Reversible compression machines

In addition to the concepts already discussed, there are also so-called RHPs. These machines can be used as both HP and CC, depending on their operating status. The working principle is the same as for normal compression machines, but RHPs can supply both heat as well as cold to, e.g., an internal space by operating in either heating or cooling mode. This is made possible by using a so-called 4-way reversing valve which allows to reverse the flow of refrigerant and thus also the external heat flows. This reversing process causes the two HXs to swap their roles. The condenser becomes the evaporator, and the evaporator becomes the condenser. The 4-way reversing valve has four connections and two switching states, which can be controlled by means of a solenoid coil and is installed next to the compressor where it is connected to its refrigerant inlet and outlet. This setup allows for controlling the direction of the refrigerant flow in the system, depending on the switching state of the valve and thus the operating mode. Today, there is a large offer of RHPs available with investment costs comparable to those of non-reversible units. Figure 19 illustrates a RHP with a 4-way reversing valve. [10, 53–57]
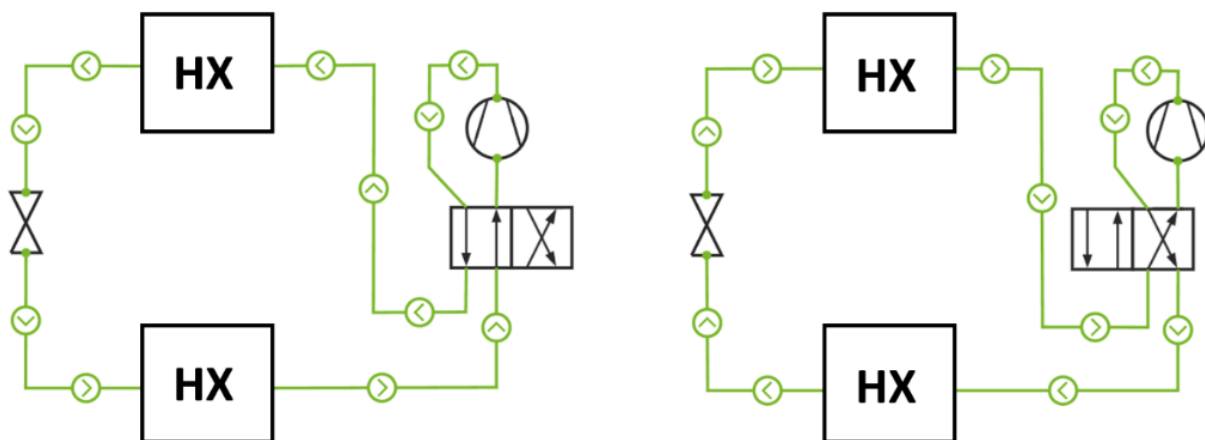
Figure 19: Illustration of a RHP with a 4-way reversing valve [54]

5.2.3 Absorption machines

The operating principle of AHPs is quite similar to that of compression HPs. The circulating working fluid is evaporated at low pressure by absorbing heat from the source, which is then transferred into the sink at higher pressure through condensation. Nevertheless, there are slight differences. In contrast to compression HPs, the compressor and thus the electrical energy supply, is replaced by a combined absorption and expulsion process. Therefore, the pressure is not increased by a conventional compressor but by an absorber-expeller unit, also called "thermal compressor". In this solvent circuit, a two-component mixture of fluids circulates. This solution, which consists of an absorption medium (the solvent) and a working fluid (the heat carrier) that has high solubility in the solvent, enables the heat transfer. The fluids are partly heavily mixed and partly separately circulated through the system. Figure 20 shows a simplified flow and functional diagram of such a machine. In this example, the two-component mixture consists of ammonia (NH_3) and water (H_2O), which are generally used when evaporation temperatures are below $0\ °C$. In AHPs with evaporating temperatures above $0\ °C$, H_2O and lithium bromide (LiBr) are typically used. [58, 59]
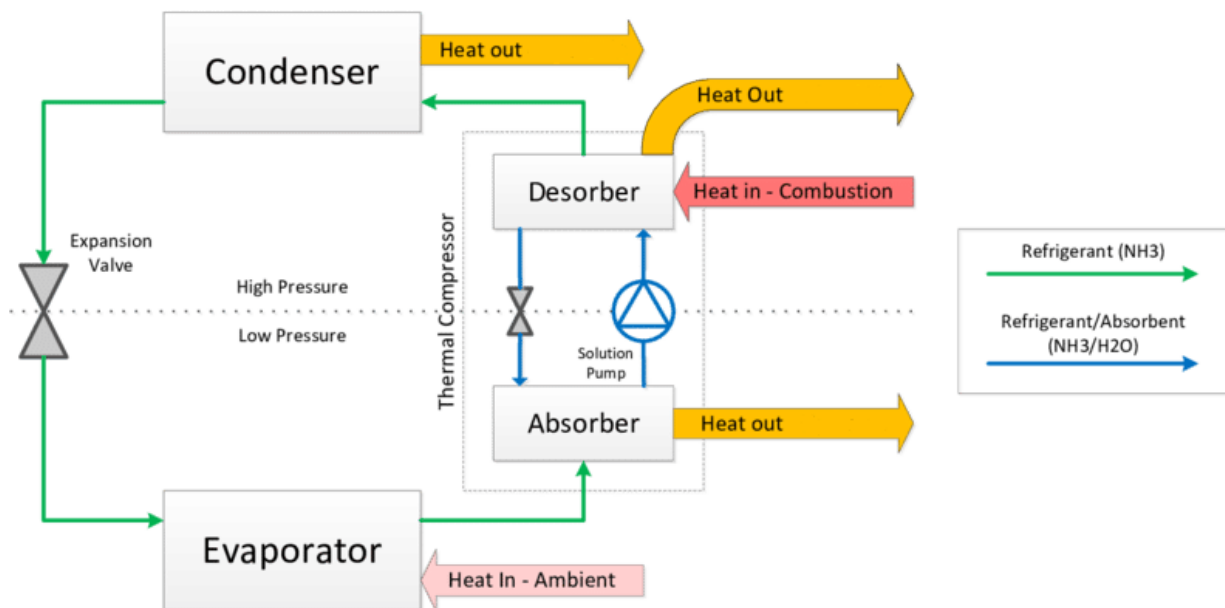
Figure 20: Simplified flow and functional diagram of an AHP [59]

In the evaporator, the low-pressure part of the system, the heat necessary for the evaporation (Q_L) is extracted from the source. The now vaporous working fluid enters the absorber, where it is absorbed by the solvent. The heat of absorption (Q_A) released during this process is generally minor in magnitude relative to the other heat quantities involved but can still be harnessed for utilization. The solution, now enriched with the working fluid, is raised to

a higher-pressure level by means of a solution pump supplied with electric power (W_{in}) and conveyed into the desorber. In the desorber, heat (Q_{in}) is supplied to separate the solvent from the working medium. Nowadays, the thermal energy required in the desorber is generally generated via solar energy or heating systems that are fired with fossil fuels. The now depleted solvent solution is fed back into the absorber through a valve, where it absorbs new working fluid. The working fluid itself, now at high temperature and pressure, enters the condenser where it undergoes a phase transition from the gaseous to the liquid state, releasing heat (Q_H) to the sink. Subsequently it is returned back to the evaporator via an expansion valve and the cycle repeats. [58]

The most important performance indicator for AHPs is the so-called heat ratio (HR). For heating operation, this dimensionless ratio is referred to as $HR_{Heating}$, while for cooling operation, it is known as $HR_{Cooling}$. [58]

$$HR_{Heating} = \frac{desired\ output}{required\ input} = \frac{Q_A + Q_H}{W_{in} + Q_{in}} \tag{4-7}$$

$$HR_{Cooling} = \frac{desired\ output}{required\ input} = \frac{Q_L}{Q_{in} + W_{in}} \tag{4-8}$$

5.3 Retrofitting DHC networks

In the following section, it is explained how HPs, CCs and AHPs can be integrated into DH networks, with a focus on HPs. Additionally, DHC network topologies are described in which reversible compression machines are used as the central heat and cold source.

5.3.1 Integration of compression and absorption machines into DH networks

Since many contemporary DH and DC systems belong to the first three generations, they need to be retrofitted. In this context, technologies such as HPs offer enormous opportunities for sustainable development, as they can efficiently provide heat and cold using electrical energy and waste heat. Thus, they allow for an increased share of renewable heat and cold in DHC systems, can contribute to the replacement of old fossil fuel boilers and create flexibility options for electrical grids. Nevertheless, in today's European DH networks, for the provision of heat at higher temperatures, HPs are still not a standard technology and play a minor role compared to the total installed DH thermal capacity of about $300\ GW$. Figure 21 shows the capacity of large HPs in European DH networks in 2021. [1, 2, 4]
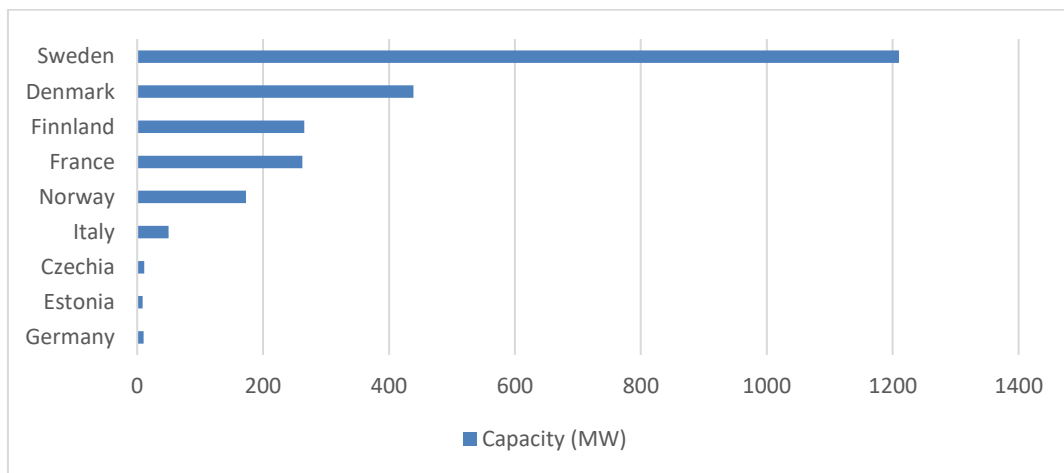
Figure 21: Production and capacity of large HPs in DH systems in 2021 [1]

Studies show that small DH networks have the greatest potential for HP implementation, while medium and large systems with efficient CHP production have less. This is because the decommissioning of CHP plants, which primarily serve the purpose of electricity generation, could mean that the demands of large cities can no longer be met reliably. However, various possibilities for enhancing overall system performance by integrating greener technologies exist in all types of DH and DC systems. If the integration is beneficial or not depends widely on the specific characteristics of the network and external factors, such as electricity and fuel prices. Relevant measures include the integration of fossil fuel heat sources, various RES, HPs, CCs, AHPs and TESs, in both decentralised and centralised ways. Figure 22 and Figure 23 compare a conventional third generation DH system to an advanced fourth generation DHC system featuring HPs, CCs and AHPs. [2, 4]
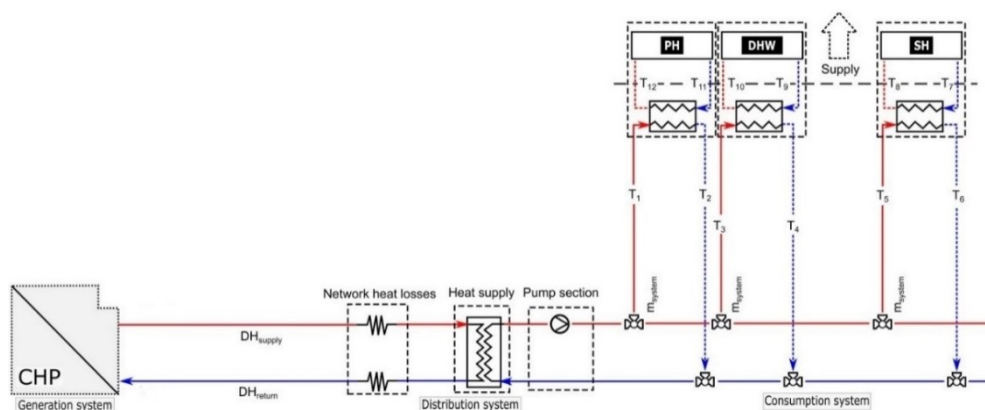
Figure 22: Conventional third generation DH system [2]

Conventional DH networks, such as the one shown in Figure 22, consist of buildings and settlements supplied with hot water from a central heat source, distributed through double pipe networks (supply and return line). In the generation system, heat from the central source is

transferred to the distribution system via an HX and then delivered to the consumer through another HX. Ultimately the heat is utilised for SH, DHW preparation or PH services. [2, 6]
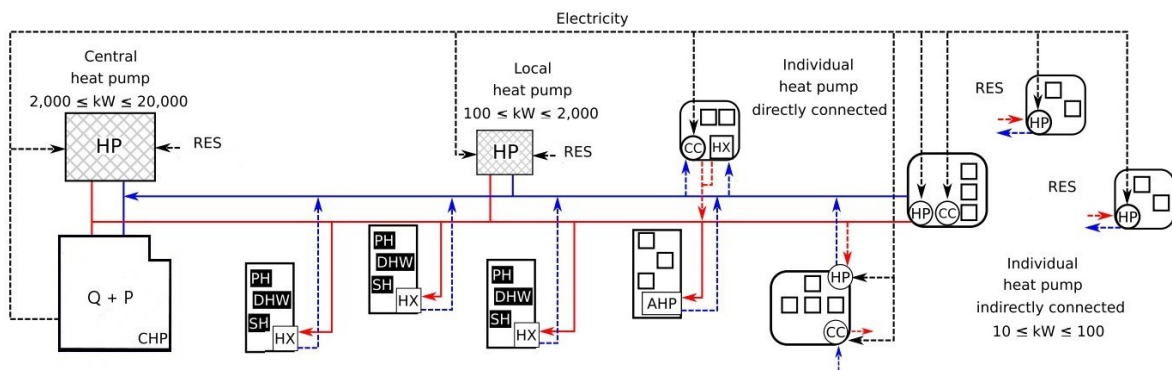
Figure 23: Fourth generation DHC system equipped with HPs, CCs and AHPs [2]

In advanced fourth generation DHC systems, such as the one illustrated in Figure 23, the network topologies are different. Unlike conventional systems, it can be observed that the system is significantly more decentralised, and that in addition to the CHP plant, a HP serves as a complementary heat source for the entire network. Moreover, the system features local and individual HPs as well as decentralised CCs and AHPs to exploit synergies between heating and cooling provision. Potential heat sources in such networks might be geothermal energy from the ground or ambient energy from rivers, lakes, the sea, underground waters and the atmosphere. Furthermore, waste heat from industrial processes and sewage water treatment facilities or urban excess heat, e.g. from the service/residential sector such as the metro, supermarkets, or data centres can be tapped. Moreover, the DHC network itself can act as a heat source. When deploying compression machines, using the ground is particularly practical as it offers the advantages of reliability, constant temperatures and the possibility to act as a TES. [1, 2, 4, 10]

The integration options for HPs can be distinguished depending on the location in the network, the connection mode and the operation mode. Table 2 provides an overview of the different integration options. [2]

Table 2: Overview of the integration options for of HPs in DHC systems [2]

Location	Connection mode	Operation mode
Central	Single	Single-source
Local	Parallel	Multi-source
Individual	Serial	High or low temperature

In the network, HPs can be installed either centralised or decentralised (local or individual location). Furthermore, they can be connected in different connection modes. Single connection mode means that a single HP provides the entire heat for the system or network node demanded by HPs. In a parallel connection mode, several HPs draw heat from the same source and discharge it into a common sink. In a serial mode, one HP heats up water and then passes it to a subsequent one for further heating. Through serial connection better COP values can be achieved as the individual HPs can operate with a smaller temperature difference. Each of these connection modes can have different operation modes. Single-source means that the HP alone provides all the thermal energy for the network. In a multi-source system, the HP serves as the primary source, while other alternatives such as CHP plants, RES or boilers are responsible to meet peak demands. If the network itself is used to evaporate the refrigerant, the operation mode also depends on whether HPs use the high-temperature supply line or the low-temperature return line as source. [2, 4]

Central HPs, or very high temperature HPs, are typically designed with high thermal capacity ranging from $2,000\ kW$ to $20,000\ kW$ and require relatively high source temperatures to adequately function as a replacement for CHP plants. This type of HPs can supply heat with up to $160\ °C$ and is therefore suitable for retrofitting second generation networks. Local HPs, also called high temperature HPs, are designed for a medium thermal capacity of approximately $100\ kW$ to $2,000\ kW$. Temperatures reaching 100 °C can be achieved, making them compatible to third generations systems. One or more of these units can be installed to provide either stable or variable capacity, depending on the available heat sources. By integrating such HPs into the network, its flexibility and reliability are increased, as the network can draw on multiple local heat sources. The power range of individual HPs lies typically between $10\ kW$ and $100\ kW$. Heat sources such as the ones mentioned above can be used and temperatures of up to $80\ °C$ can be reached at the sink, which makes them suitable for fourth and fifth generation networks. Furthermore, in fifth generation networks, individual HPs and CCs can be attached directly to piping networks that connect buildings, using them as sources and sinks. To cover the heating demand, HPs use the hot water pipe as source and discharge the cooled water into the cold water pipe. The cooling demand is met by means of CCs or HXs (in the case of direct cooling) using the cold water line as sink. The heated water is then fed back into the hot water line. Given the low temperature levels required, such topologies no longer require a central heat source. Figure 24 illustrates such a topology. [2]
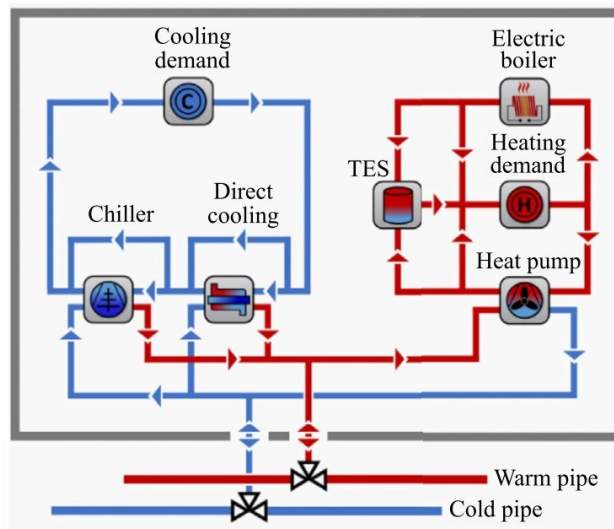
Figure 24: Integration of HPs and CCs into a fifth generation DHC system [2]

It is important to mention that the placement options for all kinds of HPs offer a lot of interesting possibilities, with a more detailed description available in the cited literature. Table 3 classifies the three different HP types according to their associated temperatures and power outputs. For commercially available very high and high temperature HPs, COP values range from 2,5 to 5,8, and the refrigerants typically used in these systems are R245fa, R717, R718, R744, R134a, and R1234ze. [2]

Table 3: Classification of HPs based on temperature ranges [2]

Type	Source temperature [°C]	Sink temperature [C°]	Thermal power range [kW]
Individual HP	$0 - 40$	$0 - 80$	$10 - 100$
Local HP	$40 - 60$	$80 - 100$	$100 - 2,000$
Central HP	$60 - 120$	$100 - 160$	$2,000 - 2,0000$

A further distinction can be made according to the uptime of the machines. There are units that are operated for between 7000 to $8000 \, h$ annually, primarily to achieve a faster return on investment and units with uptimes of around 4000 to $7000 \, h$ that are mainly utilised during the heating or cooling season to meet the increased seasonal demand. Another possibility is to operate HPs and CCs based on electricity prices. However, it is important to note that HPs today are not designed for flexible start-stop operation based on electricity prices. Nevertheless, experimental testing with advanced HP models has shown that this type of operation is feasible to some degree. If mechanical wear can be ruled out with new HP

generations or costs allow such operation in the future, this could offer attractive possibilities. [8]

A further important aspect is the integration of HPs and CCs into the wider, more encompassing energy system, especially within electric grids. In the scenario of a highly electrified energy system fed by RES and an increased use of DHC, the role of these PtH systems becomes increasingly important. In particular, large-scale electric HPs are considered critical components of smart energy systems. Moreover, the combination of CHP and HPs not only offers the advantages of fuel flexibility (such as biomass and waste) and low prices of intermittent electricity but also facilitates the expansion of RES such as solar and wind. On days with high renewable generation, CHP plants can be shut down and HPs ramped up. Conversely, on days with low renewable generation, CHP plants can be ramped up, while the HPs shut down. This approach can also be applied to better deal with fluctuating commodity prices. Another benefit of pairing these systems is the use of flue gas storages, which can be used to provide source heat and therefore achieve better SCOP values in times of very low outdoor temperatures. [8]

5.3.2 Integration of reversible compression machines

One way to provide both heating and cooling for DHC networks via a compression cycle as the primary energy source is the use of RHPs. In this case, the RHP functions alternately as both HP and CC, depending on the operating state. The system is reversed by means of a 4-way valve, effectively inversing the direction of flow through the two HXs. The topology of a network that uses RHPs for the provision of heat and cold is shown in Figure 25. In the illustration the two HX, which are alternately operated as an evaporator and a condenser, are labelled with the numbers 1 and 3. The compressor is marked with the number 4, and the expansion valve with 2. The four-way valve is labelled with 5. The curved arrows indicate the system's direction reversal. [10]
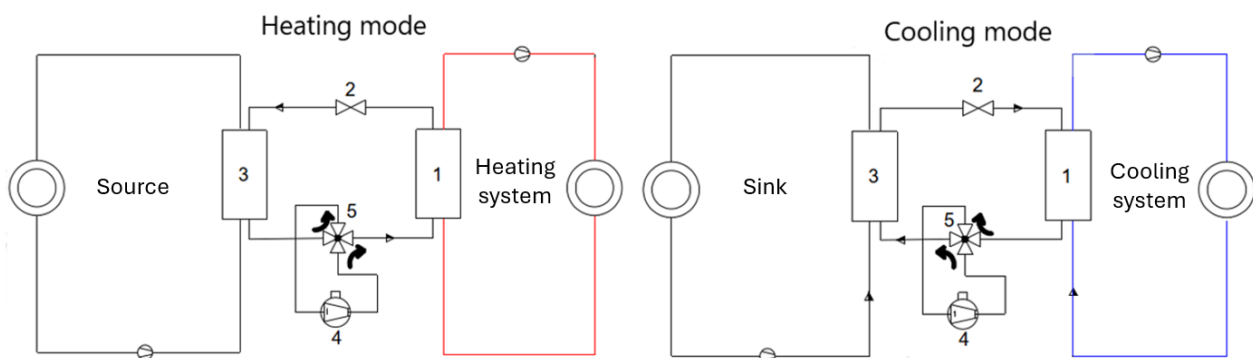
Figure 25: Topology of a DHC network fed by reversible HPs [10]

When in cooling mode, HX 3 serves as a condenser, discharging heat, while HX 1 operates as an evaporator, delivering cold to the network. In heating mode, the roles of the two HXs are reversed, with HX 3 acting as the evaporator and HX 1 as the condenser. Depending on the operating mode, the RHP are alternately connected to the heating or cooling network. The switchover between the networks is achieved through a hydraulic circuit. If the ground is used as source in heating mode and sink in cooling, improved seasonal behaviour of the system can be achieved as it has a long-term storage effect. In the best case scenario, the same amount of heat is extracted as is fed in, which results in the ground reaching the same temperature at the end of the year as at its beginning. [10]

Another way of suppling DHC networks with both heat and cold is to introduce "reversibility" into the system by a hydraulic switchover on the water side. Through this process the same behaviour as in the previously shown system can be achieved, but no RHP is required. Furthermore, by performing the switchover on the water side, it is also possible to transfer heat and cold not into the ground, but directly into the corresponding network, thus minimizing losses. Figure 26 illustrates the topology of such a system in operation with the ground serving alternately as source and sink. [10]
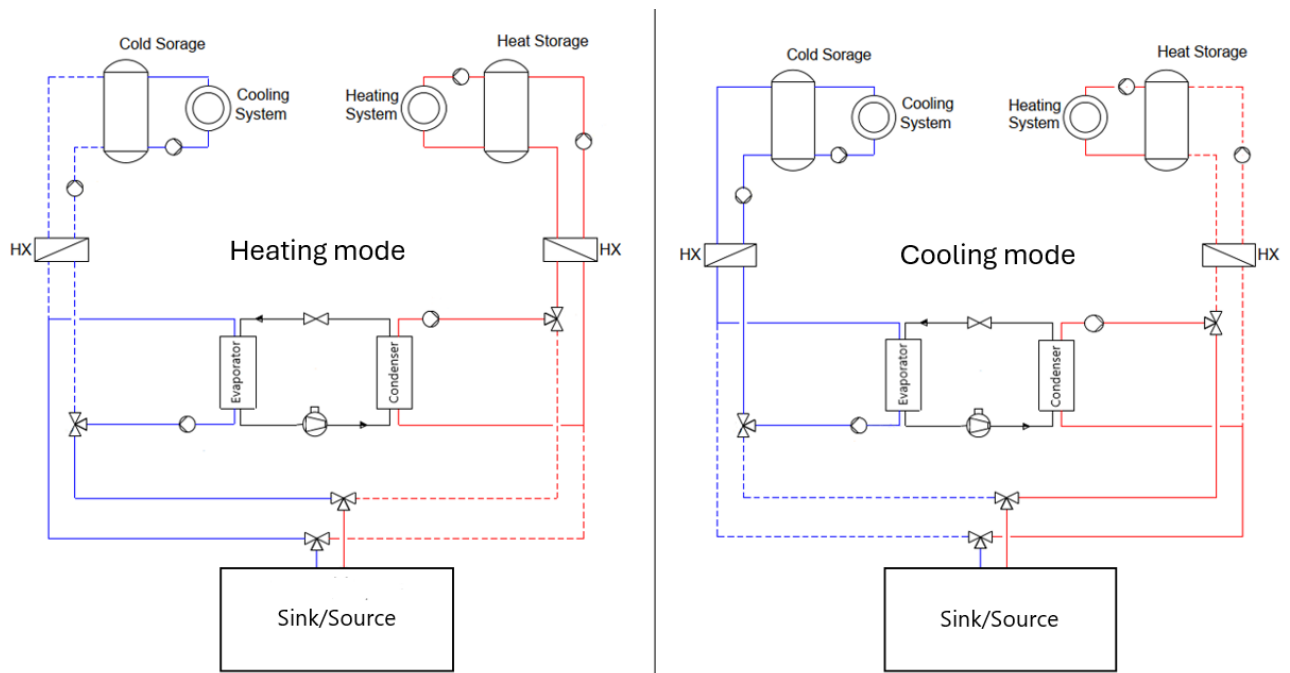
Figure 26: Topology of a reversible DHC network fed by HPs/CCs [10]

In the case of heat provision, the condenser is connected to the heating network (sink) and the evaporator is connected to the ground or cooling network (source). If cooling is to be provided, the evaporator draws heat from the cooling network (source) and releases it into the ground or heating network (sink) via the condenser. Typically, water brine solutions are used

to avoid frosting, which is why HXs are necessary to decouple the HP system from the DHC network. As the ground works as a heat reservoir, in the ideal case it reaches the same temperature at the end of the year as at the beginning. [10]

6 Thermal energy storages

The following chapter provides an overview of TESs, as these are also essential components of the TRNSYS model used in this work and regarded as key technology for the optimisation of DH and DC networks. As this is a very broad topic with many different areas of application, the focus is put on TES systems that are relevant for DH and DC. Therefore, an overview of the importance and application areas of TESs is given first. This is then followed by a classification and categorization of the different technological approaches, along with a detailed explanation of TES systems with a high technological readiness level.

6.1 Application areas of thermal energy storages

TESs enable the decoupling of production and consumption, thus being able to even out the temporal mismatch between supply and demand, which makes network operations more flexible. Therefore, a possible field of application is the use of TESs as backup technology for peak load coverage. Their implementation allows the network operator to generate thermal energy at low cost, e.g. via CHP plants, which can later be utilised to meet peak demand. Therefore, the use of more expensive, climate-damaging backup units for peak load power generation can be reduced. The same principle applies when a lot of surplus heat is generated during summer by solar thermal plants. Since most of the heat is needed in winter TESs are crucial for maximum thermal solar collector exploitation as they can help to balance the seasonal offset. They can also increase utilization of industrial excess heat delivered to the network, minimize heat loss from waste incineration plants which still have to treat waste during summer and improve the performance of integrated systems. Another reason for deploying

TESs in relation to peak load coverage is that many backup technologies, such as heat only boilers, operate at a fixed power output that rarely matches the actual demand. To compensate for this mismatch, the system operator has to ramp down baseload units, resulting in more heat than necessary being generated by expensive backup technologies. TESs can be a solution to this problem as they can absorb these variations in generation, thus increasing the capacity utilization of the base load plants. The amount of expensive peak load heat that can be replaced by cheap baseload heat, i.e. sizing of the storage, depends highly on the duration curve of the individual network. Furthermore, TESs can provide heat reserves at times when the network is unable to deliver enough heat due to bottlenecks between the production plants and the customers. However, it is important to note that TESs do not increase the generation capacity of the network and should not be used as a substitute for other backup technologies such as peak boilers. TESs should rather be understood as an instrument for economic system optimisation by allocating generation units in the most efficient way and whether the investment in a TES pays off or not depends mainly on financial considerations. [4, 5, 11, 32, 60, 61]

In small and less complex DH systems supplied by CHP plants, TESs offer the possibility to make the network operation more flexible and efficient. CHP extraction plants, which have a relatively high degree of flexibility, can ramp down electric power generation when electricity prices are low if sufficient storage capacity is available. The surplus in generated low-cost heat can be stored for later sale, while at the same time electricity generation is shifted to hours with high unit prices. In contrast, in a scenario with high electricity prices, it could be beneficial for plant operators to ramp down heat production (or shut if off entirely) to maximize electricity generation. Now the TES acts as a buffer and covers the demand until the CHP plant resumes generating thermal power. In connection with the more rigid back-pressure plants, operators can produce at full capacity when electricity prices are high, without bothering about the current thermal demand, storing the cheap heat for later usage. Therefore, TESs allow for maximizing profits by making CHP plants more flexible and help to decouple electricity market-driven production in CHP plants from heat demand in DH networks. [4, 5, 11, 32, 61]

In the context of sector coupling, another possible field of application is load balancing in electrical grids. With the ever-growing share of intermittent renewables in the electrical energy system, such as wind and solar, grows the importance of TESs in DH and DC systems, as they can help to deal with the resulting volatile power generation and pricing structure. One way to use electrical excess energy could be to drive HPs or CCs at low cost and store the generated thermal energy that is not immediately required. Thereby, the frequency in electrical grids can be stabilized, without dissipating precious electrical power when no other loads are available. [4, 5, 11, 32, 61]

6.2 Classification of thermal energy storages

Heat and cold can be stored using various technologies which is why multiple ways to classify TES systems exist. First of all, a basic distinction can be made between sensible, latent and thermochemical heat storage systems. [60]

- **Sensible heat storage** leads to a change in kinetic energy of the atoms within the storage medium by supplying or removing heat, thereby causing an increase or decrease in its temperature. The amount of stored thermal energy is proportional to the caused temperature change. Solid materials (e.g. metals, stones or concrete), liquids (e.g. water, oil or molten salts) or mixtures (e.g. water and pebbles or oil and cast iron) are used as storage media. [5, 7, 11, 58, 60, 62]

- **Latent heat storage** exploits phase transitions of the storage medium. These transitions are always coupled with the absorption or release of heat at a constant temperature. Due to the constant temperature, the transferred heat is not sensible and appears to be latent. So-called phase change materials (PCM) are used, and the stored energy is equivalent to the enthalpy of fusion or solidification required for the phase transition. Typical phase transitions employed include solid-liquid phase transitions or solid-solid ones, where a change in the crystal lattice occurs. Common PCMs used are water, salts, paraffins or salt hydrates. Although enthalpies of vaporization are large, liquid-gas phase changes are not used for latent heat storage due to the large volume of the gas phase. Generally, heat from solid-liquid phase transitions is exploited. A major advantage of latent heat storage is that heat can be stored close to the phase change temperature within a narrow range and thus at a specific temperature level. [4, 5, 7, 11, 58, 60, 62]

- **Thermochemical heat storage** systems make use of reversible thermochemical reactions. Through endothermic reactions, excess heat is stored in the form of chemical compounds and then released again through the exothermic reverse reaction. The heat stored and released during this process is equivalent to the enthalpy of reaction. Thermochemical energy storage is intrinsically more complex than sensible or latent heat storage because not only heat transfer phenomena, but also mass transfer aspects and reaction kinetics play a major role. However, one advantage of such TESs is that they offer higher energy densities as reaction enthalpies are generally much larger than the enthalpy of phase transitions exploited in latent heat storages, or the sensible heat stored over a reasonable temperature range. Possible methods are the dissociation and recombination of solids or liquids as well as the use of sorption processes. However, with the exception of low temperature sorption systems, this technology is still at an early

stage of development. It should be mentioned that, strictly speaking, sorption processes are not chemical reactions but interactions between chemical compounds due to van der Waals forces. Yet, in the context of TESs, sorption processes can be categorized as thermochemical processes. [5, 7, 11, 60, 62]

Sensible heat storage is a mature technology that is already widely used and installed in various DH and DC networks. Latent and chemical heat storage technologies are still in development and currently tested in experimental field installations (latent heat) or laboratories (thermochemical). Nonetheless, the latter offer higher energy densities and less thermal losses than sensitive TESs, making them attractive for further development. A further subdivision and categorization of TESs is given in the course of this chapter. [5, 11]

6.3 Thermal energy storages in district energy systems

Depending on the type of system used, TESs allow heat or cold in district energy systems to be stored for a certain period of time. Typically, water is chosen as a storage medium due to its advantageous thermodynamic, chemical, economic, and environmental properties. These include its particularly high heat capacity, favourable density, thermal conductivity, abundance, chemical stability, low cost, easy scalability, and behaviour in the relevant temperature range. Other alternatives to store sensible heat are materials such as soil, rock or molten salts. In the case of water-based TESs, typically, large, insulated tanks or pools with a constant water content are used. Depending on the storage time, three types of TESs can be distinguished: [4, 5, 11, 32, 61]

1. Small-scale, short-term TESs for domestic heating systems
2. Large-scale, short-term TESs for DH and DC networks
3. Large-scale, long-term TESs for DH and DC networks

Since small-scale short-term TESs used in domestic heating systems play a subordinate role in the context of DH and DC systems, they are not discussed in more detail. Large-scale TESs are around 100 times cheaper than battery storage and the only proven and available energy technology to provide monthly and even seasonal storages. [1]

6.3.1 Short-term storage for district energy networks

The most common type of TES in DH and DC networks is large-scale, short-term above ground storage tanks. These tanks are lined with an insulation layer to reduce thermal losses

and depending on their operating temperatures a pressurization system is required to avoid evaporation. The technology is well proven and reliable, can be operated with a wide range of different heat sources and allows to store energy for up to $48\,h$. The ideal volume of these systems depends on many factors such as network size, duration curve and system efficiency but typically they range from one to several thousand cubic meters. Regarding siting, a further distinction can be made between centralised TESs, which are located close to large energy sources, and decentralised TESs, which are connected at strategic locations in the network. These locations are usually related to the function performed by the storages. Central storages typically provide load shaping for aggregated loads, thus reducing cost in the overall system. Decentralised systems such as buffer tanks are installed close to the loads and meet the demand of individual consumers. In addition to above ground tanks, there is also the less common option of buried underground tanks. [4, 5, 7, 11, 32, 60, 62]

In such tanks water can be stored at various temperature levels, thus allowing the energy content in the tank to vary while keeping the water content constant. Due to differences in density, hot water accumulates in the upper part of the tank while cold water remains at the bottom. This process results in the formation of a transition zone between the hot and the cold layer. In this so-called thermocline, a temperature gradient from the hot water temperature down to the cold water temperature is observable. This type of layering is referred to as stratification. Just as for TES tanks in DH, water is the most common storage medium for low temperature TESs in DC networks. However, due to the maximum value of water density at $4\,°C$, this temperature is the natural limit for thermal stratification. Typically, heat and cold are stored in separate tanks, but thermocline technology enables using one tank for both, separating them by buoyancy from density differences which offers a cost-effective alternative to two-tank systems. In addition to insulation lining and pressurization systems (if vaporization takes place), hot and cold water connectors, diffusers as well as various sensors and transmitters that monitor parameters such as pressure, temperature or the fill level are installed. The diffusers are of particular importance as they prevent the mixing of the water during the charging and discharging process by minimizing inflow turbulence, thus maintaining stable zoning. Figure 27 shows the general layout of a TES tank with water as the heat storage medium. [4, 7, 62, 63]
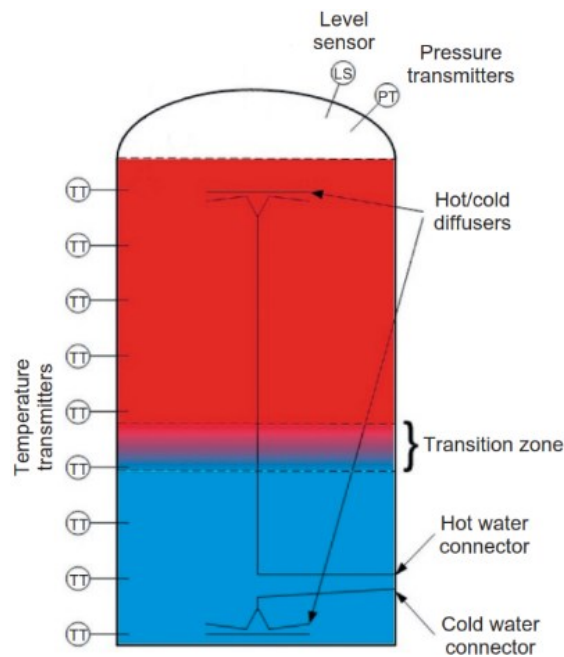
Figure 27: General layout of a TES tank with water as storage medium [4]

During the charging process, hot water is fed into the system from the DH networks supply line through the hot water diffuser, while the same amount of cold water is simultaneously drawn from the bottom of the tank and discharged into the networks return line. During discharging, the reverse process takes place. If the tank is well designed, stratification will remain intact and will only change in altitude depending on whether hot water is pumped in or out. During the charging process, the TES can be considered as a thermal load, while during the discharging process as a generation unit. [4, 11]

The supply temperature of the tank typically depends on factors such as the customer segment, network topology and variations in the demand profile. The return temperature is predetermined by the return temperature in the network. As already mentioned, in the case of supply temperatures higher than $100\,°C$, the tank as well as the pipeline must be pressurized to prevent water evaporation. As a rule of thumb, a distinction is made between non-pressurised storages ($T_{supply} < 100\,°C$) and pressurised storages ($T_{supply} > 100\,°C$). Furthermore, limits exist for the delta allowed between supply and return temperature due to thermal stresses. Non-pressurized vessels should be designed for a temperature difference of 30 to $40\,°C$, while pressurized ones for 50 to $55\,°C$. As long as there is no evaporation, the highest temperature allowed in the tank is limited to that of the energy source. [4, 11]

The amount of stored sensible thermal energy (Q_{tank}) in J can be calculated according to formula (5-1) for heat storage or formular (5-2) for cold storage. In the formulas, m is the mass in kg, c_p is the specific heat capacity of liquid water at constant pressure in $J/(kg\ K)$, and ΔT

is the change in temperature during the charging process. For heat storage, ΔT corresponds to the temperature difference between the final and initial temperature (ΔT_{hot}) and m corresponds to the mass of hot water m_{hot}, which is equal to the total mass in the tank minus the mass of the cold water and the mass of water in the transition zone. For cold storage, m corresponds to the mass of the cold water m_{cold} and ΔT corresponds to the temperature difference between the initial and final temperature (ΔT_{cold}). The same equations can be used to calculate the energy content of single heat and cold storage tanks. [4]

$$Q_{hot} = m_{hot} * c_p * \Delta T_{hot} \tag{5-1}$$

$$Q_{cold} = m_{cold} * c_p * \Delta T_{cold} \tag{5-2}$$

In the case that additional latent heat is stored in the system, formula (5-1) is extended by the term h_v (enthalpy of evaporation) in J/kg multiplied by m_{hot}. [60]

$$Q_{latent} = h_v * m_{hot} \tag{5-3}$$

$$Q_{total} = Q_{hot} + Q_{latent} = m_{hot} * c_p * \Delta T_{hot} + h_v * m_{hot} \tag{5-4}$$

When superheating the generated steam, equation (5-4) must be further extended to include a term for the sensible heat stored in the steam to determine the total energy content, considering that pressure is no longer constant. Although h_v of water is large, its liquid-gas phase transition is not used in state-of-the-art storages because of the large gas volumes and resulting high pressure levels involved. Nevertheless, research is being conducted on other PCMs, which can be used to store large quantities of latent heat through e.g. the solid-liquid transition. Furthermore, looking at the formulas, it is evident that the mass and the specific heat capacity of the storage medium play a crucial role for the amount of energy that can be stored at a given temperature level. Thus, selecting materials with good thermodynamic properties allows the storage size to be reduced. However, it is important to consider ecological, economic and safety aspects when designing these systems. [4, 11, 58, 60]

6.3.2 Long-term storage for district energy networks

Long-term or seasonal storage allows to store thermal energy for weeks or even months without significant loss, thus enabling heat to be transferred from summer to winter. These storages are of particular importance in systems predominantly fed by solar energy, which is primarily available during summer when heat demand is relatively low. The purpose of long-term storages is basically the same as for short-term, but they differ in design. One option is large, insulated underground tanks, ponds, or pools with water depths of 10 to $15\ m$ and volumetric capacities of up to $100,000\ m^3$. Such concepts are called tank thermal energy

storage (TTES) and pit thermal energy storage (PTES). TTESs are concrete or stainless-steel tanks, lined with thick insulation layers, in which water is typically used as the storage medium. These tanks operate using stratification, therefore causing the hot water to accumulate at the top and the cold at the bottom of the tank. PTESs use the stratification principle as well and are therefore very similar to TTESs from an operational point of view. However, unlike TTESs, PTESs store thermal energy in an excavated ground coated with watertight, insulating liners and besides water, gravel can serve as storage medium. From experience, it has been shown that those reservoirs allow hot water of up to $95\,°C$ to be stored with very small losses incurred. Other concepts are aquifer thermal energy storages (ATESs) and borehole thermal energy storages (BTESs). ATESs are underground water reservoirs and use a mixture of water and ground (e.g., rock or sand) to store heat. To achieve this, two wells (one hot and the other cold) are drilled into the ground for water injection and extraction. In BTESs, multiple vertical boreholes are drilled and the ground layer itself is used as the storage medium. These boreholes act as HXs (BHXs) and typically use water as heat carrier. However, BTESs and ATESs are not particularly well suited for storing heat at high temperature levels, as the soil itself is used as insulation material. Nonetheless, such systems can be an attractive storage option for advanced, low-temperature DHC networks. They can function as both source and sink for HPs and CCs, collecting heat from buildings during the warm season to then reutilise it during winter. Another known concept is cavern thermal energy storage (CTES). CTESs store hot or cold water in large underground caverns, and similar to TTES and PTES systems, stratification occurs. However, CTESs play a subordinate role in the context of DH and DC networks. Alternative technologies may use concrete, pebbles, molten salts or PCMs instead of water as thermal mass. Generally, it can be said that TTESs and PTESs have higher thermal capacities than BTESs and ATESs, but also higher construction costs. Figure 28 illustrates different types of seasonal TES relevant in the context of DH and DC. [4, 5, 11, 32, 60–62, 64]
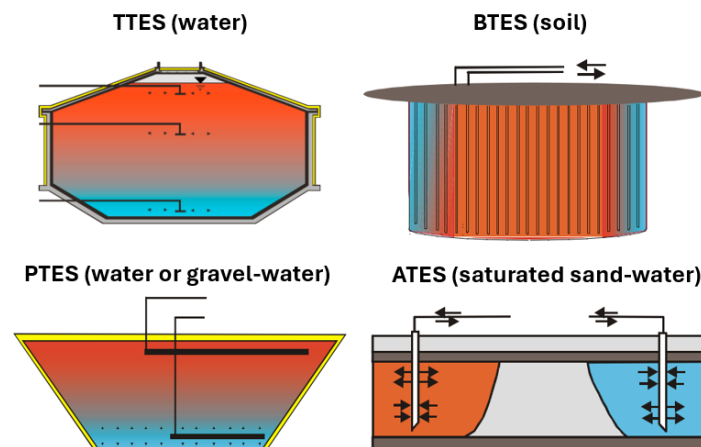
Figure 28: Types of seasonal TES relevant for DH and DC networks [61]

Due to the difference mentioned above a further distinction can be made between long-term TESs for direct usage and long-term TESs for indirect usage. In TESs for direct usage the storage temperature is the same as the temperature of the supply line whereas in TESs for indirect usage the temperature is lower and has to be raised to the appropriate level with auxiliary systems. Compared to short-term TESs, seasonal TESs have relatively low injection and withdrawal rates but high storages volumes. [11, 32]

Table 4 compares the main technological and economic characteristics of sensible long-term TESs relevant for DH and DC systems. The water equivalent corresponds to the volume occupied by the storage facility to hold the same amount of thermal energy as would be stored in one cubic meter of water. [11, 61, 65]

Table 4: Comparison of the characteristics of sensible long-term TESs [11, 61, 65]

Type	*Unit*	*TTES*	*PTES*	*ATES*	*BTES*
Container	$[-]$	*Tank*	*Insulating liners*	*Soil*	*Soil*
Storage medium	$[-]$	*Water*	*Water or gravel-water*	*Sand-water*	*Soil*
Storage density	$[\frac{kWh}{m^3}]$	$60-80$	$30-80$	$30-40$	$15-30$
Water equivalent	$[m^3]$	1	$1-2$	$2-3$	$3-5$
Application	$[-]$	*Short and long-term*	*Long-term*	*Long-term*	*Long-term*
Temperature level	$[-]$	*High*	*High*	*Low*	*Low*
Stratification	$[-]$	*Yes*	*Yes*	*No*	*No*
Cost	$[-]$	*High*	*High*	*Low*	*Low*

Nowadays it is typical to combine solar thermal production with seasonal TESs to even out the offset between supply and demand. A less common application is the combination of TESs (long and short-term) with HPs or CCs to exploit intermittent RES effectively. Through smart operation, plant operators can convert low-cost, renewable electricity into heat or cold when it is available in abundance and store for later usage while simultaneously helping to balance electrical grids. In addition, the combination with TESs allows the HPs and CCs to be operated

with more full load hours and at rated capacity, making their operation more economical. Figure 29 illustrates a smart DH system in which these synergies are exploited. [4, 5, 11]
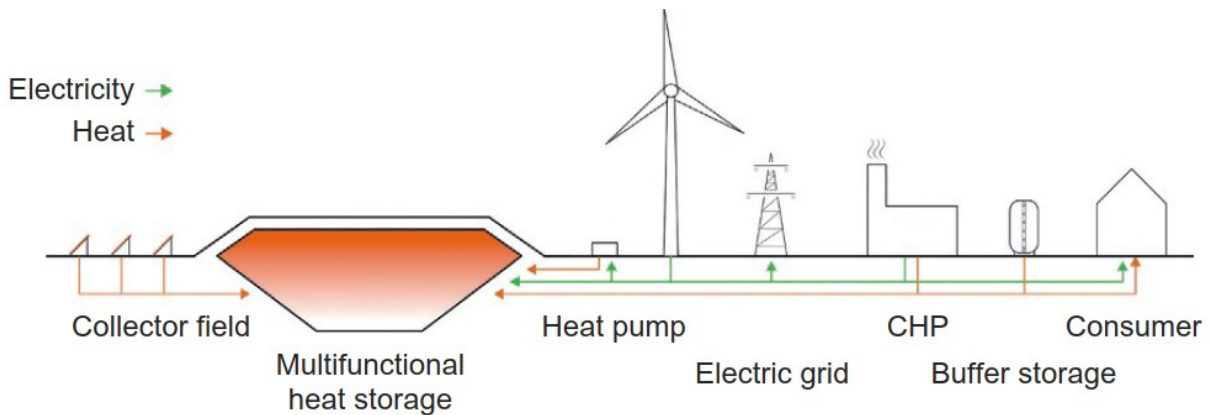
Figure 29: Illustration of a smart DH system [4]

In addition to TESs, the ability to shift heat and cold generation over time can also be found in the thermal inertia of the network itself. By increasing (DH) or decreasing (DC) the supply temperature during low demand, a certain amount of energy can temporarily be stored in the network until demand increases again. However, due to the cyclic loading, this can lead to material fatigue (especially for steel pipes) and can only be implemented with advanced control strategies. Other approaches to pre-charge the network would be to increase the mass flow through the pipes at constant supply temperatures or to use the thermal mass of buildings as decentralised storage. [5, 11]

7 Design and optimisation of a hypothetical DHC generation plant

In the following chapter, a geothermal power plant supplying a hypothetical DHC network situated in Madrid, Spain, in which the thermal energy input is primarily provided by RHPs is first designed and then optimised with regard to LCOE, CO_2 emissions and RHP coverage. For this purpose, two programs were written in Python and several simulations were conducted in the simulation environment TRNSYS. The aim here was to carry out an automated sensitivity analysis in order to identify the best topologies under the given boundary conditions. This analysis was limited only to the power plant's topology data of the TRNSYS model.

To achieve this, the first step involved analysing the DHC load data with the aim of determining a range for the number of RHPs required to effectively cover the heating and cooling demand. The goal here was to narrow down that range on the most promising scenarios (measured by total coverage) and therefore keeping the number of possible combinations in the subsequent sensitivity analysis as low as possible. Therefore, the first Python program (Appendix 2: load_data_analysis.py) was written, which enables the automated analysis of the network's heating and cooling load data and derives from it how much of the network's DHC demand can be covered with a certain number of RHPs. In the next step, the network's power plant topology was determined, and a corresponding generation facility modelled in the simulation environment TRNSYS. Subsequently, the necessary input data not obtained from TRNSYS, as well as the KPI calculation scheme, were defined. The last step was to carry out the sensitivity analysis. For this purpose, the second Python program (Appendix 3: result_analysis.py) was written, which allows for the automated calculation and graphical analysis of the previously defined KPI calculation scheme. The aim here was to

quantify and compare the target values on a consistent basis. Among other data, such as cost and emissions factors obtained from literature research, the results from the TRNSYS simulations served as the thermodynamic input data for result_analysis.py. The following chapter describes this process in detail.

7.1 Load data analysis

In order to achieve a good design of the power plant, the first step was to analyse the network's heat and cold load data, which was provided in the form of a .txt file. As already mentioned, the objective of this analysis was the determination of the most promising numbers of RHPs to effectively cover the heating and cooling demand, with the intention to keep the number of possible combinations in the subsequent sensitivity analysis as low as possible. For this purpose, the program load_data_analysis.py was written in Python, which has been attached to this work. This program first reads the load data and then automatically outputs the results graphically. For a detailed description of the program please refer to Appendix 2: load_data_analysis.py. Due to this automation, the analysis can be carried out for any kind of DHC load data that has the same file format. It is important to note that in this calculation, the influence of TESs and the thermodynamic behaviour of the system, including thermal losses, are not taken into account. Therefore, the results for the total coverage should rather be seen as an approximation of the actual values. Figure 30 shows the heating and cooling demand of the DHC network. The base load (dashed lines) was assumed to be 60 % of the corresponding highest peak.
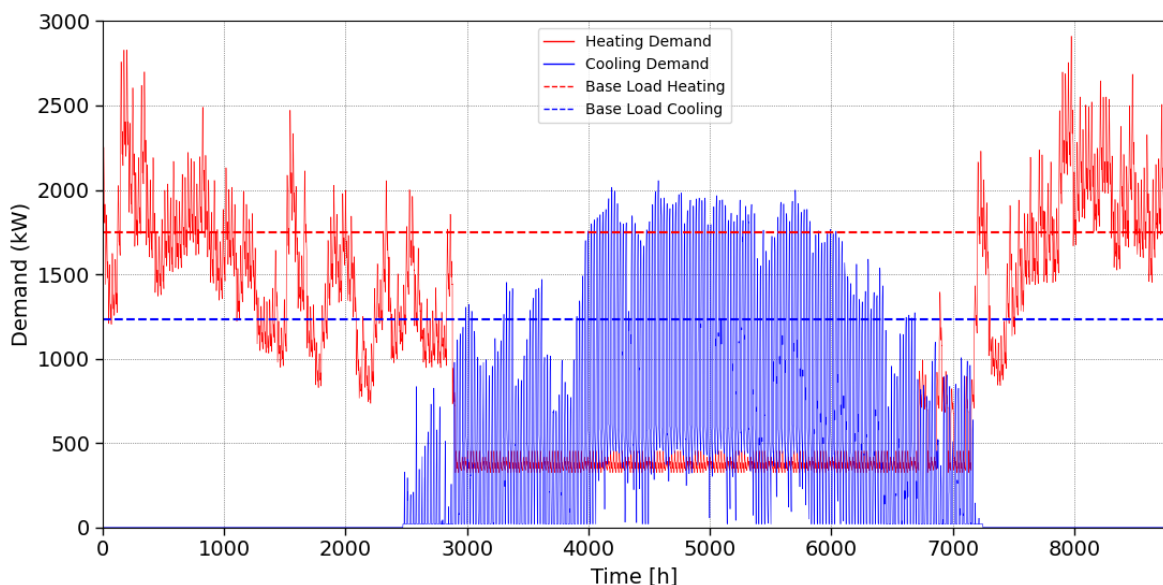
Figure 30: Heating and cooling load profile

The load profile of the heating network exhibits a bathtub shape, with the highest load peaks occurring during the winter months. Furthermore, the heating load profile shows a relatively constant load curve throughout the summer. In contrast to that, the peak loads in the cooling network occur in summer and during the winter months there is no demand at all. In order to get a better understanding of the network's characteristics, the exact same data was visualized in form of annual duration curves. Figure 31 shows the annual duration curve of the heating and cooling demand. Just as before, the base load is located at a height corresponding to 60% of the respective maximum heating demand.
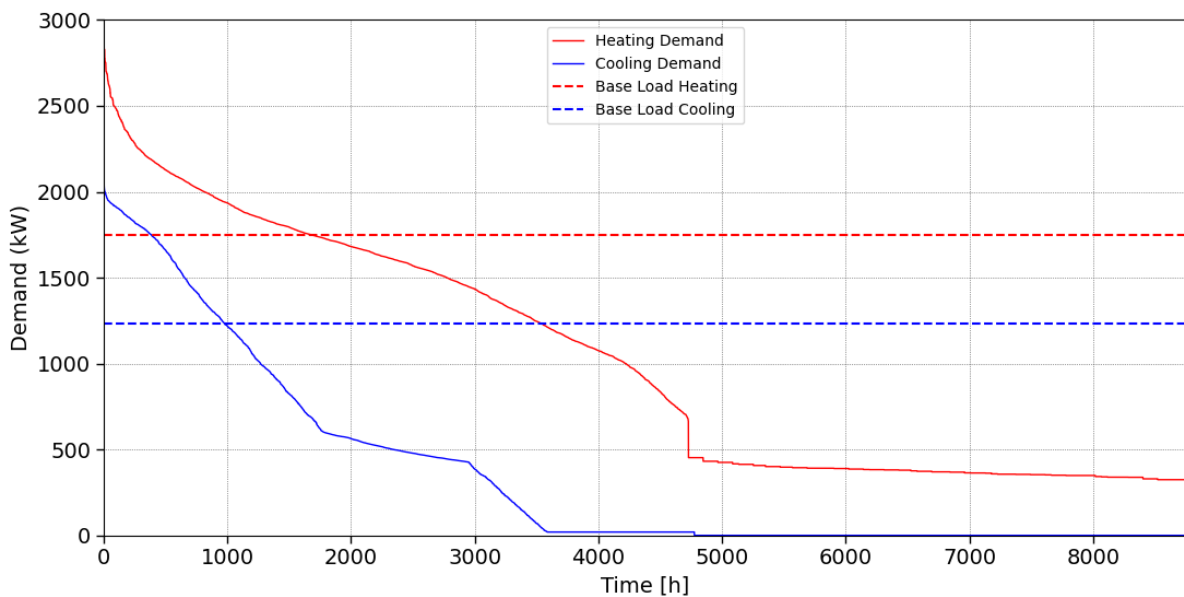
Figure 31: Annual duration curves for heating and cooling demand

From 0 up to $450\ kW$ the heat curve exhibits a flat course for approximately $4000\ h$, due to the relatively constant demand during summer. A large proportion of the heat load can therefore be covered with a small number of RHPs. Beyond this, up to approximately $2000\ kW$, the curve then displays a relatively constant gradient for another $4000\ h$. This is followed by a very steep end, which indicates that almost $1000\ kW$ of heating capacity would only be needed for around $800\ h$ per year. The annual duration curve for the cooling load is equal to 0 for about $3980\ h$ of the year. Following that, the curve exhibits a slight step-up to a very low power level for another $1200\ h$. Beyond this point, the demand shows a relatively constant gradient until reaching the highest peak.

In addition to the heating and cooling load data, the .txt file also provided data concerning the temperature requirements of the networks. Figure 32 shows the required supply and return temperatures levels in the DH and DC network.
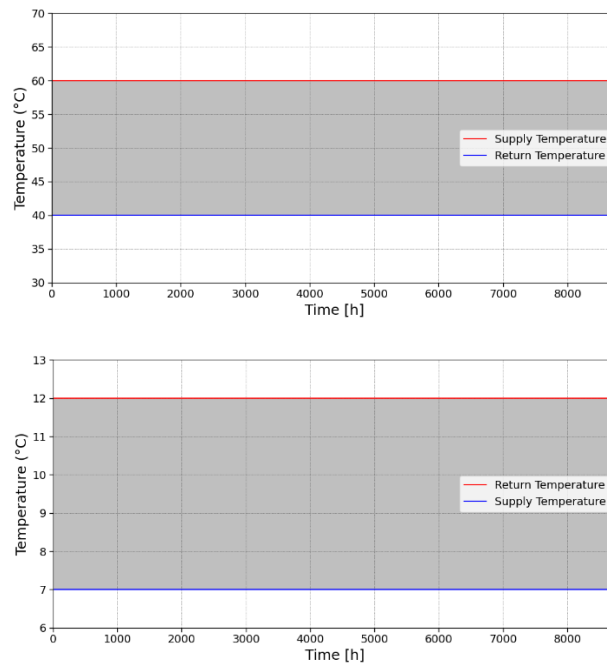
Figure 32: Required temperatures: DH network (above) and DC network (below)

As shown in Figure 32, the DH network requires a supply temperature of $60\,°C$ and a return temperature of $40\,°C$, while in the DC network a supply temperature of $7\,°C$ and a return temperature of $12\,°C$ is demanded. Table 5 summarizes the characteristic data of the DH and DC network. As already mentioned, the baseload was assumed to be $60\,\%$ of the maximum demand.

Table 5: Characteristic data of the DH and DC network

Network	*Heating*	*Cooling*	*Unit*
Annual demand	8953,00	3087,50	$[MWh]$
Maximum demand	2911,05	2055,31	$[kW]$
Minimum demand	324,22	19,39	$[kW]$
Annual peak load	1164,42	822,13	$[kW]$
Annual base load	1746,63	1233,19	$[kW]$
Supply temperature	60	40	$[°C]$
Return temperature	7	12	$[°C]$

To determine the number of RHPs required to supply such a DHC network, a RHP from the manufacturer Hirdos available on the market, that meets the technical requirements as closely as possible, was used as a reference model. The relevant technical specifications of the RHP are listed in Table 6. [66]

Table 6: Relevant technical specification of the RHP model [66]

Model name	*WHA RV* 320
Manufacturer	*Hidros*
Source	*Water*
Sink	*Water*
Heating capacity (*EN14511*)	439,4 [kW]
Cooling capacity (*EN14511*)	368,5 [kW]
COP_H (*EN14511*)	5,39 [$-$]
COP_C (*EN14511*)	4,41 [$-$]
Upper temperature limit	60 [$°C$]
Lower temperature limit	-5 [$°C$]

Using this data, it was now possible to estimate the achievable heating and cooling coverage by a given number of RHPs. As already mentioned, the code used for this estimation can be found in Appendix 2: load_data_analysis.py. What the algorithm basically tries is to approximate the coverage that can be achieved by calculating how many RHPs are needed at each hour of the year to cover the heating and cooling demand simultaneously. The data obtained is then aggregated by the number of RHPs and saved within subgroups. With the information of how many hours of the year can be covered with a corresponding number of RHPs, and by applying weighting factors, the estimate is then calculated. Given that the heating and cooling capacity of the RHP is not the same, the heating and cooling component of the network had to be evaluated first separately. Figure 33 shows the number of RHP required to meet the system's hourly heating demands throughout the year.
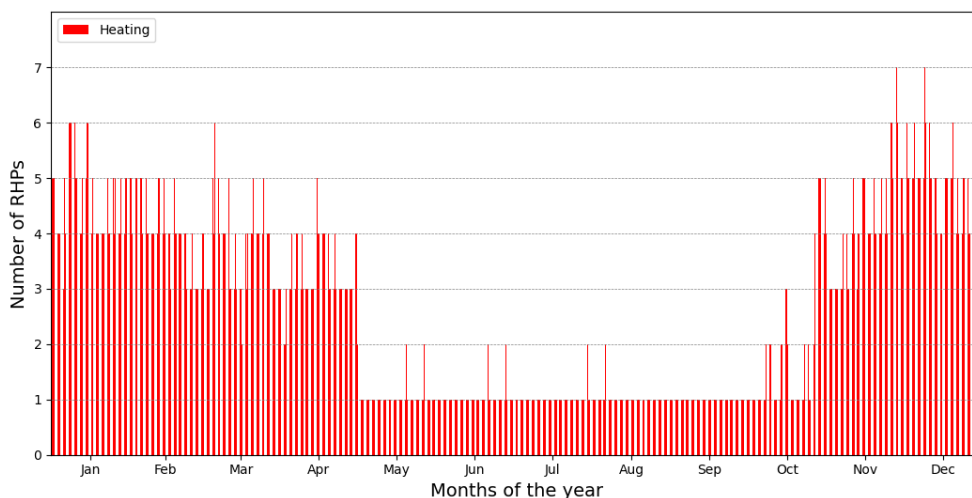
Figure 33: RHPs required to cover hourly heating demands

The same calculation was then carried out for the cooling network. Figure 34 shows the number of RHPs required to meet the system's hourly cooling demands throughout the year.
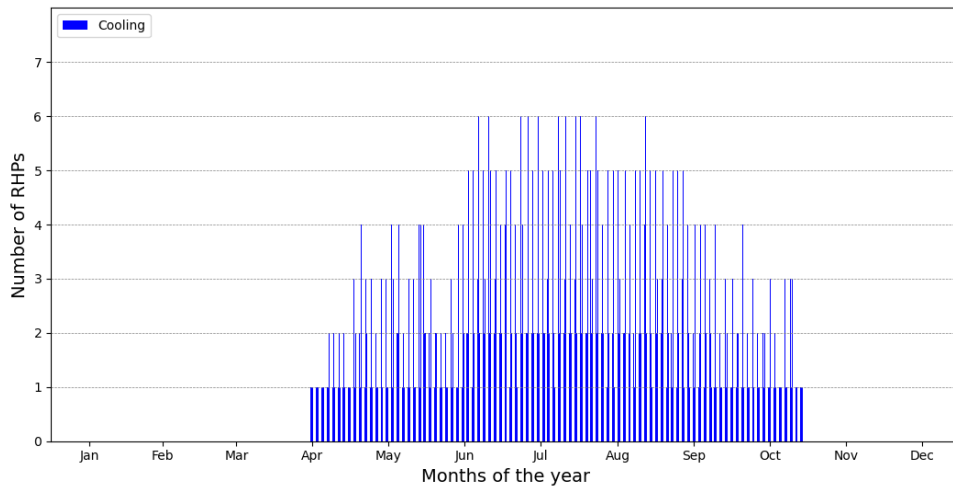
Figure 34: RHPs required to cover hourly cooling demands

By adding up the results, it was now possible to determine the number of RHPs needed to fully cover the hourly thermal demands for both heating and cooling. Figure 35 shows the number of RHPs required to meet the system's hourly heating and cooling demands throughout the year.
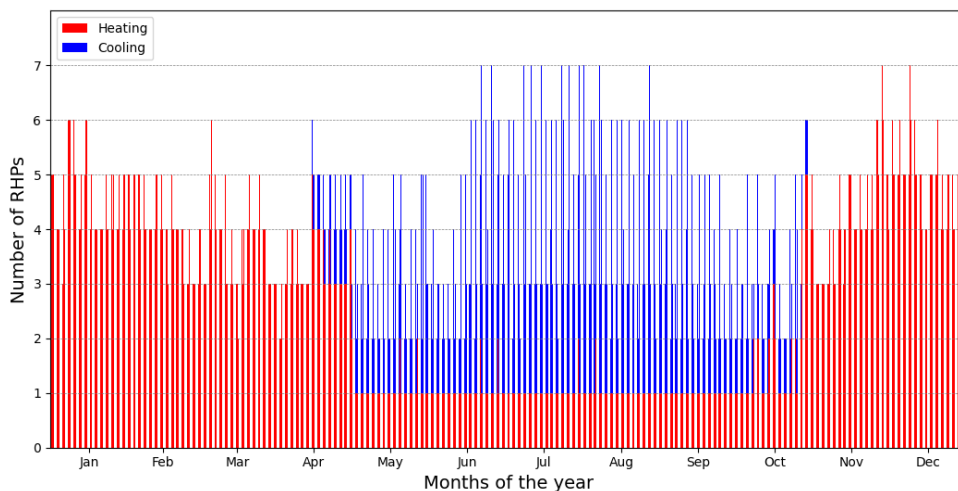
Figure 35: RHPs required to cover hourly heating and cooling demands

Figure 35 shows that with 7 RHPs the DHC demand can be covered for every hour of the year. However, it is also evident that 6 and 7 RHPs are needed for only relatively few hours of the year. In order to get a better idea of how many hours of the year can be covered exactly with a corresponding number of RHPs, the data displayed in Figure 35 is presented in form of a duration curve in Figure 36.
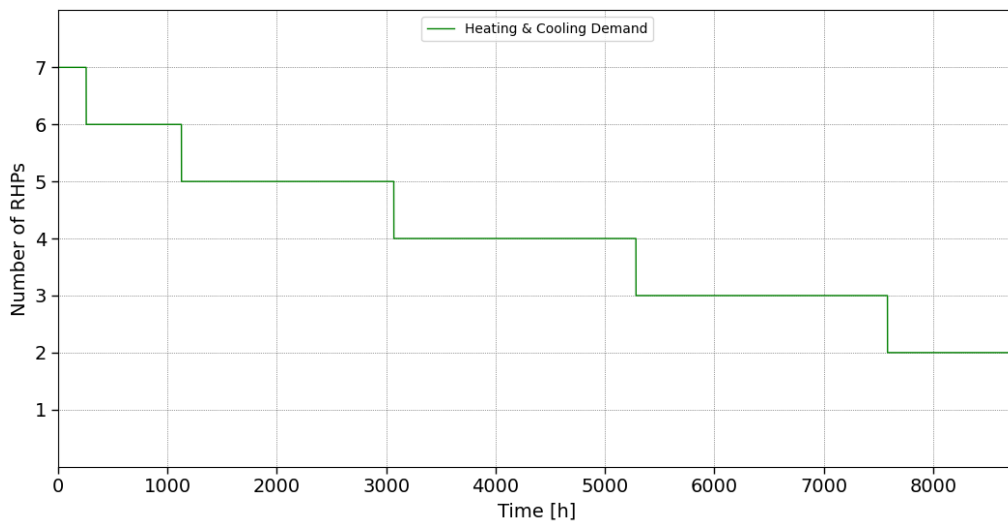
Figure 36: RHP duration curve

As the duration curve represents a quite conservative estimate for the RHP coverage, it can already be stated that a seventh RHP will probably not be integrated into the network, due to economic reasons linked to low capacity utilization. With the gathered information and by applying weighting factors, it was now possible to estimate the extent to which the demand can be covered with a given number of RHPs. The results of the calculation are shown in Figure 37.
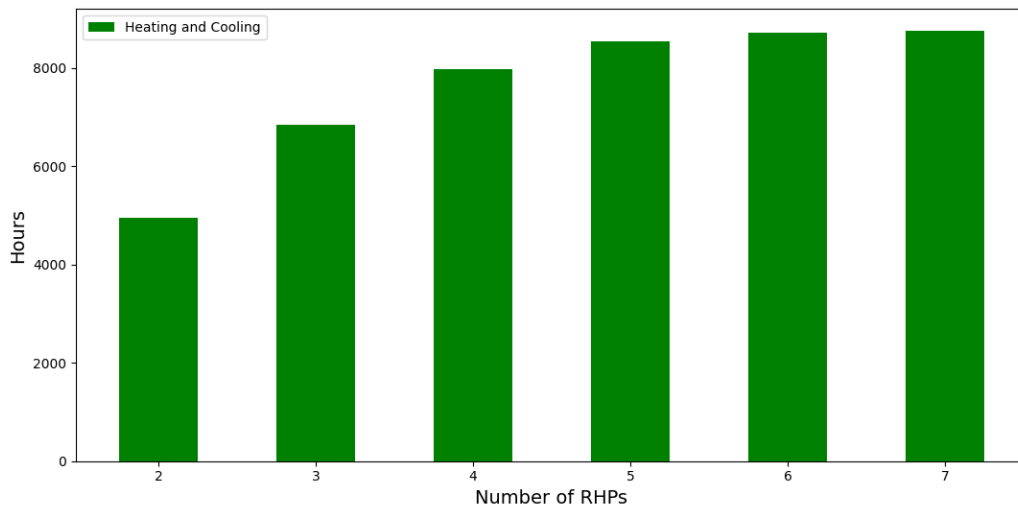
Figure 37: Absolute DHC coverage with the respective number of RHPs

In order to get a better understanding of the actual heating and cooling demand covered with the respective number of RHPs the absolute numbers shown in Figure 37 were plotted as a percentage of the 8760 yearly hours. Figure 38 shows the relative DHC coverage that can be achieved with the corresponding number of RHPs.
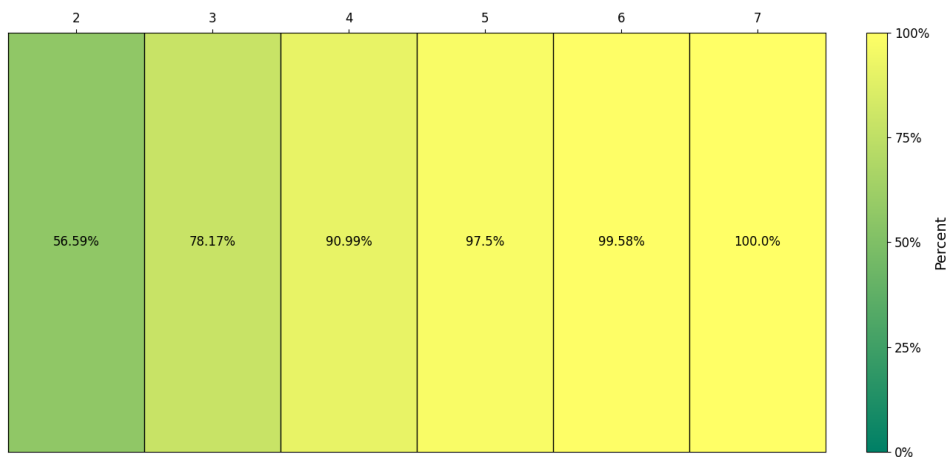
Figure 38: Relative DHC coverage with the respective number of RHPs

As maximizing DHC demand coverage via RHP is one of the main objectives, based on this estimation, a number of four, five and six RHPs was selected for the sensitivity analysis.

7.2 Power plant topology and TRNSYS model

The next step was to define the power plant's topology. After an extensive literature review, a topology consisting of vertical BHXs, reversible water to water GSHPs, and TES tanks was selected. Figure 39 shows the final power plant design in the simulation environment TRNSYS. [4, 5, 10, 47, 57, 67]
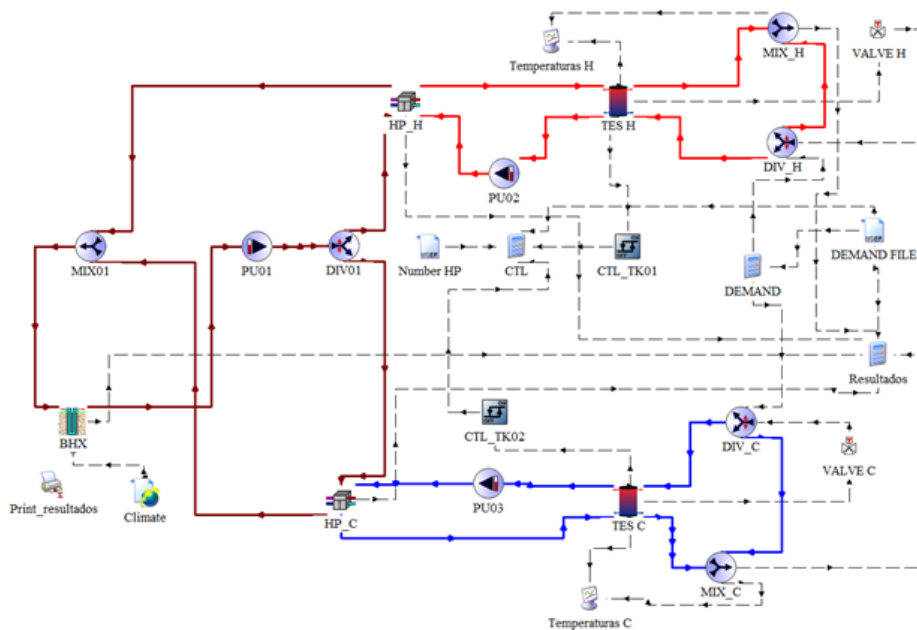
Figure 39: TRNSYS model of the DHC generation facility [68]

It is important to note that in this model, $2n$ non-reversible compression machines are used to simulate the behaviour of a power plant which deploys n RHPs, such as the one in Figure 25. In contrast to Figure 25, n RHPs connected in parallel would be used instead of one. This was achieved by integrating n HPs (HP_H) for heating and n CCs (HP_C) for cooling, with the condition that never more than n machines can be switched on at the same time. The corresponding number of HPs and CCs available for thermal energy generation at each hour of the year is determined by function plans which can be found in Appendix 1: Function Plans. These function plans ($Number\ HP$) are manually created .txt files that have been imported into the TRNSYS simulation environment and were derived using Figure 35. Since a number of four, five, and six RHPs were examined in the course of the sensitivity analysis, three of these function plans were created. Furthermore, it can be seen that two TES tanks are part of the power plant, one heat storage ($TES\ H$) and one cold storage ($TES\ C$). Whether the available HPs and CCs are active or not in each respective hour is determined by a temperature control (CTL_TK01 and CTL_TK02), which activates and deactivates the machines once the water in these tanks reaches a certain temperature level. As a result, the temperature in the tank is always slightly higher or lower than demanded by the load. However, in combination with the TESs, the temperature control allows the RHPs to be operated consistently at their rated power, eliminating the need to adjust to fluctuating loads. Furthermore, the buffer tanks allow for the coverage of load peaks that otherwise could not be met. The vertical BHXs (BHX) serve as a heat source during heating operation and as a heat sink during cooling operation. These BHXs are influenced by the given climatic conditions ($Climate$), which are imported to the model in form of a .txt file. With "$DEMAND\ FILE$", the heat and cooling load data, in the form of .txt files, are passed to TRNSYS. Based on this data, the mass flow of water required to cover the heating and cooling demand at the given temperature levels is calculated with "DEMAND". Through "CTL", the mass flows at the sources and sinks of the machines are then adjusted with the aid of pumps ($PU01$, $PU02$ and $PU03$) and a splitter ($DIV01$). The mass flows returning to the BHX are combined by means of a mixer ($MIX01$) and directed into the BHX, from where the water is then conveyed back to the splitter. Furthermore, the mass flows directed towards the load are adjusted to the required temperature level if the temperature in the tank is too high (heat) or too low (cooling) due to the temperature control. For this purpose, a certain amount of water is diverted from the mass flows coming from the load (DIV_H and DIV_C) and mixed with the mass flows going to the load using mixers (MIX_H and MIX_C). The amount of water required is calculated and adjusted through valves ($VALVE\ H$ and $VALVE\ C$) in response to the temperature levels. Since the mass flow going to the load is kept constant during the calculation, the mass flow coming from the storage is reduced by the corresponding amount. With "$Resultados$" the desired data is collected, further processed utilizing

fundamental thermodynamic equations, and converted into units that are more useful for further calculations in Python. Using "$Print\_resultados$", the results can be exported in form of a .txt file. The symbols "$Temperaturas\ C$" and "$Temperaturas\ H$" allow for a graphical display in the temperature profiles in the tanks over the course of the year and have no impact on the simulation results.

7.3 Input data

In the following, the input data for the calculation scheme, which is described in the next section, is presented. Although the calculation scheme was created first and the required data determined afterwards, the data is presented in advance for didactic reasons. The input data for the KPI calculation can be divided into five categories:

1. Power plant topology data of the TRNSYS model
2. Input data from the literature research
3. Input data from the load profiles
4. Input data from the function plans
5. Simulation results from the TRNSYS model

Table 7 shows the power plant's topology data. The sensitivity analysis was carried out with regard to TES sizes and the number of RHPs, which is why the text "varies" can be found instead of a value in the table. The concrete values selected for the analysis can be found in Chapter 7.5. The number of BHX is automatically determined by TRNSYS depending on the demand and a standard value was selected for the drilling depth. [21]

Table 7: Power plant topology data of the TRNSYS model

Quantity	Symbol	Value	Unit
Total number of installed RHPs	Nr_{RHP}	varies	$[-]$
Volume TES heating	V_{TES_H}	varies	$[m^3]$
Volume TES cooling	V_{TES_C}	varies	$[m^3]$
Number of BHX	Nr_{BHX}	223	$[-]$
Depth BHX	d_{BHX}	100	$[m]$

In Table 8 the input data derived from the literature research is shown. These factors were kept constant during the sensitivity analysis and the values represent averages from various literature sources. For electricity and gas, an average value of the prices in the EU since 2010

has been calculated. The emission factor for electricity also represents the EU average and the CO_2 certificate costs were assumed to be $80 \, €/t$. The lifetimes of the TESs and BHXs are not included in the calculation as they do not need to be replaced during the system's lifetime, which was assumed to be 30 years. However, in order to justify this no-inclusion, the respective lifetimes were researched.

Table 8: Input data derived from literature research

Quantity	Symbol	Value and Unit	Source
Investment cost compression HP	$CAPEX_{CHP_{specific}}$	$494{,}55 \, [\frac{€}{kW}]$	[69–74]
Investment cost BHX	$CAPEX_{BHX_{specific}}$	$58{,}27 \, [\frac{€}{m}]$	[65, 69, 75–78]
Investment cost boiler	$CAPEX_{B_{specific}}$	$93{,}33 \, [\frac{€}{kW}]$	[69, 74, 79]
Specific electricity cost	$Cost_{el_{specific}}$	$0{,}14 \, [\frac{€}{kWh}]$	[80]
Specific gas cost	$Cost_{gas_{specific}}$	$0{,}06 \, [\frac{€}{kWh}]$	[81]
CO_2 cost	$Cost_{CO_2}$	$8{,}00 * 10^{-5} \, [\frac{€}{g}]$	[82–84]
Heating capacity	P_H	$439{,}40 \, [kW]$	[66]
Cooling capacity	P_C	$368{,}50 \, [kW]$	[66]
Emission factor electricity	$f_{CO_{2el}}$	$266{,}73 \, [\frac{gCO_2 \, eq}{kWh}]$	[85–88]
Emission factor boiler	$f_{CO_{2B}}$	$227{,}80 \, [\frac{gCO_2 \, eq}{kWh}]$	[74, 89]
Fixed O&M factor	$f_{O\&M_{fix}}$	$3 \, [\%]$	[10, 69, 73]
Discount rate	r	$5 \, [\%]$	[69, 90]
Efficiency boiler	η_B	$90 \, [\%]$	[74, 79, 91]
SCOP of the ASHP	$SCOP_{ASHP}$	$3{,}66 \, [-]$	[51]
Lifetime compression HP	l_{CHP}	$15 \, [years]$	[92, 93]
Lifetime boiler	l_B	$15 \, [years]$	[79, 93, 94]
Lifetime BHX	l_{BHX}	$50 \, [years]$	[95, 96]
Lifetime TES	l_{TES}	$30 \, [years]$	[65, 90]

Table 9 shows the relevant data for the KPI calculation, which were derived from the load profiles. The sources of the data are .txt files provided by the Department of Energy Engineering at the Universidad Politécnica de Madrid (UPM), in Madrid, Spain.

Table 9: Input data from the load profiles

Quantity	Symbol	Value and Unit	Source
Heating demand	$Q_{H_{demand}}$	8953,00 [MWh]	UPM
Cooling demand	$Q_{C_{demand}}$	3087,50 [MWh]	UPM
Maximum heating demand	$Q_{demand_{max_H}}$	2911,05 [kW]	UPM
Maximum cooling demand	$Q_{demand_{max_C}}$	2055,31 [kW]	UPM

As already mentioned, in order to conduct the simulation in TRNSYS, a separate function plan was created for each number of RHPs. These function plans can be found in Appendix 1: Function Plans. The data from these function plans, which was used in the KPI calculation, is presented in Table 10. As data, which comes from the function plans, is different for each number of RHPs, no numerical value is provided here.

Table 10: Input data from the function plans

Quantity	Symbol and Unit	Source
Total number of installed RHPs	Nr_{RHP} [−]	Appendix 1
Number of active RHPs for heating each hour	Nr_{RHP_H} [−]	Appendix 1
Number of active RHPs for cooling each hour	Nr_{RHP_C} [−]	Appendix 1
Highest number of active RHPs for heating	$max(Nr_{RHP_H})$ [−]	Appendix 1
Highest number of active RHPs for cooling	$max(Nr_{RHP_C})$ [−]	Appendix 1

In Table 11, the input data calculated via the TRNSYS simulation environment is shown. Since the input data, which comes from TRNSYS, has been calculated for each topology separately, no numerical value is provided here.

Table 11: Simulation results from the TRNSYS model

Quantity	Symbol and Unit	Source
Hourly provided heat in heating mode at the sink	$Q_{H_{sink}}$ [kWh]	[68]
Hourly provided cold in cooling mode at the source	$Q_{C_{source}}$ [kWh]	[68]
Hourly required electrical work in heating mode	W_{in_H} [kWh]	[68]
Hourly required electrical work in cooling mode	W_{in_C} [kWh]	[68]
Hourly provided heat at the load	$Q_{H_{delivered_{RHP}}}$ [kWh]	[68]
Hourly provided cold at the load	$Q_{C_{delivered_{RHP}}}$ [kWh]	[68]

With this data, it was now possible to determine the LCOE, actual RHP coverage and specific CO_2 emissions for a given topology using the calculation scheme.

7.4 Calculation scheme

With the aim of calculating the LCOE, the RHP coverage and the specific CO_2 emissions for a given topology in a systematic and reproducible manner, a calculation scheme was defined. To achieve this objective, the first step was to define general equations for the LCOE, RHP coverage and specific CO_2 emissions on which the KPI calculation scheme is based.

The LCOE is a measure of the average net present cost of a power plant's power generation over its lifetime. It is calculated by dividing the total life cycle cost of the plant by the total amount of energy it is expected to generate during its lifetime, taking into account the time value of money. This allows the cost-effectiveness of different generation technologies to be compared on a consistent basis. However, in order to understand the LCOE, it is first important to understand the net present value (NPV). The NPV is the difference between the present value of cash inflows and cash outflows minus the initial investment (I_0) over a period of time. Therefore, the NPV indicates the profitability of a project. A positive NPV suggests a profitable investment, while a negative NPV indicates a loss. To calculate the LCOE it is assumed that the project's NPV is equal to zero. This assumption is made because the LCOE calculation aims to find the price per unit of electricity (e.g. per kWh) that would make the project break even over its lifetime. Thus, the total discounted revenue from energy sales is set to equal the total discounted expenditures of building and operating the plant, which corresponds to an NPV of zero. As previously mentioned, the project's lifetime was assumed to be 30 years, and the discount rate r was set at 5 %.

$$NPV = -I_0 + \sum_{t=0}^{t=30} \frac{Cash\ Inflow}{(1+r)^t} - \sum_{t=0}^{t=30} \frac{Cash\ Outflow}{(1+r)^t} = 0\ [\text{€}] \qquad (6\text{-}1)$$

In this case cash inflow corresponds to the product of the LCOE and the amount energy generated, while cash outflow corresponds to the expenditures.

$$NPV = -I_0 + \sum_{t=0}^{t=30} \frac{Generated\ Energy * LCOE}{(1+r)^t} - \sum_{t=0}^{t=30} \frac{Expenditures}{(1+r)^t} = 0\ [\text{€}] \qquad (6\text{-}2)$$

$$I_0 + \sum_{t=0}^{t=30} \frac{Expenditures}{(1+r)^t} = LCOE * \sum_{t=0}^{t=30} \frac{Generated\ Energy}{(1+r)^t}\ [\text{€}] \qquad (6\text{-}3)$$

By further rearranging of the equation, a general calculation formula for calculating the LCOE can be derived.

$$LCOE = \frac{-I_0 + \sum_{t=0}^{t=30} \frac{Expenditures}{(1+r)^t}}{\sum_{t=0}^{t=30} \frac{Generated\ Energy}{(1+r)^t}} = \frac{NPV\ of\ Total\ Costs\ Over\ Lifetime}{NPV\ of\ Energy\ Produced\ Over\ Lifetime} \ [\frac{€}{kWh}] \qquad (6\text{-}4)$$

The discount rate r in this formula expresses the time value of money. It acknowledges that money today is worth more than the same amount of money in the future due to its potential earning capacity. This is particularly relevant for long-term energy projects where costs and outputs are spread over many years. Furthermore, r can be interpreted as a measure of risk as a higher discount rate adjusts the LCOE upwards, making the project appear more expensive on a per-unit-of-energy basis. Thus, higher discount rates are used for projects with higher perceived risks, indicating that future earnings (in this case, cost savings or revenues from energy production) are less certain and must be greater in order to cover the initial and operational cost. Conversely, a lower discount rate results in lower LCOE, therefore reflecting less risk.

The general formulae used for calculating the specific CO_2 emissions and the RHP coverage are shown in equation (6-5) and equation (6-6).

$$Specific\ CO_2\ Emissions = \frac{\sum Total\ CO_2\ Emissions}{\sum Thermal\ Energy\ Delivered} \ [\frac{gCO_2eq}{kWh}] \qquad (6\text{-}5)$$

$$RHP\ Coverage = \frac{\sum Thermal\ Energy\ Delivered\ by\ RHPs}{\sum Thermal\ Energy\ Demanded} \ [\%] \qquad (6\text{-}6)$$

Based on this framework of general formulae, a calculation scheme was derived in order to determine the LCOE, specific CO_2 emissions and RHP coverage for any given topology. On the basis of this calculation scheme, it was then possible to carry out the sensitivity analysis. It should be mentioned in advance that it was assumed that peak loads which cannot be covered by RHPs will be met with a gas boiler and an ASHP. Direct construction cost, project engineering and development cost, project financing costs, contingency costs, decommissioning costs and residual values of the components were not included in the calculation. Additionally, as only the power plant was considered, cost and losses associated with piping and pumping in the network were also not included in the calculation. As already mentioned, the project lifetime for the calculation was assumed to be 30 years. For reasons of clarity, a distinction was made between a technology level and a system level during the KPI calculation. Furthermore, the KPIs were grouped into technical, economical, and ecological ones.

7.4.1 Technological key performance indicators

In the following, the KPIs used for evaluating the individual technologies are presented and described. All variables used in the calculation scheme are described in the subsequent text or can be found in the tables in Chapter 7.3.

7.4.1.1 Key performance indicators for reversible heat pumps

The technological KPIs that were defined for the RHPs are the SCOP in heating and cooling mode ($SCOP_H$, and $SCOP_C$), the annual performance factor (APF), the heating and cooling coverage via RHPs ($Coverage_{H_{RHP}}$ and $Coverage_{C_{RHP}}$) as well as the total coverage via RHPs ($Coverage_{HC_{RHP}}$). The APF serves as a combined SCOP for heating and cooling together and describes how efficiently the RHPs can provide thermal energy throughout the year. The coverage KPIs measure how much of the respective thermal demand can be covered by the RHPs.

$$SCOP_H = \frac{\sum_{i=1}^{i=8760} Q_{H_{sink}}}{\sum_{i=1}^{i=8760} W_{in_H}} \; [-] \tag{6-7}$$

$$SCOP_C = \frac{\sum_{i=1}^{i=8760} Q_{C_{source}}}{\sum_{i=1}^{i=8760} W_{in_C}} \; [-] \tag{6-8}$$

$$APF = \frac{\sum_{i=1}^{i=8760} Q_{H_{sink}} + \sum_{i=1}^{i=8760} Q_{C_{source}}}{\sum_{i=1}^{i=8760} W_{in_H} + \sum_{i=1}^{i=8760} W_{in_C}} \; [-] \tag{6-9}$$

$$Coverage_{H_{RHP}} = \frac{\sum_{i=1}^{i=8760} Q_{H_{delivered_{RHP}}}}{\sum_{i=1}^{i=8760} Q_{H_{demand}}} * 100 \; [\%] \tag{6-10}$$

$$Coverage_{C_{RHP}} = \frac{\sum_{i=1}^{i=8760} Q_{C_{delivered_{RHP}}}}{\sum_{i=1}^{i=8760} Q_{C_{demand}}} * 100 \; [\%] \tag{6-11}$$

$$Coverage_{HC_{RHP}} = \frac{\sum_{i=1}^{i=8760} Q_{H_{delivered_{RHP}}} + \sum_{i=1}^{i=8760} Q_{C_{delivered_{RHP}}}}{\sum_{i=1}^{i=8760} Q_{H_{demand}} + \sum_{i=1}^{i=8760} Q_{C_{demand}}} * 100 \; [\%] \tag{6-12}$$

$CAPEX_{RHP}$, $OPEX_{RHP_{H_{var}}}$, and $OPEX_{RHP_{C_{var}}}$ were defined as economic KPIs for the RHPs. The CAPEX represents the investment cost for the installation of the RHPs, while variable OPEX reflect the cost for electrical work during operation. Since the heating capacity is greater than the cooling capacity, it was used to calculate $CAPEX_{RHP}$.

$$CAPEX_{RHP} = CAPEX_{CHP_{specific}} * Nr_{RHP} * P_H \; [€] \tag{6-13}$$

$$OPEX_{RHP_{H_{var}}} = \sum_{i=1}^{i=8760} W_{in_H} * Cost_{el_{specific}} \ [\text{€}] \tag{6-14}$$

$$OPEX_{RHP_{C_{var}}} = \sum_{i=1}^{i=8760} W_{in_C} * Cost_{el_{specific}} \ [\text{€}] \tag{6-15}$$

To take into account the emissions caused by the RHPs due to their electricity consumption, $m_{CO_{2_{RHP_H}}}$ and $m_{CO_{2_{RHP_C}}}$ were defined as ecological KPIs. By means of the emission factor for electricity, these KPIs could be calculated.

$$m_{CO_{2_{RHP_H}}} = \sum_{i=1}^{i=8760} W_{in_H} * f_{CO_{2_{el}}} \ [gCO_2eq] \tag{6-16}$$

$$m_{CO_{2_{RHP_C}}} = \sum_{i=1}^{i=8760} W_{in_C} * f_{CO_{2_{el}}} \ [gCO_2eq] \tag{6-17}$$

7.4.1.2 Key performance indicators for thermal energy storages

Only economic KPIs were considered for the TESs. In order to calculate the CAPEX, first the specific costs for the TESs ($Cost_{TES_{specific_H}}$ and $Cost_{TES_{specific_C}}$) were determined as a function of their storage volume. [65]

$$Cost_{TES_{specific_H}} = 5294{,}6 * V_{TES_H}^{-0.435} \ \left[\frac{\text{€}}{m^3}\right] \tag{6-18}$$

$$Cost_{TES_{specific_C}} = 5294{,}6 * V_{TES_C}^{-0.435} \ \left[\frac{\text{€}}{m^3}\right] \tag{6-19}$$

Based on the specific costs, the investment costs for the TESs ($CAPEX_{TES_H}$ and $CAPEX_{TES_C}$) could be calculated in the next step.

$$CAPEX_{TES_H} = Cost_{TES_{specific_H}} * V_{TES_H} \ [\text{€}] \tag{6-20}$$

$$CAPEX_{TES_C} = Cost_{TES_{specific_C}} * V_{TES_C} \ [\text{€}] \tag{6-21}$$

7.4.1.3 Key performance indicators for borehole heat exchangers

For the evaluation of the BHXs, only a single economic KPI was utilised. The following equation shows how the investment costs for the BHX ($CAPEX_{BHX}$) were calculated.

$$CAPEX_{BHX} = CAPEX_{BHX_{specific}} * Nr_{BHX} * d_{BHX} \ [\text{€}] \tag{6-22}$$

7.4.1.4 Key performance indicators for the gas boiler

As already mentioned, it was assumed that a natural gas boiler is used to cover peak heat loads which cannot be covered by the RHPs. In order to calculate the investment cost for the boiler ($CAPEX_B$), it was first necessary to estimate the required boiler capacity. Therefore, the product of the RHP heating capacity and the maximum number of RHPs available for heating

was subtracted from the maximum required heating demand. Based on this information, it was possible to determine the CAPEX.

$$CAPEX_B = \left(Q_{demand_{max_H}} - max\left(Nr_{RHP_H}\right) * P_H\right) * CAPEX_{B_{specific}} \; [€]$$ (6-23)

In order to determine the OPEX for the boiler operation, the next step was to calculate the amount of heat required from the boiler (Q_B).

$$Q_B = \sum_{i=1}^{i=8760} Q_{H_{demand}} - \sum_{i=1}^{i=8760} Q_{H_{delivered_{RHP}}} \; [kWh]$$ (6-24)

Knowing Q_B and taking into account the boiler efficiency (η_B), the gas demand (D_{gas}) and thus the variable OPEX for boiler ($OPEX_{B_{var}}$) operation could now be calculated.

$$D_{gas} = \frac{Q_B}{\eta_B} \; [MWh]$$ (6-25)

$$OPEX_{B_{var}} = D_{gas} * Cost_{gas_{specific}} \; [€]$$ (6-26)

Due to the combustion of gas, an ecological KPI ($m_{CO_{2_B}}$) was calculated in addition to the economical ones, to account for the emissions caused. By means of the emission factor of the boiler, the KPI could be calculated.

$$m_{CO_{2_B}} = Q_B * f_{CO_{2_B}} \; [gCO_2eq]$$ (6-27)

7.4.1.5 Key performance indicators for the air source heat pump

Furthermore, it was assumed that an ASHP is used to cover peak cold loads which cannot be covered by the RHPs. In order to calculate the investment cost for the ASHP ($CAPEX_{ASHP}$), it was first necessary to determine the required ASHP capacity. Therefore, the product of the RHP cooling capacity and the maximum number of RHPs available for cooling was subtracted from the maximum required cooling demand. Based on this information, it was now possible to calculate the CAPEX.

$$CAPEX_{ASHP} = \left(Q_{demand_{max_C}} - max\left(Nr_{RHP_C}\right) * P_C\right) * CAPEX_{CHP_{specific}} \; [€]$$ (6-28)

In order to determine the OPEX for the ASHP operation, the next step was to calculate the amount of cold required from the ASHP (Q_ASHP).

$$Q_{ASHP} = \sum_{i=1}^{i=8760} Q_{C_{demand}} - \sum_{i=1}^{i=8760} Q_{C_{delivered_{RHP}}} \; [kWh]$$ (6-29)

Knowing Q_ASHP and taking into account the SCOP of ASHPs, the electricity demand (D_{el}) and thus the variable OPEX for the ASHP operation ($OPEX_{ASHP}$) could now be estimated.

$$D_{el} = \frac{Q_{ASHP}}{SCOP_{ASHP}} \; [kWh]$$ (6-30)

$$OPEX_{ASHP_{var}} = D_{el} * Cost_{el_{specific}} \ [€] \tag{6-31}$$

Due to the consumption of electrical energy, an ecological KPI ($m_{CO_{2_{ASHP}}}$) was calculated in addition to the economical ones, to take into account the emissions caused. By means of the emission factor for electricity, the KPI could be calculated.

$$m_{CO_{2_{ASHP}}} = D_{el} * f_{CO_{2_{el}}} \ [gCO_2eq] \tag{6-32}$$

7.4.2 Systemic key performance indicators

The next step was to merge the KPIs of the individual technologies into systemic KPIs to enable an overall assessment of the system. To equitably allocate the CAPEX of technologies that are used for both heating and cooling the respective application, a cooling share (CS) was introduced. This cooling share was derived from the function plans. More precisely, it was calculated by dividing the sum of the hourly available RHPs for cooling by the sum of the hourly available RHPs for heating and cooling.

$$CS = \frac{\sum_{i=1}^{i=8760} Nr_{RHP_C}}{\sum_{i=1}^{i=8760} Nr_{RHP_C} + \sum_{i=1}^{i=8760} Nr_{RHP_H}} \ [-] \tag{6-33}$$

To calculate the present value of the investment cost for the heat and cold production (PV_{CAPEX_H} and PV_{CAPEX_C}), the CAPEX of the individual technologies was summed up, considering that some parts of the system are used for both heating and cooling. Since certain components (RHPs, boiler and ASHP) reach the end of their life after 15 years and need to be replaced, the present value of these future investments was also taken into account.

$$PV_{CAPEX_H} = (CAPEX_{RHP} + CAPEX_{BHX} + \frac{CAPEX_{RHP}}{(1+r)^{l_{CHP}}}) * (1 - CS) + CAPEX_{TES_H} + CAPEX_B + \frac{CAPEX_B}{(1+r)^{l_B}} \ [€] \tag{6-34}$$

$$PV_{CAPEX_C} = (CAPEX_{RHP} + CAPEX_{BHX} + \frac{CAPEX_{RHP}}{(1+r)^{l_{CHP}}}) * CS + CAPEX_{TES_C} + CAPEX_{ASHP} + \frac{CAPEX_{ASHP}}{(1+r)^{l_{CHP}}} \ [€] \tag{6-35}$$

Fixed OPEX ($OPEX_{H_{fix}}$ and $OPEX_{C_{fix}}$) incurred over the project's lifetime due to operation and maintenance were assumed to be a fixed percentage of the CAPEX.

$$OPEX_{H_{fix}} = CAPEX_H * f_{O\&M_{fix}} \ [€] \tag{6-36}$$

$$OPEX_{C_{fix}} = CAPEX_C * f_{O\&M_{fix}} \ [€] \tag{6-37}$$

In order to determine the variable OPEX for heating and cooling of the overall system, the total amount of the emitted CO_2 ($m_{CO_{2_H}}$ and $m_{CO_{2_C}}$) as well as the corresponding costs ($Cost_{CO_{2_H}}$ and $Cost_{CO_{2_C}}$) had to be calculated first.

$$m_{CO_{2_H}} = m_{CO_{2_{RHP_H}}} + m_{CO_{2_B}} \ [gCO_2eq] \tag{6-38}$$

$$m_{CO_{2_c}} = m_{CO_{2_{RHP_C}}} + m_{CO_{2_{ASHP}}} \; [gCO_2eq] \tag{6-39}$$

$$Cost_{CO_{2_H}} = Cost_{CO_2} * m_{CO_{2_H}} \; [\text{€}] \tag{6-40}$$

$$Cost_{CO_{2_c}} = Cost_{CO_2} * m_{CO_{2_c}} \; [\text{€}] \tag{6-41}$$

Taking into account the cost of CO_2, the variable OPEX for heating and cooling ($OPEX_{H_{var}}$ and $OPEX_{C_{var}}$) could now be calculated.

$$OPEX_{H_{var}} = OPEX_{RHP_{H_{var}}} + OPEX_{B_{var}} + Cost_{CO_{2_H}} \; [\text{€}] \tag{6-42}$$

$$OPEX_{C_{var}} = OPEX_{RHP_{C_{var}}} + OPEX_{ASHP_{var}} + Cost_{CO_{2_c}} \; [\text{€}] \tag{6-43}$$

In the next step, the total OPEX for heat and cold production ($OPEX_H$ and $OPEX_C$) were calculated by adding up fixed and variable OPEX.

$$OPEX_H = OPEX_{H_{fix}} + OPEX_{H_{var}} \; [\text{€}] \tag{6-44}$$

$$OPEX_C = OPEX_{C_{fix}} + OPEX_{C_{var}} \; [\text{€}] \tag{6-45}$$

Based on this information, it was now also possible to calculate the specific emissions for heating, cooling as well as for heating and cooling combined. Due to the assumption that the boiler and the ASHPs will cover the demand that cannot be met by RHPs, the thermal energy supplied is equal to the demand.

$$m_{CO_{2_{H_{specific}}}} = \frac{m_{CO_{2_H}}}{Q_{H_{demand}}} \left[\frac{gCO_2eq}{kWh} \right] \tag{6-46}$$

$$m_{CO_{2_{C_{specific}}}} = \frac{m_{CO_{2_c}}}{Q_{C_{demand}}} \left[\frac{gCO_2eq}{kWh} \right] \tag{6-47}$$

$$m_{CO_{2_{HC_{specific}}}} = \frac{m_{CO_{2_H}} + m_{CO_{2_C}}}{Q_{H_{demand}} + Q_{C_{demand}}} \left[\frac{gCO_2eq}{kWh} \right] \tag{6-48}$$

The next step necessary for the determination of the LCOE was the calculation of the present value of the OPEX and the thermal energy supplied for heating (PV_{OPEX_H} and $PV_{Q_{H_{demand}}}$), for cooling (PV_{OPEX_C} and $PV_{Q_{C_{demand}}}$) as well as for heating and cooling ($PV_{OPEX_{HC}}$ and $PV_{Q_{HC_{demand}}}$) over the projects lifespan t.

$$PV_{OPEX_H} = \sum_{t=1}^{t=30} \frac{OPEX_H}{(1+r)^t} \; [\text{€}] \tag{6-49}$$

$$PV_{Q_{H_{delivered}}} = \sum_{t=1}^{t=30} \frac{Q_{H_{demand}}}{(1+r)^t} \; [kWh] \tag{6-50}$$

$$PV_{OPEX_C} = \sum_{t=1}^{t=30} \frac{OPEX_C}{(1+r)^t} \; [\text{€}] \tag{6-51}$$

$$PV_{Q_{C_{delivered}}} = \sum_{t=1}^{t=30} \frac{Q_{C_{demand}}}{(1+r)^t} \; [kWh] \tag{6-52}$$

$$PV_{OPEX_{HC}} = \sum_{t=1}^{t=30} \frac{OPEX_H + OPEX_C}{(1+r)^t} \; [kWh] \tag{6-53}$$

$$PV_{Q_{HC_{delivered}}} = \sum_{t=1}^{t=30} \frac{Q_{H_{demand}} + Q_{C_{demand}}}{(1+r)^t} \; [kWh] \tag{6-54}$$

Knowing the present values, all the information necessary for the LCOE calculation was now established. Therefore, in the final step, the LCOE for heating ($LCOE_H$), for cooling ($LCOE_C$), and for the combined provision of heating and cooling ($LCOE_{HC}$) were calculated.

$$LCOE_H = \frac{PV_{CAPEX_H} + PV_{OPEX_H}}{PV_{Q_{H_{demand}}}} \; \left[\frac{€}{kWh}\right] \tag{6-55}$$

$$LCOE_C = \frac{PV_{CAPEX_C} + PV_{OPEX_C}}{PV_{Q_{C_{demand}}}} \; \left[\frac{€}{kWh}\right] \tag{6-56}$$

$$LCOE_{HC} = \frac{PV_{CAPEX_H} + PV_{CAPEX_C} + PV_{OPEX_{HC}}}{PV_{Q_{HC_{demand}}}} \; \left[\frac{€}{kWh}\right] \tag{6-57}$$

7.5 Sensitivity analysis

The next and final step was carrying out the sensitivity analysis. To achieve this, first the TRNSYS simulation environment was used to determine the necessary thermodynamic input data for the calculation scheme. Table 12 shows the different number of RHPs and volumes of the storage tanks for which the behaviour of the system was analysed.

Table 12: Values for which the system was analysed for its sensitivity

Quantity	*Value*	*Unit*
Total number of installed RHPs	$4 - 5 - 6$	$[-]$
TES volume heating	$500 - 1000 - 1500 - 2000$	$[m^3]$
TES volume cooling	$5500 - 6000 - 6500 - 7000$	$[m^3]$

In contrast to the number of RHPs, volumes at which good coverage is achieved were first found by trial and error and then values around these volumes were investigated. Further input data for the thermodynamic simulation were the heating and cooling capacity of the RHP as well as the COP values for heating and cooling, which can be found in Table 6. A simulation was carried out in TRNSYS for each of the resulting 48 different topology combinations to generate the necessary input data for the KPI calculation shown in Table 11. In order to calculate the LCOE, RHP coverage, specific CO_2 emissions as well as the other quantities for all topologies as described in the KPI calculation scheme, the relevant data from each of the

resulting TRNSYS result files was automatically read and graphically analysed using the second python program which is attached to this work as Appendix 3: result_analysis.py. To ensure the accuracy of this program, the calculation for one case was also carried out "manually" in Excel. The results generated are presented and discussed in the next chapter.

8 Results and discussion

In the following chapter, the results of the sensitivity analysis for all 48 topologies examined are graphically presented and interpreted. The target variables for measuring system performance during the analysis were the LCOE, the specific CO_2 emissions and the load coverage achieved by RHPs alone. Furthermore, the efficiency of the RHPs for the respective application was analysed. For the sake of clarity and due to space constraints, the analysis of all KPIs was conducted in a single figure. Moreover, due to the large amount of data, a direct comparison of all results would not have been effective. Therefore, the results for each number of RHPs are first presented and interpreted separately in Chapter 8.1. Subsequently, Chapter 8.2 draws conclusions that only become apparent when all data is considered.

8.1 Results of the sensitivity analysis

In the following section, the results of the sensitivity analysis for four, five and six RHPs are presented separately. For each case, the overall system along with its heating and cooling components were examined. This was necessary because the overall system involves superimposed results and some of the observed trends could only be explained through a more detailed breakdown.

8.1.1 Topologies with four reversible heat pumps

Subsequently, the results for topologies with a number of four RHPs are presented. Figure 40 shows the results for the overall system.
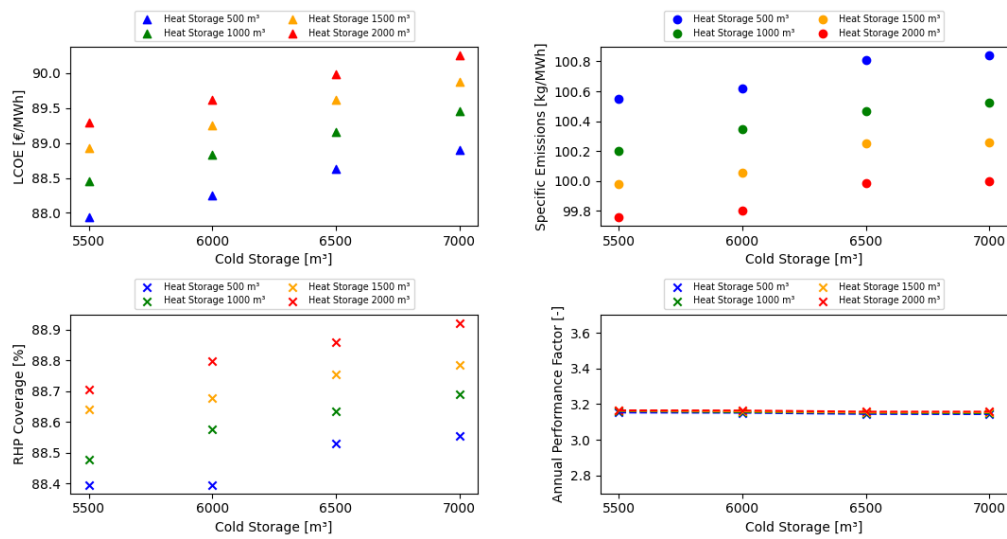
Figure 40: Results for four RHPs (heating and cooling)

As one might assume, the results show trends of increasing LCOE and RHP coverage for larger TES volumes (both heat and cold), though the variations within the studied range are relatively minor. The APF remains constant for all topologies at a value of around 3,16. Furthermore, while an increase in the size of the heat storage leads to lower specific emissions, these become higher as the size of the cold storage increases. Since the graph shows superimposed values of the results for heating and cooling, they had to be considered separately to understand this trend. Figure 41 shows the results for the heating network.
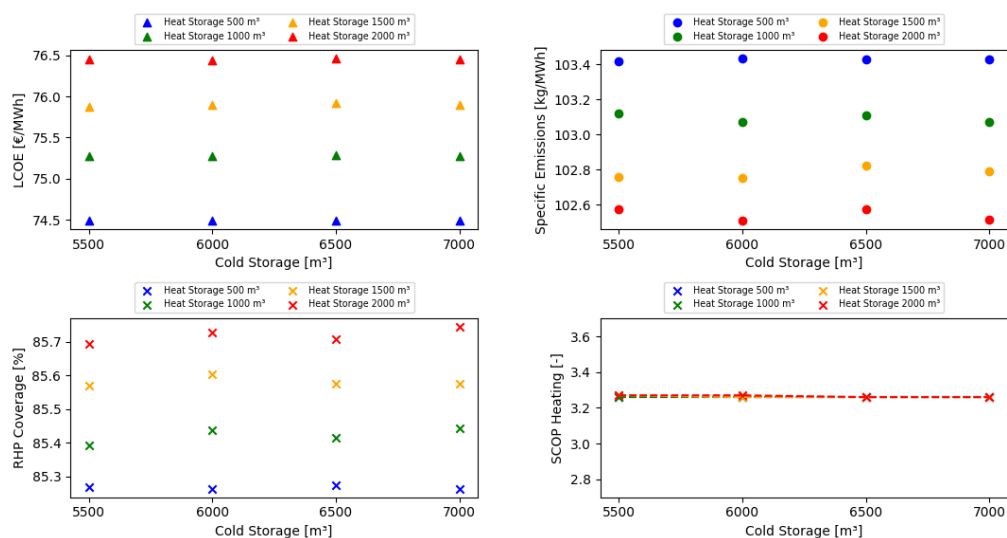
Figure 41: Results for four RHPs (heating)

As expected, the figure shows that the size of the cold storage has no effect on the LCOE, RHP coverage and specific CO_2 emissions related to the heating network. Larger heat storage tanks lead to elevated LCOE due to the higher CAPEX and decreased specific emissions, as

the gas consumption is lower due to the improved RHP coverage. Similar to the APF, the SCOP for heating remains constant for all topologies, but has a slightly higher value of around $3{,}27$. Figure 42 shows the results for the cooling network.
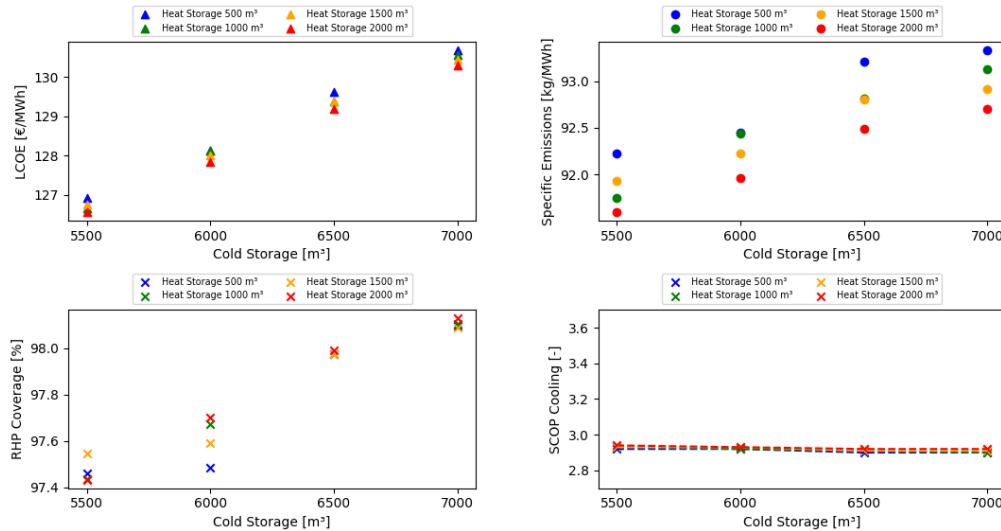
Figure 42: Results for four RHPs (cooling)

As anticipated, Figure 42 shows that the size of the heat storage has no effect on neither the LCOE nor the RHP coverage. The minor discrepancies observed in RHP coverage for $5500 \ m^3$ and $6000 \ m^3$ are attributable to inaccuracies in the simulation's calculation methods. Similarly, the specific emissions exhibit slight variations across identical cold storage volumes, deviating from the expected uniformity, due to the numerical methods used in the simulation. Larger cold storage tanks lead to higher LCOE due to increased CAPEX as well as better RHP coverage. Almost full coverage can already be achieved with just four RHPs. Similar to the APF, the SCOP for cooling remains constant, but at a slightly lower value of around $2{,}93$. To understand the trend of increasing specific emissions for larger cold storage tanks, three effects need to be considered. Firstly, within the calculation scheme, the thermal energy supplied to the load always matches the demand due to the auxiliary ASHP. Therefore, the denominator for the calculation of the specific emissions remains constant throughout all scenarios. Secondly, there is a proportionality between the RHP coverage and specific emissions. This is because the SCOP of the ASHP, at $3{,}66$, is higher than the SCOP of the RHPs, which leads to an increase in emissions when more cooling is provided by the RHPs. Thirdly, the thermal cooling losses need to be considered. Among other things, losses are incurred because the storage tanks are charged to unnecessarily high levels by the RHPs at hours of low demand due to the temperature control described in Chapter 7.2. As this produces cold that is not immediately fed into the grid but is subject to thermal losses, a certain amount of additional CO_2 is emitted over the course of the year. As this effect becomes more

pronounced with increasing tank sizes, it also leads to an increase in the specific emissions. In other words, for larger tank sizes, more cooling energy is provided to meet the same demand. As the cold provided is proportional to the CO_2 emissions this results in higher specific emissions. Figure 43 shows the thermal cooling losses for the different tank sizes.
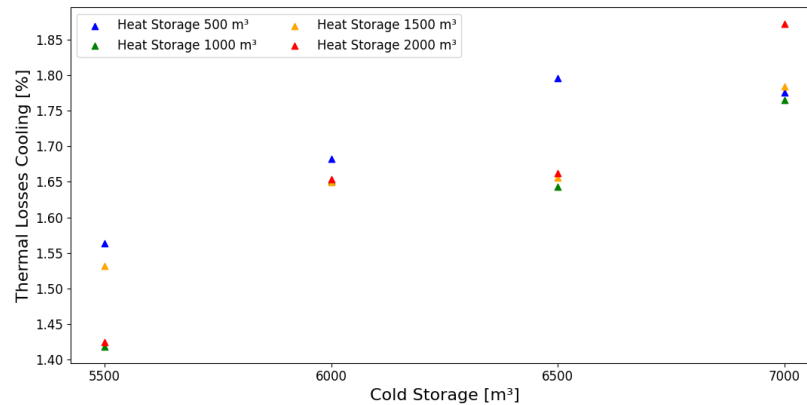
Figure 43: Thermal cooling losses for four RHPs

8.1.2 Topologies with five reversible heat pumps

In the next step, the calculation was carried out for topologies with five RHPs. Figure 44 shows the results.

Figure 44: Results for five RHPs (heating and cooling)

Apart from the same trends observed in Figure 40, with five RHPs the RHP coverage has significantly increased by around 7 %, while LCOE experiences only a marginal rise of around 1,5 €/MWh. Furthermore, the specific CO_2 emissions demonstrate a decline of approximately 7 kg/MWh, which is attributable to the reduced gas consumption due to the increased use of

RHPs. As well as for four RHPs the APF is constant but has a slightly smaller value of around 3,1. Next, the cooling and heating network were analysed separately again. Figure 45 shows the results for the heating network.
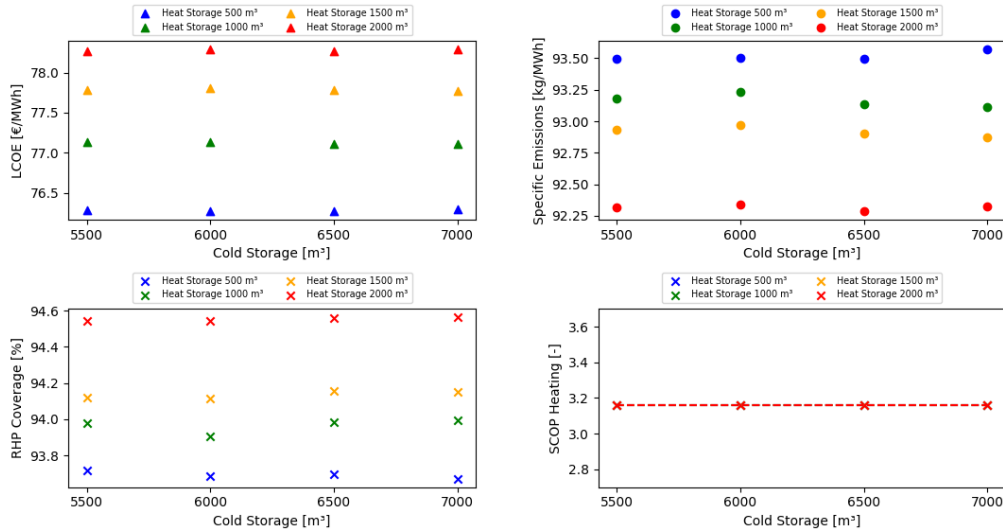
Figure 45: Results for five RHPs (heating)

Due to the fifth RHP higher LCOE and RHP coverage along with reduced specific emissions can be observed in the heating network. Furthermore, in comparison to four RHPs, slightly lower SCOP values are achieved. Apart from that, the trends for five RHPs align with those observed for four and are caused by the same phenomena. Figure 46 shows the results for the cooling network.
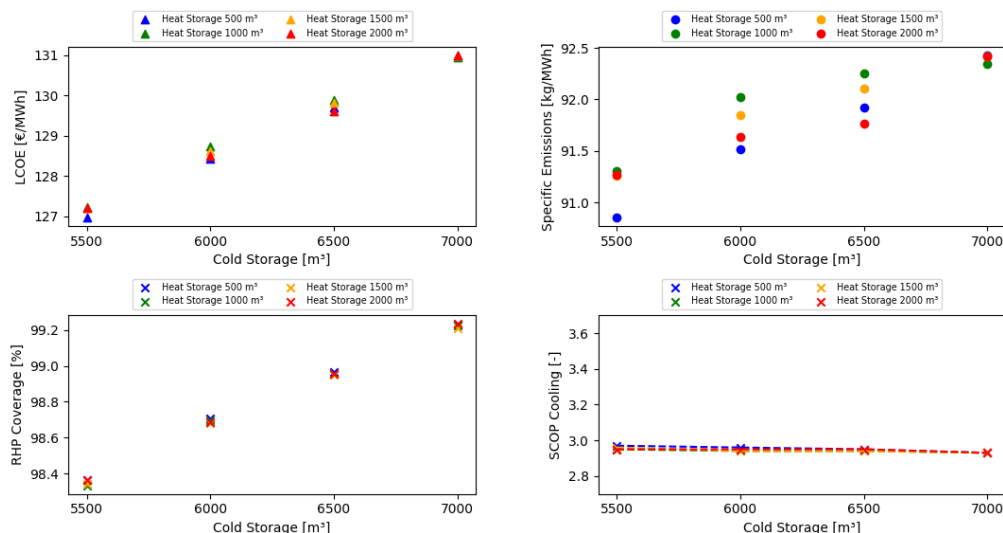
Figure 46: Results for five RHPs (cooling)

In addition to a minor increase in LCOE, RHP coverage and SCOP values, deploying five RHPs also resulted in a decline in specific cooling-related emissions. Apart from that, the

analysis reveals similar trends to those observed in the power plant with four RHPs. However, the deviations in RHP coverage for cold storage volumes of $5500\ m^3$ and $6000\ m^3$ are no longer present, and the values for specific emissions exhibit better convergence than for four RHPs. An examination of the RHP coverage and thermal cooling losses again explains the trend of increasing specific emissions for larger cold storages. Figure 47 shows the thermal losses for different cold tank volumes.
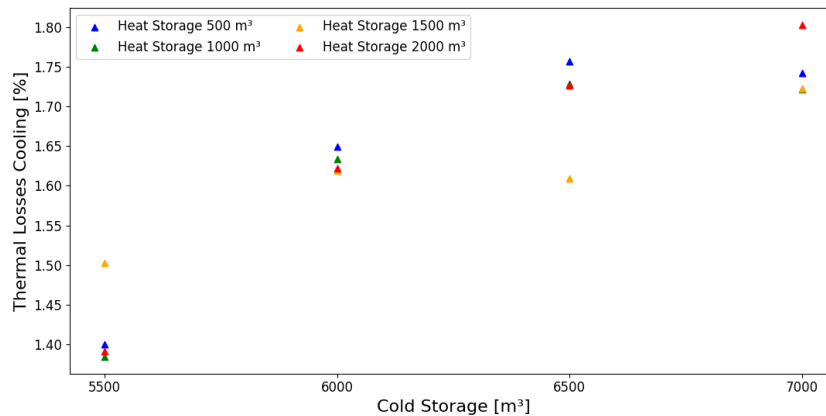
Figure 47: Thermal cooling losses for five RHPs

8.1.3 Topologies with six reversible heat pumps

In the following step the calculation was carried out for topologies with six RHPs. Figure 48 shows the results.
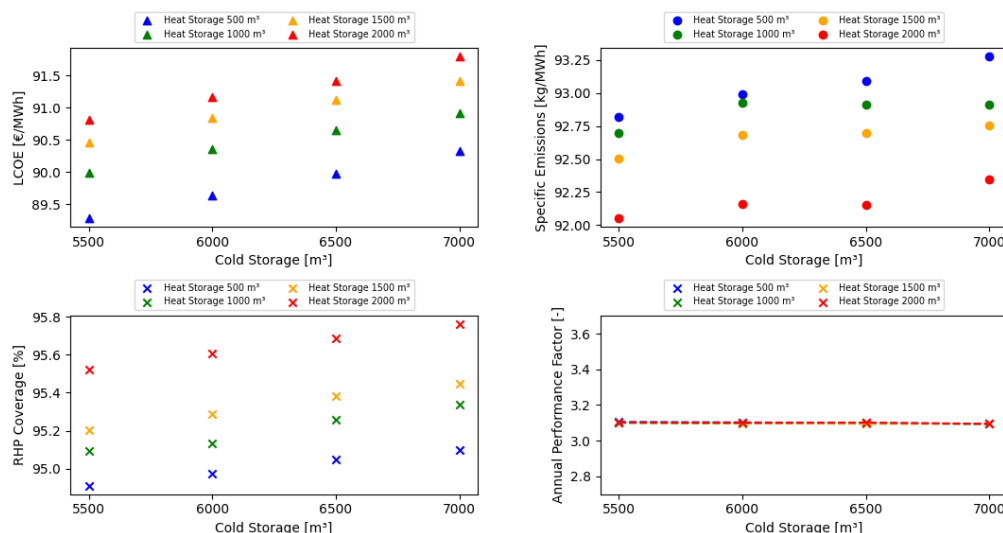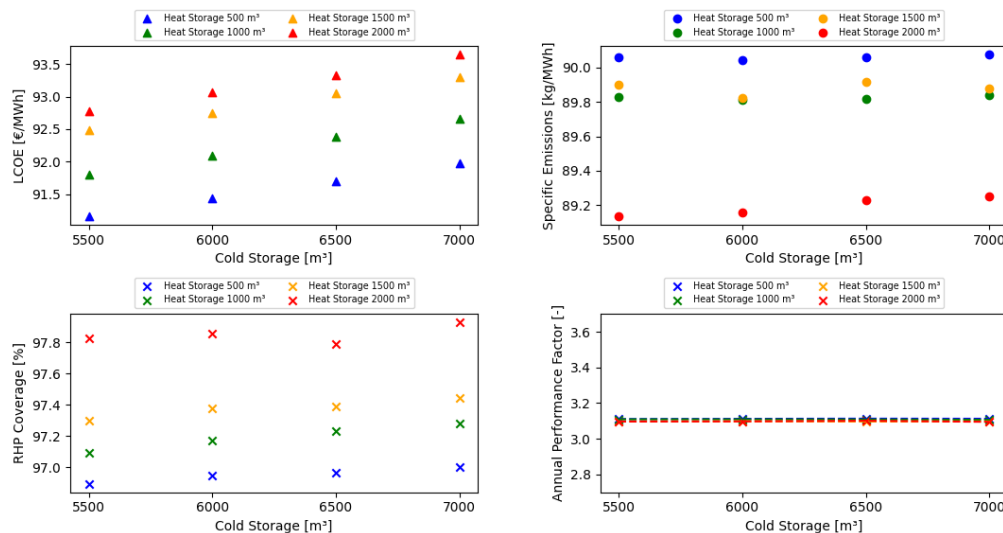

Figure 48: Results for six RHPs (heating and cooling)

Consistent with the observations for four and five RHPs, a trend towards elevated LCOE and RHP coverage is discernible for larger tank volumes. As well as for five RHPs, the APF is

constant and has a value of around 3,1. However, a sixth RHP leads to a further increase in RHP coverage of around 2 % as well as a decline in specific emissions of around 3 kg/MWh. This indicates that six RHPs would allow the thermal demand to be covered almost exclusively by RHPs with minimal specific emissions. The increase in LCOE of around 1,5 €/MWh is again relatively low. Furthermore, by deploying six RHPs, the proportional relationship between cold storage volume and specific emissions, observed in the previous setups, is only recognizable in the topology featuring the 2000 m^3 heat tank. Moreover, a deviation from the trend towards lower emissions with greater heat storages can be observed for a heating tank size of 1500 m^3. To understand these trends, the heating and cooling network were considered separately again. Figure 49 shows the results of the analysis for the heating network.
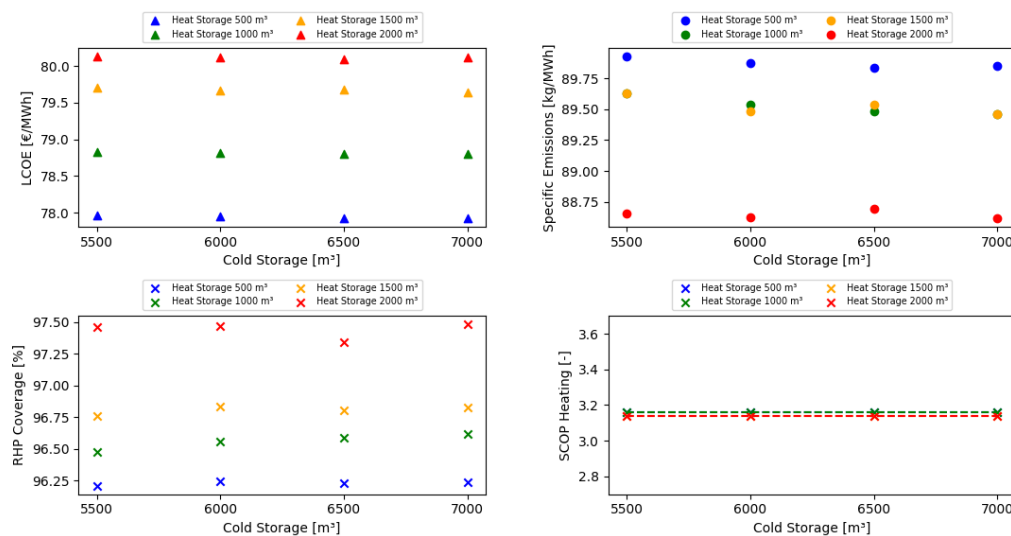
Figure 49: Results for six RHPs (heating)

The addition of a sixth RHP leads to a further increase in LCOE as well as RHP coverage, while simultaneously further reducing specific emissions. The heating-related SCOP values reach their minimum for such topologies. Apart from that, the same trends as for four and five RHPs can be observed. However, the trend of decreasing heating-related emissions for increasing heat storage volumes shows a deviation for a tank size of 1500 m^3. The deviation observed in Figure 48 can thus be directly attributed to the heating network. Depending on the size of the tank, almost complete coverage of the heating demand is now possible exclusively with RHPs. The next step was to examine the cooling network for topologies with six RHPs. Figure 50 shows the results of the analysis.
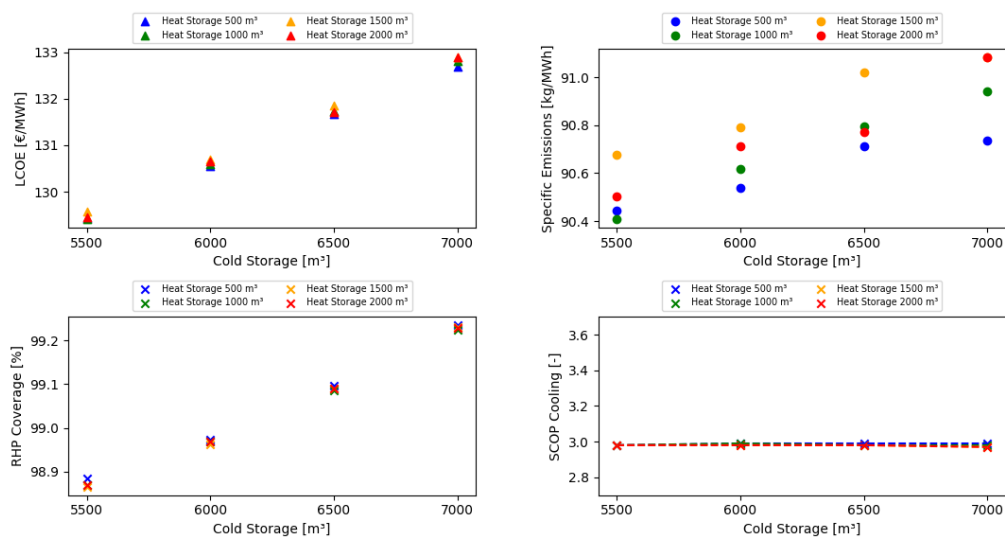
Figure 50: Results for six RHPs (cooling)

With the addition of a sixth RHP, the LCOE continue to increase, while the specific emissions can be further reduced. Cooling-related SCOP values reach their maximum for such topologies. Since almost full coverage can already be achieved with four RHPs, the addition of a sixth one does not result in any significant improvement compared to five. Apart from that, the same trends as for four and five RHPs can be observed. Just as for five RHPs, the values for the RHP coverage converge well in this scenario, whereas those for the specific emission once again are more widely spread. The trend towards an increase in cooling-related emissions for larger cold tank volumes can be attributed again to the higher RHP coverage and greater losses caused by larger tanks. Figure 51 shows the thermal cooling losses for the different tank sizes.
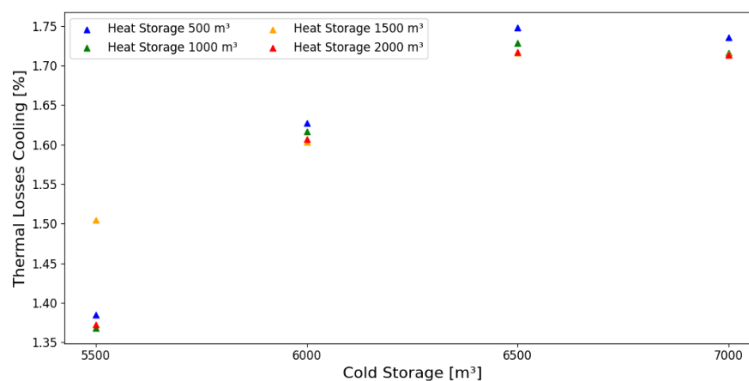
Figure 51: Thermal cooling losses for six RHPs

Therefore, the reason why the proportional relationship between cold storage tank size and specific emissions for tank sizes smaller than 2000 m^3 is no longer as pronounced for six RHPs

cannot be directly attributed to the cooling network. It results from the superposition of several effects that impact the results and are difficult to separate from one another.

8.2 Conclusions regarding all topologies

In the following section, conclusions are drawn that only become apparent when all topologies are considered. First the overall system is analysed and subsequently the heating and the cooling component are discussed separately.

8.2.1 Overall system

As it can be expected, the comparison of Figure 40, Figure 44 and Figure 48 shows that the LCOE and the RHP coverage increase with an increasing number of RHPs. An opposite trend can be observed for the specific emissions, which is due to the lower gas consumption. The APF and SCOP heating are approximately the same in all topologies, although the highest values are achieved by deploying four RHPs. In contrast, the SCOP cooling reaches its maximum by deploying six RHPs, although the values are also very close to each other. Figure 52 shows the APF, the SCOP in heating mode, as well as the SCOP in cooling mode for all topologies. Since the values for some topologies are identical, not all data points are visible.
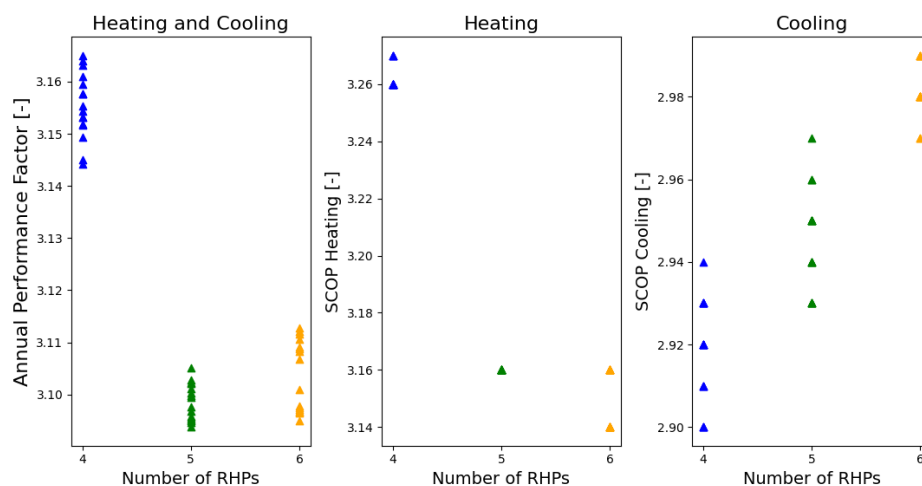
Figure 52: APF and SCOP values for all topologies

By increasing the number of RHPs from four to six, RHP coverage can be enhanced by around $10\,\%$ and specific CO_2 emissions reduced by around $10\,\mathrm{kg/MWh}$, while LCOE at the same time only experience a relatively minor rise of approximately $3\,€/MWh$. Therefore, for

the given demand profile and boundary conditions, six RHPs were identified as the optimal number for covering the heating and cooling load most efficiently when aiming to optimise cost, RHP coverage and specific CO_2 emissions. The corresponding optimal tank sizes identified are $2000\ m^3$ for the heat storage tank and $5500\ m^3$ for the cold storage tank, as this configuration achieves a very good RHP coverage with moderate LCOE and the lowest emissions. The trend towards lower specific emissions also shows the potential of HPs in terms of sustainable development. Although the average emission factor of the EU's electricity mix ($266{,}73\ \mathrm{k}g/MWh$) is higher than that of gas boilers ($227{,}80\ kg/MWh$), due to the APF of around $3{,}1$, the RHPs enable the provision of thermal energy with specific emission of $86{,}00\ \mathrm{k}g/MWh$ and thus make it possible to save CO_2.

8.2.2 Heating component

The conclusions pertaining to the heating network are clear and straightforward. By comparing Figure 41, Figure 45 and Figure 49 it can be observed that increasing the number of RHPs from four to six, results in approximately $11{,}5\ \%$ better RHP coverage and a significant reduction in heating-related emissions of around $14\ \mathrm{kg}/MWh$ due to the decreased gas consumption. Meanwhile, the LCOE experience only minor rise of about $3{,}5\ €/MWh$. These trends are clearly reflected in the overall system. The SCOP values in heating mode slightly decrease for an increasing number of RHPs. Furthermore, as it can be expected from the calculation scheme, the enlargement of the cold storage tank has virtually no influence on the results related to the heating network. The minor discrepancies observed are attributable to inaccuracies due to the numerical methods within the simulation.

8.2.3 Cooling component

The results for the cooling network, on the other hand, are less intuitive. By comparing Figure 42, Figure 46 and Figure 50 it is evident that the specific emissions in the cooling network for four RHPs are about $1{,}5\ \mathrm{kg}/MWh$ higher than for six. Nevertheless, as Table 8 shows, the SCOP of the ASHP has a value of $3{,}66$, therefore surpassing the SCOP of the RHPs in cooling mode of around $2{,}95$. This suggests that topologies with lesser RHPs are expected to yield better performance in terms of specific cooling-related emissions compared to those with a higher number of RHPs. However, the results indicate that this is not the case. The explanation can be found in a more detailed analysis of the system's efficiencies. Figure 52 clearly shows that within the cooling network, topologies with six RHPs achieve better SCOP values compared to those with five, which in turn surpass the SCOP values of topologies with four

RHPs. This variation of the SCOP values in cooling mode suggests that in topologies with a greater number of RHPs, the RHPs emit less CO_2 than in topologies with a smaller number. Combined with the fact that the ASHP plays a secondary role, since almost full coverage of approximately 97,5 % is already achieved with four RHPs and the smallest storage tank, this discrepancy in SCOP values leads to lower specific emissions for topologies with a high number of RHPs. In addition to that, the thermal cooling-related losses are somewhat lower for higher numbers of RHPs. Figure 53 shows a comparison of the thermal cooling losses.
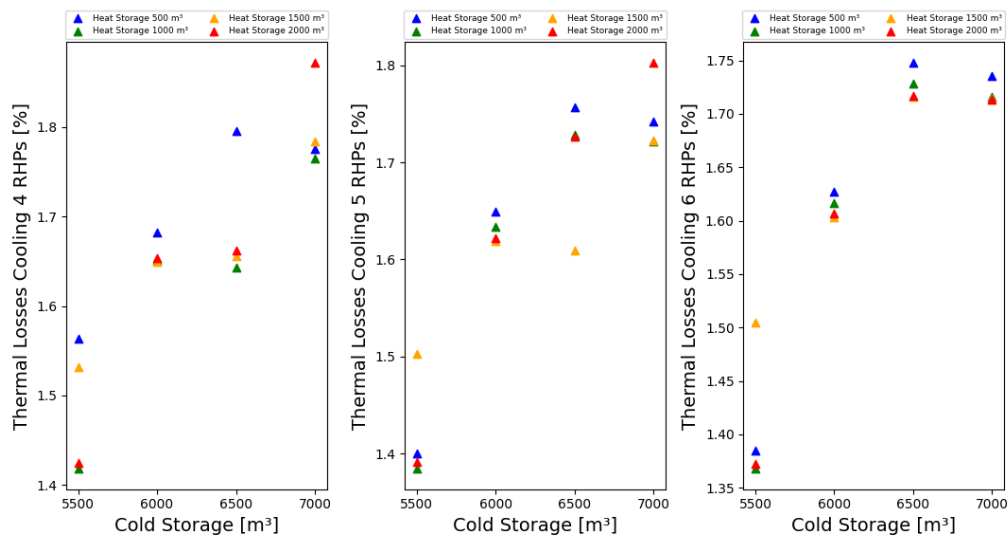
Figure 53: Comparison of the thermal cooling losses

Apart from that, the trends in the cooling network are also quite straightforward. An increase from four to six RHPs leads to a minor rise in LCOE of around $3 \, €/MWh$ and enhances RHP coverage by about 1,3 %. As expected, the enlargement of the heat storage tank has virtually no influence on parameters related to the cooling network. The minor discrepancies observed are attributable to inaccuracies due to the numeric methods applied within the simulation. Furthermore, the results show that almost complete coverage of the cooling demand can be already achieved with just four RHPs and the smallest cold storage tank, indicating that the units are oversized in terms of cooling provision. However, this is to some extent unavoidable, as a lower number of RHPs would mean that good coverage of the heating demand during winter, and therefore good coverage in the overall system, cannot be achieved.

9 Summary and future outlook

The following chapter summarizes the key findings from the literature review as well as the outcomes of the practical part of the work. Furthermore, possible paths for future endeavours regarding these aspects are outlined.

9.1 Geothermal energy in the district heating and cooling sector

In 2023, the heating and cooling sector accounted for half of Europe's final energy consumption and about 70 % of this energy was generated by the use of fossil fuels. This shows that the potential for decarbonization and greater energy independence through Europe's heating and cooling sector is substantial but remains largely untapped. Policymakers seek ways to expedite transformation in the thermal energy sector, enacting policies aimed at decarbonizing the sector and enhancing security of supply by valorising local resources. DHC systems exemplify best practice approaches for delivering locally available, cost-effective, and low-carbon thermal energy. Furthermore, they provide various interesting possibilities for the substitution of climate-damaging generation technologies through greener options in the heating and cooling sector on a large-scale. Within the context of fourth and fifth generation networks, the exploitation of the shallow geothermal potential presents a very promising pathway, as it provides the right temperature levels required for GSHP operation. In 2021, Europe saw the announcement of 13 new geothermal heating and cooling plants being integrated into district energy systems. This includes the development of Europe's largest geothermal (DH) facility in Aarhus, Denmark, which is expected to become partially operational by 2025. Furthermore, HPs and CCs are considered key technologies for the fossil fuel phase

out, with their use within DHC networks expected to increase significantly across Europe. Operating these machines in a reversible manner decreases CAPEX as one device can simultaneously offer cooling and heating. This applies to the reversible operation of standard compression machines as well as to RHPs, since their costs are comparable. Investment plans from some of the largest European DHC operators indicate that the capacity of large HPs is going to increase by at least 80 % by 2030. However, contemporary DHC systems are not on track to meet the climate targets set for 2050 by the IEA, so that in 2021 nearly 90 % of district heat was still generated via fossil fuels. Many DHC systems currently in operation are from the first three generations and need to be modernized. Especially, DC networks require more attention, as currently no comprehensive framework at the EU level to recognize and address the cooling challenge exists. With the anticipated expansion of existing networks and the emergence of new projects driven by increasing incomes, growing populations, and rising temperatures, the urgency for rapid improvement and greater integration of RES into DHC networks, to allow them to fully realize their potential in the energy transition, is evident. Moreover, the technologies discussed in this thesis present significant opportunities for achieving a sustainable low-carbon future in the district energy sector. They have the potential to efficiently generate heating and cooling by utilizing electrical energy and recovering waste heat. As a result, these technologies can increase the proportion of renewable energy in contemporary DHC systems, facilitate the transition away from fossil fuel-based individual generation units and enhance the flexibility in the overall energy systems. However, despite these advantages, technologies such as HPs and CCs are not commonly used for providing heat and cold in today's energy system. Furthermore, two aspects that were only peripherally addressed in this thesis but deserve much more attention are the thermal envelope of loads connected to the networks and how PtH technologies can be utilised in the future to provide flexibility in electrical grids. Future research should thus focus on how heating requirements of buildings can be reduced and how cross-sector integration can be best achieved.

9.2 Calculation model

Regarding the current state of the calculation model and the results obtained, the following points can be stated:

- A framework has been successfully developed to analyse large datasets from the TRNSYS simulation software and integrate this data into an overarching calculation scheme to enable a highly automated sensitivity analysis.

- The program written to estimate the RHP coverage (Appendix 2: load_data_analysis.py), with the aim of keeping the scope of the sensitivity analysis as limited as possible, shows promising results. The average error between the predicted coverage and the actual value is approximately 2,32 %. This program can be applied to any load profile provided as .txt or .csv with the same data structure.

- The results, and thus the conclusion drawn in Chapter 8, are dependent on the specific input parameters. For instance, in scenarios with very high electricity prices, CAPEX and increased operation and maintenance cost, it might be preferable to opt for a generation plant with five RHPs, accepting slightly lower coverages and higher emissions. Therefore, it must always be considered that the best possible options are heavily influenced by the specific boundary conditions. Especially in the context of renewable energy, this variability in cost structure is more pronounced than with fossil fuels, as there is no generic solution that can be applied universally. In fact, a significant challenge is that geothermal DHC systems are strongly tied to regional circumstances, including the availability of local heating and cooling resources and urban demands. To address this issue, local conditions must be compiled and quantified at regional, national, and international levels. Thus, it is important to know that the results obtained in this thesis are not generally applicable and may vary for different input values.

Regarding further optimisation and refinement of the calculation model, the following points could be considered:

- Due to the multitude of influencing factors and the resulting high number of different possibilities in the sensitivity analysis, this study focused exclusively on evaluating the impact of the power plant's topology on the specified target metrics. Subsequent analyses could therefore investigate how changes in electricity prices, emission factors, CO_2 prices, CAPEX, etc., impact these KPIs. The program written for the sensitivity analysis of the system (Appendix 3: result_analysis.py) provides a framework that has been developed for this purpose, as the input parameters can be easily adjusted, and the corresponding results calculated.

- The input data for the program can be improved and extended as the program's structure allows for an easy adoption of new variables. Although a thorough literature review has already been conducted, prices are subject to temporal fluctuations, and the cost structure can be further specified when more detailed information about the project is available. Direct construction costs, project engineering and development costs, project financing costs, contingency costs, decommissioning costs and residual values of the components are examples of how the costs could be specified in more detail.

Furthermore, the model used EU averages for variables such as the electricity price, emission factors and the gas prices. These variables can be adjusted to better align with local values.

- The TRNSYS model for the generation plant can be improved and expanded. The next steps would involve the simulation of the boiler and the ASHP in TRNSYS to better account for their thermodynamic behaviour. Furthermore, the model could be supplemented with a solar park, potentially reducing the oversizing of the cooling components, since heat generated in the summer could be stored and used in the winter. In this way, heat could be supplied from a TES rather than relying on the RHPs, potentially also enhancing their SCOP values.

10 Bibliography

[1] Piel, E., Mata, C., Lucas, P. and Pesce, G., DHC Market Outlook - Insights & Trends, https://www.euroheat.org/data-insights/outlooks/market-outlook-2023.

[2] Barco-Burgos, J., Bruno, J. C., Eicker, U., Saldaña-Robles, A. L. and Alćantar-Camarena, V., Review on the integration of high-temperature heat pumps in district heating and cooling networks (2021). DOI: 10.1016/j.energy.2021.122378.

[3] Rezaie, B. and Rosen, M. A., District heating and cooling: Review of technology and potential enhancements (2011). DOI: 10.1016/j.apenergy.2011.04.020.

[4] Wiltshire, Robin (Ed.), 2016, Advanced District Heating and Cooling (DHC) Systems, WOODHEAD PUBLISHING.

[5] Djurić, D. I., Classification of Measures for Dealing with District Heating Load Variations - A systematic Review (2020). DOI: 10.3390/en14010003.

[6] Sarbu, I., Mirza, M. and Muntean, D., Integration of Renewable Energy Sources into Low-Temperature District Heating Systems: A Review (2022). DOI: 10.3390/en15186523.

[7] Schönberger, Technisches Energiemanagement, 2022.

[8] Andrei, D., Mathiesen, B. V., Averfalk, H., Werner, S. and Lund, H., Heat Roadmap Europe: Large-Scale Electric Heat Pumps in District Heating Systems (2017). DOI: 10.3390/en10040578.

[9] Jangsten, M., Filipsson, P., Lindholm, T. and Dalenbäck, J.-O., High Temperature District Cooling: Challenges and Possibilities Based on an Existing District Cooling System and its Connected Buildings (2020). DOI: 10.1016/j.energy.2020.117407.

[10] Stephan, W., Dentel, A., Madjidi, M., Dippel, T., Schmid, J., Gu, B. and André, P., Design Handbook for Reversible Heat Pump Systems with and without Heat Recovery, https://iea-ebc.org/Data/publications/EBC_Annex_48_Final_Report_R4.pdf.

[11] Guelpa, E. and Verda, V., Thermal energy storage in district heating and cooling systems: A review (2019). DOI: 10.1016/j.apenergy.2019.113474.

[12] Rehman, O. A., Palomba, V., Frazzica, A., Charalampidis, A., Karellas, S. and Cabeza, L. F., Numerical and Experimental Analysis of a Low-GWP Heat Pump Coupled to Electrical and Thermal Energy Storage to Increase the Share of Renewables across Europe (2023). DOI: 10.3390/su15064973.

[13] Gang, W., Wang, S., Xiao, F. and Gao, D., District cooling systems: Technology integration, system optimization, challanges and opportunities for applications (2015). DOI: 10.1016/j.rser.2015.08.051.

[14] Popovski, E., Aydemir, A., Fleiter, T., Bellstädt, D., Büchele, R. and Steinbach, J., The role and costs of large-scale heat pumps in decarbonising existing district heating networks - A case study for the city of Herten in Germany (2019). DOI: 10.1016/j.energy.2019.05.122.

[15] Romaní, Joaquim; Ivancic, Aleksandar; All partners (Eds.), 2020, W.E. DISTRICT Heating & Cooling Solutions - D2.2 KPIs definition, European Union.

[16] Dodds, P. E., Staffell, I., Hawkes, A. D., Li, F., Grünewald, P., McDowall, W. and Ekins, P., Hydrogen and fuell cell technologie for heating: A review (2015). DOI: 10.1016/j.ijhydene.2014.11.059.

[17] Poul, Ø. A. and Lund, H., A renewable energy system in Frederikshavn using low-temperature geothermal energy for district heating (2010). DOI: 10.1016/j.apenergy.2010.03.018.

[18] Gudmundsson, O. and Thorsen, J. E., Source-to-sink efficiency of blue and green district heating and hydrogen-based heat supply systems (2022). DOI: 10.1016/j.segy.2022.100071.

[19] Böhm, H., Moser, S., Puschnigg, S. and Zauner, A., Power-to-hydrogen & district heating: Technology-based and infrastructure-priented analysis of (future) sector coulping potentials (2021). DOI: 10.1016/j.ijhydene.2021.06.233.

[20] Lund, H., Werner, S., Wiltshire, R., Scendsen, S., Thorsen, J. E., Hvelplund, F. and Mathiesen, B. V., 4th Generation District Heating (4GDH) (2014). DOI: 10.1016/j.energy.2014.02.089.

[21] Borge-Diez, David; Rosales-Asensio, Enrique (Eds.), 2023, Geothermal Heat Pump Systems, Springer Nature Sqitzerland AG.

[22] Gracía-Céspedes, J., Herms, I., Arnó, G. and Juan de Felipe, J., Fifth-Generation District Heating and Cooling Networks Based on Shallow Geothermal Energy: A Review and Possible Solutions for Mediterranean Europe (2022). DOI: 10.3390/en16010147.

[23] Interreg North-West Europe, Different generations of DHC, https://5gdhc.eu/different-generations-of-dhc/.

[24] Boesten, S., Ivens, W., Dekker, S. C. and Eijdems, H., 5th generation district heating and cooling systems as a solution for renewable urban thermal energy supply (2019). DOI: 10.5194/adgeo-49-129-2019.

[25] Østergaard, P. A., Werner, S., Dyrelund, A., Lund, H., Arabkoohsar, A., Sorknæs, P. et al., The four generations of district cooling - A categorization of the development in district cooling from origin to future prospect (2022). DOI: 10.1016/j.energy.2022.124098.

[26] Werner, S., International review of district heating and cooling (2017). DOI: 10.1016/j.energy.2017.04.045.

[27] Vogl, B., Stadt Wien - Energieplanung, https://www.wien.gv.at/stadtentwicklung/energie/erp/pdf/bericht-erp-1040.pdf.

[28] Wien Energie, Fernkälte, https://www.wienenergie.at/business/produkte/kaelte/fernkaelte/.

[29] Lischtansky, S. and Hölller, O., Technische Richtlinie - LEITFADEN ALLGEMEINGÜLTIGE BESTIMMUNGEN, https://dokumente.wienenergie.at/wp-content/uploads/tr-2017-leitfaden-allgemeingueltige-bestimmungen.pdf.

[30] Lischtansky, S. and Höller, O., Technische Richtlinie - Technische Auslegungsbedingungen, https://dokumente.wienenergie.at/wp-content/uploads/tr-technische-auslegungsbedingungen-2013.pdf#:~:text=Die%20Technische%20Richtline%20Technische%20Auslegungsbedingungen,Betrieb%20der%20Hausstationen%20und%20%2Danlagen.

[31] Pechtl, S., Raus aus dem Gas: Aber wie? (2022).

[32] Aue, G. and Burger, A., Heating & cooling, mobility, electricity: Scenarios for decarbonisation of Viennas's energy system by 2040,

https://positionen.wienenergie.at/wp-content/uploads/2021/10/WE-DECARB21-Study-English.pdf.

[33] Stadt Wien, Wiener Klimafahrplan - 4.7 Strom- und Fernwärmeerzeugung, https://www.wien.gv.at/spezial/klimafahrplan/klimaschutz-wien-wird-klimaneutral/strom-und-fernwarmeerzeugung/.

[34] Wien Energie, Saubere Kälte: So wird Fernwärme zur Fernkälte, https://www.wienenergie.at/blog/saubere-kaelte-so-wird-fernwaerme-zur-fernkaelte/.

[35] Zeh, R., Ohlsen, B., Philipp, D., Bertermann, D., Kotz, T., Jocić, N. and Stockinger, V., Large-Scale Geothermal Collector Systems for 5th Generation District Heating and Cooling Networks (2021). DOI: 10.3390/su13116035.

[36] Ministry of Foreign Affairs and Trade of Hungary, ENERGY STORAGE, https://energy.danube-region.eu/wp-content/uploads/sites/6/sites/6/2021/03/Energy_storage2021FINAL_03.25.pdf.

[37] Yan, Introduction to Engineering Thermodynamics, 2022.

[38] Holzer et al., Technische Thermodynamik, 2018.

[39] Kienberger, Thermische Energietechnik, 2020.

[40] Kulterer, K., Mair, O., Sulzer, T., Betrand, A., Tudor, H., Blaser, M. et al., LEITFADEN FÜR ENERGIEAUDITS IN KÄLTESYSTEMEN (2015).

[41] Hua, T., Yitai, M., Minxia, L., Chuntao, L. and Li, Z., The status and development trend of the water chiller energy efficiency standard in China (2010). DOI: 10.1016/j.enpol.2010.06.020.

[42] Lorenzo, C. and Narvarte, L., Performance indicators of photovoltaic heat-pumps (2019). DOI: 10.1016/j.heliyon.2019.e02691.

[43] Raupenstrauch, Mühlbacher, Wärmetechnik, 2019.

[44] Gamsjäger, Strömungslehre, 2017.

[45] Yu, F. W., Chan, K. T., Sit, R. K. Y. and Yang, J., Review of Standards for Energy Performance of Chiller Systems Serving Commercial Buildings (2014). DOI: 10.1016/j.egypro.2014.12.308.

[46] Allahyarzadeh-Bidgoli, A., Dezan, D. J. and Yanagihara, J. I., COP optimization of propane pre-cooling cycle by optimal Fin design of heat exchangers: Efficiency and sustainability improvement (2020). DOI: 10.1016/j.jclepro.2020.122585.

[47] Fischer, D. and Madani, H., On heat pumps in smart grids: A review (2016). DOI: 10.1016/j.rser.2016.11.182.

[48] Østergaard, P. A. and Andersen, A. N., Booster heat pumps and central heat pumps in district heating (2016). DOI: 10.1016/j.apenergy.2016.02.144.

[49] Piechurski, K., Szulgowska-Zgrzywa, M. and Danielcewicz, J., The impact of the work under partial load on the energy efficiency of an air-to-water heat pump (2017). DOI: 10.1051/e3sconf/20171700072.

[50] Pieper, H., Krupenski, I., Markussen, W. B., Ommen, T., Siirde, A. and Volkova, A., Method of linear approximation of COP for heat pumps and chillers based on thermodynamic modelling and off-design operation (2021). DOI: 10.1016/j.energy.2021.120743.

[51] Kaneko, C. and Yoshinaga, M., Long-term operation analysis of a ground source heat pump with an air source heat pump as an auxiliary heat source in a warm region (2023). DOI: 10.1016/j.enbuild.2023.113050.

[52] Pieper, H., Ommen, T., Elmegaard, B. and Markussen, W. B., Assessment of a combination of three heat sources for heat pumps to supply district heating 2019. DOI: 10.1016/j.energy.2019.03.165.

[53] Nuclear Power, Reversible Heat Pumps – Heating and Cooling, https://www.nuclear-power.com/nuclear-engineering/thermodynamics/thermodynamic-cycles/heating-and-air-conditioning/reversible-heat-pumps-heating-and-cooling/.

[54] TLK Energy, Reversing Valve in Heat Pumps, https://tlk-energy.de/blog-en/heat-pump-reversing-valve.

[55] Rajapaksha, L. and Suen, K. O., Influence of liquid receiver on the performance of reversible heat pumps using refrigerant mixtures (2003). DOI: 10.1016/S0140-7007(03)00092-6.

[56] Rajapaksha, L. and Suen, K. O., Influence of reversing methods on the performance of a reversible water-to-water heat pump (2003). DOI: 10.1016/S1359-4311(02)00136-9.

[57] Urbanucci, L., Testi, D. and Bruno, J. C., Integration of Reversible Heat Pumps in Trigeneration Systems for Low-Temperature Renewable District Heating and Cooling Microgrids (2019). DOI: 10.3390/app9153194.

[58] Doletschek, Hammer, Thermische Energietechnik (Teil 1 nicht fossil), 2014.

[59] Glanville, P., Vadnal, H. and Garrabrant, M., Field Testing of a Prototype Residential Gas-Fired Heat Pump Water Heater (2016).

[60] Bauer, T., Steinmann, W.-D., Laing, D. and Tamme, R., Thermal energy storage materials and systems (2012). DOI: 10.1615/AnnualRevHeatTransfer.2012004651.

[61] Dahash, A., Ochs, F., Janetti, M. B. and Streicher, W., Advances in seasonal thermal energy storage for solar district heating applications: A crtical review on large-scale hot-water tank and pit thermal energy storage systems (2019). DOI: 10.1016/j.apenergy.2019.01.189.

[62] Zahoransky, Richard (Ed.), 2013, Energietechnik: Systeme zur Energieumwandlung. Kompaktwisen für Studium und Beruf. With assistance of Hans-Josef Allelein, Elmar Bollin, Helmut Oehler, Udo Schelling, Harald Schwarz. 6. Auflage, Springer Viewewg.

[63] Lou, W., Fan, Y. and Luo, L., Single-tank thermal energy storage systems for concentrated solar power: Flow distribution optimization for thermocline evolution management (2020). DOI: 10.1016/j.est.2020.101749.

[64] Alfasfos, R., Cavern Thermal Energy Storage for District Cooling: Feasability Study on Mixing Mechanism in Cold Thermal Energy Storage, Master Thesis, KTH School of Industrial Engineering and Management, 2017.

[65] Sveinbjörnsson, D., Jensen, L. L., Trier, D., Bava, F., Hassine, I. B. and Jobard, X., D2.3 - Large Storage Systems for DHC networks (2019).

[66] Hidros Thermal Solutions, WHA - Ground Source Water to Water Heat Pumps, https://www.hidros.it/wp-content/uploads/2021/12/WHA_ENG.pdf.

[67] Ellerbrok, C., Potentials of Demand Side Management Using Heat Pumps with Building Mass as a Thermal Storage (2014). DOI: 10.1016/j.egypro.2014.01.175.

[68] Klein, S., 2017, TRNSYS 18: A Transient System Simulation Program, Solar Energy Laboratory, University of Wisconsin, Madison, USA.

[69] Cambronero, Victoria; Saint-sardos, Christophe; Cervero, Claudia Sanroman; Velasco, Alberto Abánades (Eds.), 2023, W.E. DISTRICT Heating & Cooling Solutions - D5.8. Virtual demo designs, European Union.

[70] Cox, J., Belding, S., Campos, G. and Lowder, T., High-Temperature Heat Pump Model Documentation and Case Studies, https://www.nrel.gov/docs/fy23osti/84560.pdf.

[71] Galletti Group, 2023, Commercial proposal, Phone call to Paul Stipper, Madrid, 04.12.2023.

[72] Enerblue, 2023, Commercial proposal, E-Mail to Paul Stipper, Madrid, 03.12.2023.

[73] Hansen, K., Decision-making based on energy costs: Comparing levelized cost of energy and energy system costs (2019). DOI: 10.1016/j.esr.2019.02.003.

[74] Dorotić, H., Pukšec, T. and Duić, N., Analysis of displacing natural gas boiler units in district heating systems by using multi-objective optimization and different taxing approaches (2019). DOI: 10.1016/j.enconman.2019.112411.

[75] Liu, X., Polsky, Y., Qian, D. and Mcdonald, J., An Analysis on Cost Reduction Potential of Vertical Bore Gound Heat Exchangers Used for Ground Source Heat Pump Systems (2019).

[76] Luo, J., Zhang, Y. and Rohn, J., Analysis of thermal performance and drilling costs of borehole heat exchanger (BHE) in a river deposited area (2019). DOI: 10.1016/j.renene.2019.11.019.

[77] Milanowski, M., Cazorla-Marín, A. and Montagud-Montalvá, C., Energy Analysis and Cost-Effective Design Solutions for a Dual-Source Heat Pump System in Representative Climates in Europe (2022). DOI: 10.3390/en15228460.

[78] Luo, J., Rohn, J., Bayer, M. and Priess, A., Thermal performance and economic evaluation of double U-tube borehole heat exchanger with three different borehole diameters (2013). DOI: 10.1016/j.enbuild.2013.08.030.

[79] Somma, M. D., Yan, B., Bianco, N., Graditi, G., Luh, P. B., Mongibello, L. and Naso, V., Design optimization of a distributed energy system through cost and exergy assessments (2017). DOI: 10.1016/j.egypro.2017.03.706.

[80] eurostat, Electricity prices for non-household consumers - bi-annual data (from 2007 onwards), https://ec.europa.eu/eurostat/databrowser/view/nrg_pc_205__custom_9019650/default/table?lang=en.

[81] eurostat, Gas prices for non-household consumers - bi-annual data (from 2007 onwards), https://ec.europa.eu/eurostat/databrowser/view/nrg_pc_203__custom_10023296/default/table?lang=en.

[82] BOERSE.DE GROUP AG, CO2 Emissionsrechte, https://www.boerse.de/rohstoffe/Co2-Emissionsrechtepreis/XC000A0C4KJ2.

[83] Trading Economics, EU Carbon Permits, https://tradingeconomics.com/commodity/carbon.

[84] Umwelt Bundesamt, Der Europäische Emissionshandel,
https://www.umweltbundesamt.de/daten/klima/der-europaeische-
emissionshandel#teilnehmer-prinzip-und-umsetzung-des-europaischen-
emissionshandels.

[85] Scarlat, N., Prussi, M. and Padella, M., Quantification of the carbon intensity of electricity
produced and used in Europe (2021). DOI: 10.1016/j.apenergy.2021.117901.

[86] European Environment Agency, Greenhouse gas emission intensity of electricity
generation, https://www.eea.europa.eu/data-and-maps/daviz/co2-emission-intensity-
14/#tab-googlechartid_chart_41.

[87] Our World in Data, Carbon intensity of electricity generation,
https://ourworldindata.org/grapher/carbon-intensity-
electricity?tab=chart&time=earliest.2022&region=Europe&country=ESP~OWID_EU27.

[88] Ember-Climate, European Union, https://ember-climate.org/countries-and-
regions/regions/european-union/.

[89] Casasso, A., Sethi, R., Capodaglio, P. and Simonetto, F., Environmental and Economic
Benefits from the Phase-out of Residential Oil Heating: A Study from the Aosta Valley
Region (Italy) (2019). DOI: 10.3390/su11133633.

[90] Yang, T., Liu, W., Kramer, G. J. and Sun, Q., Sesonal thermal energy storage: A techno-
economic literature review (2021). DOI: 10.1016/j.rser.2021.110732.

[91] Department of Climate Change and Energy Efficiency, Factsheet Boiler Efficiency,
https://www.energy.gov.au/sites/default/files/hvac-factsheet-boiler-efficiency.pdf.

[92] Toleikyte, Agne; Roca Reina, Juan Carlos; Volt, Jonathan; Carlsson, Johan; Lyons,
Lorcan; Gasparella, Andrea et al. (Eds.), The Heat Pump Wave: Opportunities and
Challenges: Analysis of the largesacle deployment of heat pumps by 2030 following the
REPowerEU plan, European Comission.

[93] Cozzi, L., Monschauer, Y., Wetzel, D. and Bouckaert, S., The Future of Heat Pumps,
https://iea.blob.core.windows.net/assets/4713780d-c0ae-4686-8c9b-
29e782452695/TheFutureofHeatPumps.pdf.

[94] Department for Business, Energy & Industrial Strategy, Improving Boiler Standards and
Efficiency,
https://assets.publishing.service.gov.uk/media/63e25c96e90e076266ed429c/Improving
_boiler_standards_and_efficiency_consultation.pdf.

[95] Zhang, F., Yu, M., Sørensen, B. R., Cui, P., Zhang, W. and Fang, Z., Heat extraction capacity and its attenuation of deep borehole heat exchanger array (2022). DOI: 10.1016/j.energy.2022.124430.

[96] Korhonen, K., Markó, Á., Bischoff, A., Szijártó, M. and Mádl-Szönyi, J., Infinite borehole field model - A new approach to estimate the shallow geothermal potential of urban areas applied to central Budapest, Hungary (2023). DOI: 10.1016/j.renene.2023.03.043.

Appendix 1: Function Plans

4 RHPs

Hours	RHPs available for heating	RHPs available for cooling
0 − 2450	4	0
2450 – 2850	3	1
2850 – 6700	1	3
6700 – 7200	2	2
7200 – 8760	4	0

5 RHPs

Hours	RHPs available for heating	RHPs available for cooling
0 – 1250	5	0
1250 – 2450	4	0
2450 – 2880	3	2
2880 – 3900	1	3
3900 – 6450	1	4
6450 – 6700	2	3
6700 – 7180	2	2
7180 – 8760	5	0

6 RHPs

Hours	*RHPs available for heating*	*RHPs available for cooling*
0 – 150	4	0
150 – 350	6	0
350 – 1250	5	0
1250 – 2450	4	0
2450 — 2880	3	2
2880 – 3900	1	3
3900 – 6200	1	5
6200 – 6450	1	4
6450 – 6700	1	3
6700 – 7180	2	2
7180 – 7280	5	1
7280 — 7870	5	0
7870 – 8500	6	0
8500 – 8760	5	0

Appendix 2: load_data_analysis.py

Program description: The purpose of this program is to automate the task of estimating how much of the DHC demand can be covered with a corresponding number of RHPs. Therefore, the program first imports the load data for heating and cooling provided in form of a .txt file and then exports this data in form of a .csv file. From this .csv file, the load data is read and stored in lists to facilitate further data analysis. Subsequently, the program derives basic metrics such as the base and peak load, the annual thermal energy demand, etc., from the data. Following this, the actual analysis, with the aim of estimating how much of the DHC demand can be met with a corresponding number of RHPs, begins. The algorithm approximates the RHP coverage achievable by calculating the number of units needed at each hour of the year to simultaneously cover the heating and cooling demand. This data is then summarized in a dictionary where the keys correspond to the number of RHPs and the values to the number of hours during which this number of RHPs is required. Based on that information, and by applying weighting factors, an estimate is calculated. The calculation logic of these weighting factors is demonstrated in the program using this case as an example but has also been automated to allow for the calculation with any load profile. The code used for the graphical representation of the data is not included due to its extensive space requirements.

```python
import pandas as pd
from pathlib import Path
import csv
import matplotlib.pyplot as plt
import math
import numpy as np
from itertools import zip_longest
```

```python
###############################################################################
'''Importing data'''

# cooling - 4Generation_Demand_Cooling_3087500 kWh/year
read_file = pd.read_csv(
    r'C:\Users\pauls\Desktop\master_thesis\Thesis\python\load_data\cooling_dem
and_M8200_Type_9_excl_header.txt',
    delimiter=',',
    header=0,
)

read_file.to_csv(
    r'C:\Users\pauls\Desktop\master_thesis\Thesis\python\load_data\cooling_dem
and_M8200_Type_9_excl_header.csv',
    index=None
)

# heating - MAD_DH01_20230206_8953000 kWh/year
read_file = pd.read_csv(
    r'C:\Users\pauls\Desktop\master_thesis\Thesis\python\load_data\heating_dem
and_M8100_Type_9_excl_header.txt',
    delimiter=',',
    header=0,
)

read_file.to_csv(
    r'C:\Users\pauls\Desktop\master_thesis\Thesis\python\load_data\heating_dem
and_M8100_Type_9_excl_header.csv',
    index=None
)

def get_dhc_data(path, QDEM_kWh, TRET, TFOR, demand_index, ret_index,
        for_index):
    """Get QDEM_kWh, TRET, TFOR, from the .csv file."""
    # Read the file and chain the splitlines() method to get a list of all
lines in the file
    lines = path.read_text().splitlines()
    # The reader object can be used to parse each line in the file
    reader = csv.reader(lines)
    # The next function returns the next line in the file, starting form the
beginning
    header_row = next(reader)

    for index, column_header in enumerate(header_row):
        print(index, column_header.lstrip())

    n = 0
```

```python
    # Extract QDEM_kWh, TRET, TFOR
    '''
    Note that the reader object continues from where it left off in the CSV
file
    and automatically returns each line following its current position.
Because we've
    already read the header row, the loop will begin at the second line where
the acutal data begins!
    '''

    for row in reader:
        n=n+1
        try:
            demand = float(row[demand_index])
            t_ret = float(row[ret_index])
            t_for = float(row[for_index])
        except ValueError:
            print(f"Missing data in line {n}")
        else:
            QDEM_kWh.append(demand)
            TFOR.append(t_for)
            TRET.append(t_ret)

    if len(QDEM_kWh) == 8760 and len(TRET) == 8760 and len(TFOR) == 8760:
        print(F"All data has been extracted\n")
    else:
        print(F"Some data is missing")

# Get cooling data
path_C =
Path(r'C:\Users\pauls\Desktop\master_thesis\Thesis\python\load_data\cooling_de
mand_M8200_Type_9_excl_header.csv')
QDEM_kWh_C, TRET_C, TFOR_C = [], [], []

get_dhc_data(path_C, QDEM_kWh_C, TRET_C, TFOR_C, demand_index=0, ret_index=1,
        for_index=2)


# Get heating data
path_H =
Path(r'C:\Users\pauls\Desktop\master_thesis\Thesis\python\load_data\heating_de
mand_M8100_Type_9_excl_header.csv')
QDEM_kWh_H, TRET_H, TFOR_H = [], [], []

get_dhc_data(path_H, QDEM_kWh_H, TRET_H, TFOR_H,  demand_index=0, ret_index=1,
        for_index=2)


##############################################################################
```

```python
'''Calculation of all values required for plotting'''

# Since the required amount of energy is given in kWh per hour, this also
corresponds to the power
QDEM_kW_C = QDEM_kWh_C
QDEM_kW_H = QDEM_kWh_H

# Check whether the annual energy requirement matches that in the text file
annual_demand_H = sum(QDEM_kWh_H)
annual_demand_C = sum(QDEM_kWh_C)
print(F"Annual heating demand: {annual_demand_H} kWh")
print(F"Annual cooling demand: {annual_demand_C} kWh")
# Cooling - 4Generation_Demand_Cooling_3087500 kWh/year (3087.5MWh/year)
# Heating - MAD_DH01_20230206_8953000 kWh/year (8953MWh/year)

max_dem_h = max(QDEM_kW_H)
max_dem_c = max(QDEM_kW_C)
min_dem_h = min(QDEM_kW_H)
min_dem_c = min(x for x in QDEM_kW_C if x != 0)

peak_load_factor = 0.4
base_load_h = max_dem_h*(1-peak_load_factor)
base_load_c = max_dem_c*(1-peak_load_factor)
peak_load_h = max_dem_h*peak_load_factor
peak_load_c = max_dem_c*peak_load_factor

print(F"\nMaximum heating demand: {max_dem_h} kW")
print(F"Maximum cooling demand: {max_dem_c} kW")
print(F"Minimum heating demand: {min_dem_h} kW")
print(F"Minimum cooling demand: {min_dem_c} kW")
print(F"\nPeak load heating: {peak_load_h} kW")
print(F"Peak load cooling: {peak_load_c} kW")
print(F"Base load heating: {base_load_h} kW")
print(F"Base load cooling: {base_load_c} kW")

# The reversing factor (rf) corresponds to the ratio between the heating and
cooling capcity of the RHP
rf=368.5/439.4
heating_capacity_RHP = 439.4
cooling_capacity_RHP = heating_capacity_RHP*rf

# Consistency check:
# heating_capacity_RHP = 100
# cooling_capacity_RHP = min_dem_c*0.5

print(F"\nHeating Capacity RHP: {heating_capacity_RHP} kW")
print(F"Cooling Capacity RHP: {cooling_capacity_RHP} kW")
```

```python
# Sorting of the demand values to create the duration curves
sorted_QDEM_kW_C = sorted(QDEM_kW_C, reverse=True)
sorted_QDEM_kW_H = sorted(QDEM_kW_H, reverse=True)

# Calculation of the number of RHPs (for every hour of the year) that need to
be activated to cover the hourly heating and cooling demands
num_RHPs_activated_each_hour_H = []
num_RHPs_activated_each_hour_C = []

for hourly_demand_H in QDEM_kW_H:
    num_RHPs_H = math.ceil(hourly_demand_H/heating_capacity_RHP)
    num_RHPs_activated_each_hour_H.append(num_RHPs_H)

for hourly_demand_C in QDEM_kW_C:
    num_RHPs_C = math.ceil(hourly_demand_C/cooling_capacity_RHP)
    num_RHPs_activated_each_hour_C.append(num_RHPs_C)

# Calculation of the number of RHPs that need to be activated to cover the
respective the total hourly demand for heating and cooling simultaneously
num_RHPs_activated_each_hour_HC = [num_RHPs_H + num_RHPs_C for num_RHPs_H,
num_RHPs_C in zip(num_RHPs_activated_each_hour_C,
num_RHPs_activated_each_hour_H)]

# Sorting of values to create the duration curves
num_RHPs_activated_each_hour_HC_sorted =
sorted(num_RHPs_activated_each_hour_HC, reverse=True)

# Consistency check
print(F"\nConsistency check:\nThis value should be equal to 8760:
{len(num_RHPs_activated_each_hour_H)}")
print(num_RHPs_activated_each_hour_H[3000:3050])
print(num_RHPs_activated_each_hour_H[0:50])
print(F"\nConsistency check:\nThis value should be equal to 8760:
{len(num_RHPs_activated_each_hour_C)}")
print(num_RHPs_activated_each_hour_C[3000:3050])
print(num_RHPs_activated_each_hour_C[0:50])
print(F"\nConsistency check:\nThis value should be equal to 8760:
{len(num_RHPs_activated_each_hour_HC)}")
print(F"These lists should correspond to the sum of the lists
above:\n{num_RHPs_activated_each_hour_HC[3000:3050]}\n{num_RHPs_activated_each
_hour_HC[0:50]}")
print(F"Number of RHPs required to cover the entire heating and cooling demand
at any time simultaneously: {max(num_RHPs_activated_each_hour_HC)}")
print(F"Minimum number of RHPs that are activated for heating and cooling:
{min(num_RHPs_activated_each_hour_HC)}")

# The following code block counts and records the frequency of each non-zero
value in the list calculated previously
```

```python
# It creates a dictionary where each key is a unique value (number of RHPs
actviated) from the list, and the corresponding value is the count of how many
times that number appears in the list
# Therefore this process effectively measures how many hourly demands can be
met by a certain number of RHPs
num_h_covered_with_num_RHP_unsorted_HC = {}

for number in num_RHPs_activated_each_hour_HC:
    if number != 0:
        if number in num_h_covered_with_num_RHP_unsorted_HC:
            num_h_covered_with_num_RHP_unsorted_HC[number] += 1
        else:
            num_h_covered_with_num_RHP_unsorted_HC[number] = 1

#  The following code sorts the key-value pairs in the dictionary by their
keys in ascending order
#  The output is a list of tuples, where each tuple is a key-value pair from
the respective original dictionary.
num_h_covered_with_num_RHP_HC_sorted =
sorted(num_h_covered_with_num_RHP_unsorted_HC.items())

# The following code unpacks and separates the sorted key-value pairs,
creating two tuples.
# This process effectively splits the sorted pairs into two separate
sequences: one for the keys (number of RHPs) and one for the values (hours).
num_RHPs_HC_sorted, covered_hours_HC_sorted =
zip(*num_h_covered_with_num_RHP_HC_sorted)

# In the following, the hours that can be covered with the respective number
of RHPs are corrected upwards with weighting factors
# The following code block shows the applied logic (for the load profile of
this work) which was implemented below in a for-loop for any input data (load
profiles)
percent_2RHPs = round((num_h_covered_with_num_RHP_unsorted_HC[2] +
2/3*num_h_covered_with_num_RHP_unsorted_HC[3] +
2/4*num_h_covered_with_num_RHP_unsorted_HC[4] +
2/5*num_h_covered_with_num_RHP_unsorted_HC[5] +
2/6*num_h_covered_with_num_RHP_unsorted_HC[6] +
2/7*num_h_covered_with_num_RHP_unsorted_HC[7])/8760,4)
percent_3RHPs = round((num_h_covered_with_num_RHP_unsorted_HC[2] +
num_h_covered_with_num_RHP_unsorted_HC[3] +
3/4*num_h_covered_with_num_RHP_unsorted_HC[4] +
3/5*num_h_covered_with_num_RHP_unsorted_HC[5] +
3/6*num_h_covered_with_num_RHP_unsorted_HC[6] +
3/7*num_h_covered_with_num_RHP_unsorted_HC[7])/8760,4)
percent_4RHPs = round((num_h_covered_with_num_RHP_unsorted_HC[2] +
num_h_covered_with_num_RHP_unsorted_HC[3] +
num_h_covered_with_num_RHP_unsorted_HC[4] +
```

```
4/5*num_h_covered_with_num_RHP_unsorted_HC[5] +
4/6*num_h_covered_with_num_RHP_unsorted_HC[6] +
4/7*num_h_covered_with_num_RHP_unsorted_HC[7])/8760,4)
percent_5RHPs = round((num_h_covered_with_num_RHP_unsorted_HC[2] +
num_h_covered_with_num_RHP_unsorted_HC[3] +
num_h_covered_with_num_RHP_unsorted_HC[4] +
num_h_covered_with_num_RHP_unsorted_HC[5] +
5/6*num_h_covered_with_num_RHP_unsorted_HC[6] +
5/7*num_h_covered_with_num_RHP_unsorted_HC[7])/8760,4)
percent_6RHPs = round((num_h_covered_with_num_RHP_unsorted_HC[2] +
num_h_covered_with_num_RHP_unsorted_HC[3] +
num_h_covered_with_num_RHP_unsorted_HC[4] +
num_h_covered_with_num_RHP_unsorted_HC[5] +
num_h_covered_with_num_RHP_unsorted_HC[6] +
6/7*num_h_covered_with_num_RHP_unsorted_HC[7])/8760,4)
percent_7RHPs = round((num_h_covered_with_num_RHP_unsorted_HC[2] +
num_h_covered_with_num_RHP_unsorted_HC[3] +
num_h_covered_with_num_RHP_unsorted_HC[4] +
num_h_covered_with_num_RHP_unsorted_HC[5] +
num_h_covered_with_num_RHP_unsorted_HC[6] +
num_h_covered_with_num_RHP_unsorted_HC[7])/8760,4)
control_coverage = [percent_2RHPs, percent_3RHPs, percent_4RHPs,
percent_5RHPs, percent_6RHPs, percent_7RHPs]

# print(F"TEST {covered_hours_HC_sorted}")
# print(F"TEST {num_h_covered_with_num_RHP_unsorted_HC}")
print(F"TEST {control_coverage}")

# AUTOMATION
# Generation of an x-value for every hour of the year. The following code
creates a list and populates it with integers ranging from 0 to 8759.
hours_per_year = []
for i in range(8760):
    hours_per_year.append(i)

total_hours = len(hours_per_year)  # Total hours for percentage calculation
coverage_percent = []  # Initialize list to hold coverage percentages
coverage_hours = [] # Initialize list to hold total hours

# Dynamically determine the range of RHP values based on the keys in the
dictionary
keys = sorted(num_h_covered_with_num_RHP_unsorted_HC.keys())
min_key = min(keys)
max_key = max(keys)

for rhp_num in range(min_key, max_key + 1):
    num_h_RHPs = 0
    # Adjust the calculation to correctly sum the applicable proportions
```

```python
    for key in keys: # key = denominator
        if rhp_num >= key:  # Correct this condition to include the RHP itself
            factor = 1  # When rhp_num is equal to or greater than key, factor
is 1
        else:
            factor = rhp_num / key  # Apply proportion for partial coverage
        num_h_RHPs += factor *
float(num_h_covered_with_num_RHP_unsorted_HC[key])
    # Normalize the sum to get the percentage

    percent = (num_h_RHPs / total_hours)*100
    percent_rounded = round(percent,2)
    coverage_hours.append(num_h_RHPs)
    coverage_percent.append(percent_rounded)

print(f"TEST {coverage_percent}")
print(F"TEST {coverage_hours}")
```

Appendix 3: result_analysis.py

Program description: The purpose of this program is to automate the calculation of the calculation scheme described in Chapter 7.4, with the aim to facilitate the analysis of large data volumes during sensitivity analysis. Initially, the program reads the characteristic data of the various cases being analysed in TRNSYS, available in form of a .csv file after the simulation. Based on this data, file paths are created to access and import all the relevant thermodynamic data from the TRNSYS result .txt files into Python. This is followed by the initialization of a function that calculates the calculation scheme for any given input data and outputs the results in form of a dictionary. Subsequently, this function is applied to all TRNSYS result .txt files. The resulting dictionaries are then grouped according to certain criteria and stored in an overarching dictionary to facilitate the graphical evaluation of the sensitivity analyse. The code used for the graphical representation of the data is not included due to its extensive space requirements.

```python
import pandas as pd
import os
import matplotlib.pyplot as plt
from matplotlib.ticker import MultipleLocator

'''Creation of filepaths for accessing the TRNSYS results files in order to be
able to automatically read the results into Python'''

# Path for accesing characterizing case data such as folder names and
corresponding TES tank sizes, number of RHPs, etc., required to create file
paths
case_characterizing_data =
r'C:\Users\pauls\Desktop\master_thesis\Thesis\python\análisis_resultados\Resul
tados\SimJobIndex.csv'
```

```python
# Import of data characterizing case data such as folder names and
corresponding TES tank sizes, number of RHPs, etc., required to create file
paths
data_frame = pd.read_csv(case_characterizing_data, sep=",")

# Display the first rows of the dataframe to confirm the import
# with pd.option_context('display.max_columns', None):  # None means all
columns will be shown
#     print(df_0.head(15))

# Convert each column into a separate list
data_frame_lists = {col: data_frame[col].tolist() for col in
data_frame.columns}
# data_frame_lists is a dictionary where each key is a column name and each
value is a list of that column's data
# For example, to access the list of data for a column named 'Column1', use
column_lists['Column1']

# Generating file paths to automatically access all data and storing them in
the list 'file_paths'
folder_names = data_frame_lists['Job_ID']
base_directory =
r"C:\Users\pauls\Desktop\master_thesis\Thesis\python\análisis_resultados\Resul
tados"
file_name = "Resultados.txt"
file_paths = [os.path.join(base_directory, folder, file_name) for folder in
folder_names]

################################################################################
'''Definition of a function (analyse_file) that automatically executes the
calculation scheme on each result file and stores the outcomes in a
dictionary'''

def analyse_file(file_path):

    df = pd.read_csv(file_path, sep="\s+", skiprows=[0], nrows=8760)
    # The sep="\s+" parameter indicates that the separator between fields in
the result file is one or more whitespace characters
    # skiprows=[0]: This tells Pandas to skip the first row of the file. Rows
are zero-indexed, so [0] refers to the very first row.
    # This is used to skip the header row as the header is not needed and not
formatted in a way that is not useful for creating the data frame.
    # The use of nrows=8760 in the pd.read_csv function in Pandas, instructs
the function to read 8760 rows of data from the CSV file, starting from the
first row after any skipped rows.
    # Since skiprows=[0] is used to skip the very first row (row 0), the rows
actually read will be from row 1 to row 8760 of the original file.
```

```python
    # So, the total number of rows read into the data frame will be 8760,
covering row 1 through row 8760 of the CSV file. The initial row (row 0) is
not included in this count because it's skipped.
    # In this way, the relevant data from the file is imported. Test: With
nrows=8761 the last value is NaN.

    # Display the first or last few rows of the data frame to confirm the
import
    # with pd.option_context('display.max_columns', None):  # None means all
columns will be shown
        # print(df.head(15))
        # print(df.iloc[1245:1255])
        # print(df.iloc[2448:2470])
        # print(df.iloc[3000:3030])
        # print(df.tail(20))

    # Convert each column into a separate list
    df_lists = {col: df[col].tolist() for col in df.columns}
    # df_lists is a dictionary where each key is a column name and each value
is a list of that column's data
    # For example, to access the list of data for a column named 'Column1',
use column_lists['Column1']

    '''Input data for the calculation scheme'''
    # COP heating mode RGSHP [-]
    # COP_heating_RGSHP = df_lists['HP01_COPrated_H'][0]

    # COP cooling mode RGSHP [-]
    # COP_cooling_RGSHP = df_lists['HP01_COPrated_C'][0]

    # Heating capacity per RGSHP [kW]
    heating_capacity_RGSHP = df_lists['HP01_QHNomkW'][0]

    # Cooling capacity per RGSHP [kW]
    cooling_capacity_RGSHP = df_lists['HP01_QCNomkW'][0]

    # Total number of RGSHPs [-]
    total_num_RGSHP = df_lists['HP01_Num'][0]

    # Maximum number of RGSHPs used for heating at the same time [-]
    max_num_RGSHP_heating_simultaneously = max(df_lists['HP_NumON_H'])

    # Maximum number of RGSHPs used for cooling at the same time [-]
    max_num_RGSHP_cooling_simultaneously = max(df_lists['HP_NumON_C'])

    # Volume TES heating [m³]
    vol_TES_heating = df_lists['TK01_Vol'][0]
```

```python
# Volume TES cooling [m³]
vol_TES_cooling = df_lists['TK02_Vol'][0]

# Depth BHX [m]
depth_BHX = df_lists['BHX_Depth'][0]

# Number BHX [-]
number_BHX = df_lists['BHX_No'][0]

# CAPEX compression HP [€/kW]
CAPEX_per_kW_compression_HP = 494.5515521

# SCOP cooling ASHP [-]
SCOP_cooling_ASHP = 3.66

# CAPEX Boiler [€/kW]
CAPEX_per_kW_boiler = 93.33333

# Specific cost BHX [€/m]
specific_cost_BHX = 58.27357117

# Gas cost [€/kWh]
specific_cost_gas = 0.056488889

# Electricity cost [€/kWh]
specific_cost_electricity = 0.137755556

# CO2 cost [€/g]
specific_cost_CO2 = 80 / 1000000

# Fixed operation and maintenance (O&M) cost in % of investment [-]
fixed_OM_cost_in_percent_of_investment = 0.03

# Lifetime compression HP [years]
lifetime_compression_HP = 15

# Lifetime Boiler [years]
lifetime_boiler = 15

# Lifetime TES [years]
lifetime_TES = 30

# Lifetime BHX [years]
lifetime_BHX = 50

# Emission factor electrcity [gCO2eq/kWh]
f_emission_electricity = 266.73
```

```python
    # Emission factor gas boiler [gCO2eq/kWh]
    f_emission_gas_boiler = 227.8025

    # Boiler efficiency [-]
    efficiency_boiler = 0.9

    # Discount rate [-]
    discount_rate = 0.05

###############################################################################
    '''Calculating KPIs'''
    '''Reversible ground source heat pumps'''

    # Seasonal COP heating mode [-]
    W_RGSHP_total_heating = sum(df_lists['RES_W_HP_H'])
    Q_RGSHP_sink_total_heating = sum(df_lists['RES_Q_HP_H'])
    SCOP_heating_RGSHP =
round(Q_RGSHP_sink_total_heating/W_RGSHP_total_heating,2)
    # print(f"Seasonal COP heating RGSHPs: {SCOP_heating_RGSHP} [-]")

    # Seasonal COP cooling mode [-]
    W_RGSHP_total_cooling = sum(df_lists['RES_W_HP_C'])
    Q_RGSHP_source_total_cooling = sum(df_lists['RES_Q_HP_C'])
    SCOP_cooling_RGSHP =
round(Q_RGSHP_source_total_cooling/W_RGSHP_total_cooling,2)
    # print(f"Seasonal COP cooling RGSHPs: {SCOP_cooling_RGSHP} [-]")

    # Annual performance factor [-]
    Annual_performance_factor_RGSHP = (Q_RGSHP_sink_total_heating +
Q_RGSHP_source_total_cooling)/(W_RGSHP_total_heating + W_RGSHP_total_cooling)
    # print(f"Annual performance factor RGSHPs:
{Annual_performance_factor_RGSHP} [-]")
    W_RGSHP_total_heating_and_cooling = (W_RGSHP_total_cooling +
W_RGSHP_total_heating)/1000
    # print(f"Total electrical energy consumption RGSHPs heating:
{W_RGSHP_total_heating} [kWh]")
    # print(f"Total electrical energy consumption RGSHPs cooling:
{W_RGSHP_total_cooling} [kWh]")
    # print(f"Total electrical energy consumption RGSHPs heating and cooling:
{W_RGSHP_total_heating_and_cooling} [MWh]")

    # Heating coverage with RHPs [%]
    # Annual heating demand: 8952999.999974359 kWh (from the other file)
    annual_demand_heating = sum(df_lists['RES_Q_Hdemand'])
    # print(f"\nAnnual heating demand: {annual_demand_heating}")
    Q_RGSHP_supplied_total_heating = sum(df_lists['RES_Q_Hsuplied'])
    heating_coverage =
(Q_RGSHP_supplied_total_heating/annual_demand_heating)*100
```

```python
    # print(f"Heating coverage: {heating_coverage} [%]")

    # Cooling coverage with RHPs [%]
    # Annual cooling demand: 3087500.000349187 kWh (from the other file)
    annual_demand_cooling = sum(df_lists['RES_Q_Cdemand'])
    # print(f"\nAnnual cooling demand: {annual_demand_cooling}")
    Q_RGSHP_supplied_total_cooling = sum(df_lists['RES_Q_Csuplied'])
    cooling_coverage =
(Q_RGSHP_supplied_total_cooling/annual_demand_cooling)*100
    # print(f"Cooling coverage: {cooling_coverage} [%]")

    # Total coverage with RHPs [%]
    total_coverage = ((Q_RGSHP_supplied_total_cooling +
Q_RGSHP_supplied_total_heating)/(annual_demand_cooling +
annual_demand_heating))*100
    # print(f"\nTotal coverage: {total_coverage} [%]")

    # Total CAPEX RGSHPs [€]
    CAPEX_RGSHPs = CAPEX_per_kW_compression_HP * total_num_RGSHP *
heating_capacity_RGSHP
    # print(f"\nCAPEX for RGSHPs: {CAPEX_RGSHPs} [€]")

    # OPEX RGSHP heating [€]
    OPEX_RGSHPs_heating_variable = specific_cost_electricity *
W_RGSHP_total_heating
    # print(f"OPEX RGSHP heating: {OPEX_RGSHP_heating_variable} [€]")

    # OPEX RGSHP cooling [€]
    OPEX_RGSHPs_cooling_variable = specific_cost_electricity *
W_RGSHP_total_cooling
    # print(f"OPEX RGSHP cooling: {OPEX_RGSHP_cooling_variable} [€]")

    # CO2 emissions RGSHPs [gCO2eq/year]
    CO2_emissions_RGSHPs_heating = W_RGSHP_total_heating *
f_emission_electricity
    CO2_emissions_RGSHPs_cooling = W_RGSHP_total_cooling *
f_emission_electricity
    CO2_emissions_RGSHPs_total = CO2_emissions_RGSHPs_heating +
CO2_emissions_RGSHPs_cooling
    # print(f"\nCO2 emissions RGSHPs total: {CO2_emissions_RGSHPs_total}
[gCO2eq/year]")
    # print(f"CO2 emissions RGSHPs heating: {CO2_emissions_RGSHPs_heating}
[gCO2eq/year]")
    # print(f"CO2 emissions RGSHPs cooling: {CO2_emissions_RGSHPs_cooling}
[gCO2eq/year]")

    # Thermal losses cooling [%]
```

```python
    losses_cooling = (1-
(Q_RGSHP_supplied_total_cooling/Q_RGSHP_source_total_cooling))*100


    ##################################################################
    '''Thermal energy storages'''

    # Specific cost thermal energy storages [€/m³]
    specific_cost_TES_heating = 5294.6 * vol_TES_heating ** -0.435
    specific_cost_TES_cooling = 5294.6 * vol_TES_cooling ** -0.435
    # print(f"\nSpecific cost TES heating: {specific_cost_TES_heating} [€]")
    # print(f"Specific cost TES cooling: {specific_cost_TES_cooling} [€]")

    # CAPEX thermal energy storages [€]
    CAPEX_TES_heating = vol_TES_heating * specific_cost_TES_heating
    CAPEX_TES_cooling = vol_TES_cooling * specific_cost_TES_cooling
    # print(f"CAPEX for TES heating: {CAPEX_TES_heating} [€]")
    # print(f"CAPEX for TES cooling: {CAPEX_TES_cooling} [€]")


    ##################################################################
    '''Borehole heat exchanger'''

    # CAPEX borhole HX [€]
    CAPEX_BHXs = specific_cost_BHX * depth_BHX * number_BHX
    # print(F"\nCAPEX for borehole HXs: {CAPEX_BHXs} [€]")

    # Energy delta at the end of the year in the borehole [kWh]
    delta_Q_BHX = sum(df_lists['RES_Q_BH'])
    delta_Q_BHX_2 = sum(df_lists['RES_Q_Resource_H']) +
sum(df_lists['RES_Q_Resource_C'])
    # print(f"\nEnergy delta at the end of the year in the borehole:
{delta_Q_BHX} [kWh]\n-Positive if more energy was supplied than was fed in\n-
Negative if more energy was fed in than was supplied")
    # print(f"\nEnergy delta (consitency check) at the end of the year in the
borehole: {delta_Q_BHX_2} [kWh]\n-Positive if more energy was supplied than
was fed in\n-Negative if more energy was fed in than was supplied")


    ##################################################################
    '''Cooling share'''

    # Calculation of the cooling share [-]
    cooling_share = sum(df_lists['HP_NumON_C'])/(sum(df_lists['HP_NumON_H']) +
sum(df_lists['HP_NumON_C']))
    # print(F"\nCooling share: {cooling_share}")


    ##################################################################
    '''Boiler'''

    peak_demand_heating = max((df_lists['RES_Q_Hdemand']))
```

```python
    # print(F"\nPeak demand heating: {peak_demand_heating} kW")

    # CAPEX boiler [€]
    CAPEX_boiler = (peak_demand_heating - max_num_RGSHP_heating_simultaneously
* heating_capacity_RGSHP) * CAPEX_per_kW_boiler

    # CO2 emissions boiler [gCO2eq/year]
    remaining_heat_demand_kWh = annual_demand_heating -
Q_RGSHP_supplied_total_heating
    gas_demand_kWh = remaining_heat_demand_kWh/efficiency_boiler
    gas_demand_GJ = gas_demand_kWh * 0.0036
    OPEX_boiler_variable = gas_demand_kWh * specific_cost_gas
    CO2_emissions_boiler = remaining_heat_demand_kWh * f_emission_gas_boiler
    # print(f"Gas demand: {gas_demand_kWh} [kWh]")
    # print(f"Gas demand: {gas_demand_GJ} [GJ]")

###############################################################################
    '''Air source heat pump'''

    peak_demand_cooling = max((df_lists['RES_Q_Cdemand']))
    # print(F"\nPeak demand cooling: {peak_demand_cooling} kW")

    # CAPEX ASHP [€]
    CAPEX_ASHPs = (peak_demand_cooling - max_num_RGSHP_cooling_simultaneously
* cooling_capacity_RGSHP) * CAPEX_per_kW_compression_HP

    # CO2 emissions ASHP [gCO2eq/year]
    remaining_cold_demand_kWh = annual_demand_cooling -
Q_RGSHP_supplied_total_cooling
    electricity_demand_ASHPs_kWh = remaining_cold_demand_kWh/SCOP_cooling_ASHP
    OPEX_ASHPs_variable = electricity_demand_ASHPs_kWh *
specific_cost_electricity
    CO2_emissions_ASHPs = electricity_demand_ASHPs_kWh *
f_emission_electricity

###############################################################################
    '''CAPEX, OPEX and CO2 cost of the system per year'''

    # CAPEX system [€]
    CAPEX_heating = (CAPEX_RGSHPs + CAPEX_BHXs +
CAPEX_RGSHPs/((1+discount_rate)**lifetime_compression_HP)) * (1-cooling_share)
+ CAPEX_TES_heating + CAPEX_boiler +
CAPEX_boiler/((1+discount_rate)**lifetime_boiler)
    CAPEX_cooling = (CAPEX_RGSHPs + CAPEX_BHXs +
CAPEX_RGSHPs/((1+discount_rate)**lifetime_compression_HP)) * cooling_share +
CAPEX_TES_cooling + CAPEX_ASHPs +
CAPEX_ASHPs/((1+discount_rate)**lifetime_compression_HP)
```

```python
    # CAPEX_RGSHPs/((1+discount_rate)**lifetime_compression_HP) is the present
value of the costs for replacing the RGSHPs when they reach the end of their
service life
    # CAPEX_boiler/((1+discount_rate)**lifetime_boiler is the present value of
the costs for replacing the boilers when they reach the end of their service
life
    # CAPEX_ASHPs/((1+discount_rate)**lifetime_compression_HP is the present
value of the costs for replacing the ASHPs when they reach the end of their
service life
    # print(f"\nCAPEX heating: {CAPEX_heating} [€]")
    # print(f"CAPEX cooling: {CAPEX_cooling} [€]")

    # Fixed OPEX system [€]
    OPEX_heating_fixed = CAPEX_heating *
fixed_OM_cost_in_percent_of_investment
    OPEX_cooling_fixed = CAPEX_cooling *
fixed_OM_cost_in_percent_of_investment

    # Variable OPEX [€] and specific CO2 Emissions of the system [gCO2eq/year
& gCO2eq/kWh]
    total_CO2_emissions_heating = CO2_emissions_RGSHPs_heating +
CO2_emissions_boiler
    total_CO2_emissions_cooling = CO2_emissions_RGSHPs_cooling +
CO2_emissions_ASHPs
    total_CO2_emissions_heating_and_cooling = total_CO2_emissions_heating +
total_CO2_emissions_cooling

    cost_CO2_heating = specific_cost_CO2 * total_CO2_emissions_heating
    cost_CO2_cooling = specific_cost_CO2 * total_CO2_emissions_cooling
    cost_CO2_total = cost_CO2_heating + cost_CO2_cooling

    OPEX_heating_variable = OPEX_RGSHPs_heating_variable +
OPEX_boiler_variable + cost_CO2_heating
    OPEX_cooling_variable = OPEX_RGSHPs_cooling_variable  + cost_CO2_cooling +
OPEX_ASHPs_variable

    specfic_emissions_heating = total_CO2_emissions_heating /
annual_demand_heating
    specfic_emissions_cooling = total_CO2_emissions_cooling /
annual_demand_cooling
    specfic_emissions_heating_and_cooling =
total_CO2_emissions_heating_and_cooling / (annual_demand_heating +
annual_demand_cooling)

    # print(f"\nSpecific CO2 emissions heating: {specfic_emissions_heating}
[gCO2eq/kWh] = [kgCO2eq/MWh]")
    # print(f"Specific CO2 emissions cooling: {specfic_emissions_cooling}
[gCO2eq/kWh] = [kgCO2eq/MWh]")
```

```python
    # print(f"Specific CO2 emissions heating and cooling:
{specfic_emissions_heating_and_cooling} [gCO2eq/kWh] = [kgCO2eq/MWh]")

    # print(f"\nTotal CO2 Emissions heating and cooling:
{total_CO2_emissions_heating_and_cooling} [gCO2eq/year]")
    # print(f"Total CO2 Emissions heating: {total_CO2_emissions_heating}
[gCO2eq/year]")
    # print(f"Total CO2 Emissions cooling: {total_CO2_emissions_cooling}
[gCO2eq/year]")

    # OPEX system [€]
    OPEX_heating = OPEX_heating_fixed + OPEX_heating_variable
    OPEX_cooling = OPEX_cooling_fixed + OPEX_cooling_variable
    # print(f"\nOPEX heating: {OPEX_heating} [€]")
    # print(f"OPEX cooling: {OPEX_cooling} [€]")

################################################################################
    '''Levelized cost of energy (NPV = 0)'''

    # Calculating the LCOE [€/kWh]
    commissioning = 1
    decommissioning = 30  # Project lifetime in years

    years = []
    present_value_OPEX_heating = 0
    present_value_OPEX_cooling = 0
    present_value_annual_demand_heating = 0
    present_value_annual_demand_cooling = 0
    present_value_OPEX_heating_cooling = 0
    present_value_annual_demand_heating_cooling = 0
    test = 0

    for i in range(commissioning, decommissioning + 1):  # + 1 to include the
end value
        years.append(i)
        present_value_OPEX_heating = present_value_OPEX_heating +
OPEX_heating/((1+discount_rate)**i)
        present_value_OPEX_cooling = present_value_OPEX_cooling +
OPEX_cooling/((1+discount_rate)**i)
        present_value_annual_demand_heating =
present_value_annual_demand_heating +
annual_demand_heating/((1+discount_rate)**i)
        present_value_annual_demand_cooling =
present_value_annual_demand_cooling +
annual_demand_cooling/((1+discount_rate)**i)
        present_value_OPEX_heating_cooling =
present_value_OPEX_heating_cooling + (OPEX_heating +
OPEX_cooling)/((1+discount_rate)**i)
```

```python
        present_value_annual_demand_heating_cooling =
present_value_annual_demand_heating_cooling + (annual_demand_heating +
annual_demand_cooling)/((1+discount_rate)**i)
        test = test + i
        # print(test)
        # 'range(start, stop):' generates a sequence of numbers from 'start'
to 'stop - 1'
        # This loop will run 30 iterations, adding the value of i (which
represents the current year) each time.

    LCOE_heating_per_kWh = (CAPEX_heating +
present_value_OPEX_heating)/present_value_annual_demand_heating
    LCOE_cooling_per_kWh = (CAPEX_cooling +
present_value_OPEX_cooling)/present_value_annual_demand_cooling
    LCOE_heating_cooling_per_kWh = (CAPEX_heating + CAPEX_cooling +
present_value_OPEX_heating_cooling)/present_value_annual_demand_heating_coolin
g

    LCOE_heating_per_MWh = LCOE_heating_per_kWh*1000
    LCOE_cooling_per_MWh = LCOE_cooling_per_kWh*1000
    LCOE_heating_and_cooling_per_MWh = LCOE_heating_cooling_per_kWh*1000

    # print(f"\nLCOE heating: {LCOE_heating_per_kWh} [€/kWh]")
    # print(f"LCOE cooling: {LCOE_cooling_per_kWh} [€/kWh]")
    # print((f"LCOE heating and cooling: {LCOE_heating_cooling_per_kWh}
[€/kWh]"))

    # print(f"\nLCOE heating: {LCOE_heating_per_MWh} [€/MWh]")
    # print(f"LCOE cooling: {LCOE_cooling_per_MWh} [€/MWh]")
    # print(f"LCOE heating and cooling: {LCOE_heating_and_cooling_per_MWh}
[€/MWh]")

    #############################################################################
    # Generating a results dictionary with all data relevant for further
analysis

    results = {
        'SCOP_heating_RGSHP': SCOP_heating_RGSHP,
        'SCOP_cooling_RGSHP': SCOP_cooling_RGSHP,
        'Annual_performance_factor_RGSHP': Annual_performance_factor_RGSHP,
        'LCOE_heating_per_MWh': LCOE_heating_per_MWh,
        'LCOE_cooling_per_MWh': LCOE_cooling_per_MWh,
        'LCOE_heating_and_cooling_per_MWh': LCOE_heating_and_cooling_per_MWh,
        'Specfic_emissions_heating_per_MWh': specfic_emissions_heating,
        'Specfic_emissions_cooling_per_MWh': specfic_emissions_cooling,
        'Specfic_emissions_heating_and_cooling_per_MWh':
specfic_emissions_heating_and_cooling,
        'heating_coverage': heating_coverage,
```

```python
        'cooling_coverage': cooling_coverage,
        'total_coverage': total_coverage,
        'losses_cooling': losses_cooling,
    }

    return results

###############################################################################
'''Store the calculation results for every topology in a comprehensive
structure for further analysis and plotting'''

# print(file_paths)
# print(column_lists_0['@@TK01_Vol@@'])
# print(column_lists_0['@@TK02_Vol@@'])
# test_path =
r'C:\Users\pauls\Desktop\master_thesis\Thesis\python\análisis_resultados\Resul
tados.txt'

tanksizes_heating = data_frame_lists['@@TK01_Vol@@']
tanksizes_cooling = data_frame_lists['@@TK02_Vol@@']
number_RGSHPs = data_frame_lists['@@HP01_Num@@']

# Initialize a dictionary to hold grouped data
grouped_data = {}
grouped_data_2 = {}

# Loop over zipped lists to be able to store the result data separately using
group keys.
for file_path, tanksize_heating, number_RGSHP in zip(file_paths,
tanksizes_heating, number_RGSHPs):

    result = analyse_file(file_path)
    # The corresponding sizes of the cooling tanks can be found in the
SimJobIndex.csv file
    # It is important that these are calculated in ascending order during the
TRNSYS simulation, so that the SimJobIndex.csv file has the same format
    # The first value in each list corresponds to the smallest cold storage
tank, the second to the second smallest, the third to the third smallest and
so on

    # Create a unique key for each group
    group_key_1 = (number_RGSHP, tanksize_heating)
    group_key_2 = number_RGSHP

    # Initialize lists for the group if it doesn't exist
    if group_key_1 not in grouped_data:
        grouped_data[group_key_1] = {
            'SCOP_heating_RGSHP': [],
```

```python
            'SCOP_cooling_RGSHP': [],
            'Annual_performance_factor_RGSHP': [],
            'LCOE_heating_per_MWh': [],
            'LCOE_cooling_per_MWh': [],
            'LCOE_heating_and_cooling_per_MWh': [],
            'Specfic_emissions_heating_per_MWh': [],
            'Specfic_emissions_cooling_per_MWh': [],
            'Specfic_emissions_heating_and_cooling_per_MWh': [],
            'heating_coverage': [],
            'cooling_coverage': [],
            'total_coverage': [],
            'losses_cooling': [],
        }

    if group_key_2 not in grouped_data_2:
        grouped_data_2[group_key_2] = {
            'SCOP_heating_RGSHP': [],
            'SCOP_cooling_RGSHP': [],
            'Annual_performance_factor_RGSHP': [],
        }

    # Append values to the respective lists in the group
    grouped_data[group_key_1]['SCOP_heating_RGSHP'].append(result['SCOP_heatin
g_RGSHP'])
    grouped_data[group_key_1]['SCOP_cooling_RGSHP'].append(result['SCOP_coolin
g_RGSHP'])
    grouped_data[group_key_1]['Annual_performance_factor_RGSHP'].append(result
['Annual_performance_factor_RGSHP'])
    grouped_data[group_key_1]['LCOE_heating_per_MWh'].append(result['LCOE_heat
ing_per_MWh'])
    grouped_data[group_key_1]['LCOE_cooling_per_MWh'].append(result['LCOE_cool
ing_per_MWh'])
    grouped_data[group_key_1]['LCOE_heating_and_cooling_per_MWh'].append(resul
t['LCOE_heating_and_cooling_per_MWh'])
    grouped_data[group_key_1]['Specfic_emissions_heating_per_MWh'].append(resu
lt['Specfic_emissions_heating_per_MWh'])
    grouped_data[group_key_1]['Specfic_emissions_cooling_per_MWh'].append(resu
lt['Specfic_emissions_cooling_per_MWh'])
    grouped_data[group_key_1]['Specfic_emissions_heating_and_cooling_per_MWh']
.append(result['Specfic_emissions_heating_and_cooling_per_MWh'])
    grouped_data[group_key_1]['heating_coverage'].append(result['heating_cover
age'])
    grouped_data[group_key_1]['cooling_coverage'].append(result['cooling_cover
age'])
    grouped_data[group_key_1]['total_coverage'].append(result['total_coverage'
])
    grouped_data[group_key_1]['losses_cooling'].append(result['losses_cooling'
])
```

```python
    grouped_data_2[group_key_2]['SCOP_heating_RGSHP'].append(result['SCOP_heat
ing_RGSHP'])
    grouped_data_2[group_key_2]['SCOP_cooling_RGSHP'].append(result['SCOP_cool
ing_RGSHP'])
    grouped_data_2[group_key_2]['Annual_performance_factor_RGSHP'].append(resu
lt['Annual_performance_factor_RGSHP'])

# print(grouped_data)
```